

South Dakota State University

Open PRAIRIE: Open Public Research Access Institutional Repository and Information Exchange

Electronic Theses and Dissertations

2018

Lignin Depolymerization: Mechanistic Analysis, Optimization and Application

Eric Michael Nagel

South Dakota State University

Follow this and additional works at: <https://openprairie.sdstate.edu/etd>

 Part of the [Materials Chemistry Commons](#), and the [Organic Chemistry Commons](#)

Recommended Citation

Nagel, Eric Michael, "Lignin Depolymerization: Mechanistic Analysis, Optimization and Application" (2018). *Electronic Theses and Dissertations*. 2678.

<https://openprairie.sdstate.edu/etd/2678>

This Thesis - Open Access is brought to you for free and open access by Open PRAIRIE: Open Public Research Access Institutional Repository and Information Exchange. It has been accepted for inclusion in Electronic Theses and Dissertations by an authorized administrator of Open PRAIRIE: Open Public Research Access Institutional Repository and Information Exchange. For more information, please contact michael.biondo@sdstate.edu.

LIGNIN DEPOLYMERIZATION: MECHANISTIC ANALYSIS,
OPTIMIZATION AND APPLICATION

BY

ERIC MICHAEL NAGEL

A dissertation submitted in partial fulfillment of the requirements for the

Doctor of Philosophy

Major in Chemistry

South Dakota State University

2018

LIGNIN DEPOLYMERIZATION: MECHANISTIC ANALYSIS,
OPTIMIZATION AND APPLICATION

ERIC MICHAEL NAGEL

This dissertation is approved as a credible and independent investigation by a candidate for the Doctor of Philosophy in Chemistry degree and is acceptable for meeting the dissertation requirements for this degree. Acceptance of this dissertation does not imply that the conclusions reached by the candidate are necessarily the conclusions of the major department.

Cheng Zhang, Ph.D
Dissertation Advisor

Date

Douglas ~~H~~ Kaynie, Ph.D
Head, Department of Chemistry & Biochemistry

Date

~~Dean~~, Graduate School

Date

ACKNOWLEDGEMENTS

I first would like to offer my sincere gratitude and appreciation to my advisor, Dr. Cheng Zhang for challenging me to pursue my own ideas and his unceasing guidance. I would also like to extend my gratitude to the members of my graduate committee, Dr. Fathi Halaweish and Dr. Brian Logue for your time, guidance, and assistance in research and class work. I would like to thank my former lab members, Aubrey Jone, Logan Sanow, Dan Liu, and Jianyuan Sun for your support, knowledge, and friendship.

I am especially grateful for the unwavering support and encouragement from my loving parents, Pat and Sandy Nagel. They have always supported my endeavors, pushed me to grow beyond myself, have been a wealth of practical (and sometimes impractical) advice, and so should be largely accredited for my accomplishments.

Lastly, I want to acknowledge my associate in avocation, cohort in camaraderie, and fellow TexMex aficionado, Elizabeth (Emmy) Bailey, for her constant compassion, and support. You helped to make this possible.

The author thanks and acknowledges the financial support by the South Dakota NSF EPSCoR Program (Grant No. IIA-1330842).

TABLE OF CONTENTS

LIST OF ABBREVIATIONS.....	ix
LIST OF FIGURES	xii
LIST OF SCHEMES	xiv
LIST OF TABLES.....	xvi
ABSTRACT.....	xvii
CHAPTER 1: INTRODUCTION AND BACKGROUND	1
1.1 Overall significance.....	1
1.2 Lignocellulose	3
1.3 Lignin Depolymerization	8
1.3.1 Lignin sources and models	8
1.3.2 Physicochemical and chemical methods	11
1.3.3 Oxidative methods.....	13
1.3.4 Reductive methods	14
1.3.5 Challenges and research objectives	14
CHAPTER 2: DETERMINATION OF THE HYDROTHERMAL DEGRADATION MECHANISM OF A LIGNIN DIMER UNDER NEUTRAL AND BASIC CONDITIONS	16
2.1 Introduction	16
2.2 Experimental	19

2.2.1 Materials	19
2.2.1.1 Guaiacylglycerol synthesis	20
2.2.2 Methods	21
2.2.2.1 Dimer decomposition reactions and workup	21
2.2.2.2 Guaiacylglycerol degradation	22
2.2.2.3 Isolation of (Z)- and (E)-2-methoxy-4-(2-(2-methoxyphenoxy)vinyl)phenol	23
2.2.2.4 Product characterization and quantification	25
2.3 Results and Discussion	32
2.3.1 Reactions and Data	32
2.3.2 β -O-4 bond cleavage mechanisms under neutral and basic conditions	34
2.3.3 The fate of the major β -O-4 cleavage product 11	41
2.3.4 Formation of vinyl ether 10 under strongly basic conditions	43
2.3.5 Condensation of dimer decomposition products to biochar	44
2.4 Conclusions	46
CHAPTER 3: LIGNIN DIMER DECOMPOSITION UNDER REDUCTIVE	
CONDITIONS	48
3.1 Introduction	48
3.2 Experimental	50
3.2.1 Materials	50

3.2.1.1	Preparation of 10% Nickel/Carbon Catalyst	50
3.2.1.2	Preparation of Ni/Zn Catalyst.....	51
3.2.2	Methods	51
3.2.2.1	Reductive dimer decomposition	51
3.2.2.2	Characterization and quantification.....	52
3.2.2.3	NMR	52
3.3	Results and Discussion.....	53
3.3.1	Three reductive systems Ni/C + H ₂ , Ni/C + Zn, Ni/Zn and the main reduction path	53
3.3.2	The functions of individual metals and effect of solvent on cleavage and condensation under neutral conditions	55
3.3.3	Reduction under neutral conditions.....	57
3.3.3.1	Reduction in aqueous solutions	57
3.3.3.2	Reduction pathway	60
3.3.3.3	The effect of ethanol.....	61
3.3.3.4	Homolytic β -O-4 cleavage in ethanol.....	64
3.3.4	Reduction under basic conditions.....	66
3.3.5	Vanillin formation and reduction	69
3.3.6	ZnO formation under basic conditions	70
3.3.7	Reduction mechanism of the vinyl ether (compound 10)	70

3.4 Conclusions	74
CHAPTER 4: SELECTIVE DEPOLYMERIZATION OF LIGNIN IN A RAW	
BIOMASS SUBSTRATE.....	77
4.1 Introduction	77
4.2 Experimental	80
4.2.1 Materials	80
4.2.2 Methods	80
4.2.2.1 Biomass Characterization	80
4.2.2.2 Biomass Decomposition Reactions	82
4.2.2.3 Product characterization and quantification	83
4.2.2.4 Zinc oxide synthesis	88
4.3 Results and discussion.....	89
4.3.1 Lignin depolymerization in pine sawdust with external reducing agent (H ₂ or Zn)	89
4.3.1.1 Effects of reaction conditions	89
4.3.1.2 Mechanism.....	98
4.3.2 Lignin depolymerization in pine sawdust utilizing hydrogen transfer from alcohol	108
4.3.3 Application to agricultural waste product substrates.....	115
4.4 Conclusions	119

CHAPTER 5: CONCLUSIONS AND FUTURE WORK.....	121
5.1 Conclusions	121
5.1.1 Determination of the hydrothermal degradation mechanism of a lignin dimer under neutral and basic conditions	121
5.1.2 Lignin dimer decomposition under reductive conditions.....	121
5.1.3 Selective depolymerization of lignin in a raw biomass substrate.....	122
5.2 Continued and future work.....	122
5.2.1 Application of lignin derived monophenols	122
5.2.2 Reactions and Schemes	124
REFERENCES	133

LIST OF ABBREVIATIONS

ACN: Acetonitrile

BET: Brunauer–Emmett–Teller

BHT: Butylated hydroxytoluene

CH₄: Methane

CO: Carbon monoxide

CO₂: Carbon dioxide

DCM: Dichloromethane

DFT: Density functional theory

DI: Deionized

DMF: Dimethylformamide

DMSO: Dimethylsulfoxide

ECN: Estimated carbon number

EI: Electron impact

EtOH: Ethanol

GC-MS: Gas chromatography – mass spectroscopy

GPC: Gel permeation chromatography

HPLC: High pressure liquid chromatography

HSQC: Heteronuclear single quantum correlation

H₂: Diatomic hydrogen

H₂O: Water

MeOH: Methanol

MW: Molecular weight

NBS: N-bromosuccinimide

Ni: Nickel

Ni/C: Nickel supported on activated carbon

NIST: National Institute of Standards and Technology

NMR: Nuclear magnetic resonance

OPEC: Organization of the Petroleum Exporting Countries

PCM: Polarizable continuum model

PG: 4-propylguaiacol

PS: Polystyrene

RT: Room temperature

SIM: Selective ion monitoring

TBDMS: tert-Butyldimethylsilyl

TBDMSCl: tert-Butyldimethylsilyl chloride

THF: Tetrahydrofuran

TIC: Total ion count

UV: Ultraviolet

Zn: Zinc

ZnO: Zinc oxide

LIST OF FIGURES

Figure 1. (a) Cross section of the secondary cell wall illustrating the organization of cellulose, hemicelluloses, and lignin. (b) Diagram of the cell wall illustrating the division into sections (S1-S3) ²²	4
Figure 2. Molecular diagram of the secondary cell wall illustrating the structural relationship of the constituent biopolymers: Crystalline cellulose microfibrils are covalently attached to lignin through hemicellulose.	6
Figure 3. (A) Representative softwood lignin fragment, (B) Lignin monolignols, (C) lignin number convention, and (D) bond composition. Lignin is the result of enzyme catalyzed radical polymerization of up to three monolignols. The resultant structure is primarily linked by ether bonds but also contains an appreciable amount of C-C bonds, the percentage of which depends on the monomer ratios.	8
Figure 4. Common lignin model compounds. (1) Unfunctionalized α -O-4 dimer model. (2) Unfunctionalized 4-O-5 dimer model. (3) Unfunctionalized β -O-4 model dimer. (4) Nonphenolic β -O-4 model dimer. (5) Phenolic β -O-4 dimer model. (6) Phenolic β -O-4 trimer model.....	11
Figure 5. ¹ H NMR spectrum of compound (Z)-2-methoxy-4-(2-(2-methoxyphenoxy)vinyl)phenol	24
Figure 6. ¹³ C NMR spectrum of compound (Z)-2-methoxy-4-(2-(2-methoxyphenoxy)vinyl)phenol	24
Figure 7. ¹ H NMR spectrum of compound 9 (<i>trans</i> , TBDMS-protected).	25
Figure 8. Mass distribution of products in DCM oil obtained from hydrothermal decomposition using hydroxide bases.	33
Figure 9. Mass distribution of products in DCM oil obtained from hydrothermal decomposition using carbonate bases.	34
Figure 10. GC-MS chromatogram of guaiacylglycerol degradation in 2eq NaOH. 8 eq of tetrabutylammonium fluoride was also present prior to the reaction as the hydroxy groups of guaiacylglycerol were protected by TBDMS.	39
Figure 11. GC-MS chromatogram of the products of Entry 5 (Table 4). The y-axis is the signal intensity of the MS detector and the x-axis is the retention time in minutes. The internal standard is 2-isopropylphenol.....	44
Figure 12. GC-MS chromatogram of decomposition products of β -O-4 dimer under reducing conditions in ethanol (Entry 11, Ni/C, Zn, EtOH). The y-axis is the signal intensity of the MS detector and the x-axis is the retention time in minutes. The internal standard is 2-isopropylphenol.	63
Figure 13. GC-MS chromatogram of decomposition products of β -O-4 dimer under reducing conditions in basic water (entry 14A: Ni/C + Zn + 8 eq NaOH + water). The y-axis is the signal intensity of the MS detector and the x-axis is the retention time in minutes. The internal standard is 2-isopropylphenol.....	68

- Figure 14. ^1H NMR spectrum of the product of dimer hydrothermal decomposition catalyzed by Pd/C. An appreciable amount of vinyl ether reduction product (24) is observed when Pd/C is used. Pd/C functions as a much better hydrogenation catalyst than Ni/C..... 72
- Figure 15. GC-MS chromatograms of 6h methanol entries from Table 11 depicting the amount of hemicelluloses/cellulose derived alcohols relative to the concentration of internal standard. Each chromatogram is normalized to the internal standard (peak at 6.42 minutes). Other peaks represent the abundance of 5 or 6 aliphatic carbon chains containing one or two hydroxyl groups. The lack of aromatic moieties indicates that these alcohols must be derived from polysaccharides. 93
- Figure 16. GC-MS chromatogram and peak identification of trimethylsilylated lignin monomers (1-5) and dimers (6-9) (reaction conditions: Entry 8 Table 11). The internal standard is 2-isopropylphenol. A relatively high abundance of dehydroabietic acid (15 min) is observed due to the reaction being conducted without extractive pre-treatment. 102
- Figure 17. Mass distribution of products in DCM oil of entries 1-4. Entry 1: Ni/C, Zn, H_2O . Entry 2: Ni/C, 4 atm H_2 , H_2O . Entry 3: Ni/C, Zn, 4% NaOH. Entry 4: Ni/C, 4 atm H_2 , 4% NaOH..... 104
- Figure 18. GC-MS chromatograms of 6h methanol entries from Table 12 depicting the amount of hemicelluloses/cellulose derived alcohols relative to the concentration of internal standard. Each chromatogram is normalized to the internal standard (peak at 6.42 minutes). Other peaks represent the abundance of 5 or 6 aliphatic carbon chains containing one or two hydroxyl groups. The lack of aromatic moieties indicates that these alcohols must be derived from polysaccharides. 112
- Figure 19. Mass distributions of lignin product oil from corn stover, sugarcane bagasse, and switchgrass feedstocks. 118

LIST OF SCHEMES

Scheme 1. Structures of some β -O-4 model compounds studied in the literature (top), and acidolysis (middle) and homolysis (bottom) mechanisms.....	18
Scheme 2. β -O-4 bond cleavage mechanism and downstream reactions under neutral and basic conditions.....	36
Scheme 3. Newman projections and relative probabilities of all rotamers for α S, β R and α R, β R stereoisomers. Rotamers that can undergo elimination across the β - γ bond are highlighted in red. Rotamers that can under elimination across the α - β bond have the Newman projection of the C $_{\alpha}$ -C $_{\beta}$ bond highlighted in blue.....	36
Scheme 4. β -O-4 hydrolysis (intermolecular substitution) mechanism under basic conditions and fate of guaiacylglycerol	40
Scheme 5. Possible formation mechanisms for the vinyl ether (10). Left: deprotonation of the phenol results in the formation of quinone methide and elimination of the α -OH followed by deprotonation of the γ -OH, resulting in β - γ cleavage and the release of formaldehyde. Right: deprotonation of the γ -OH results in the ejection of the α -OH by an E2 or E1cb mechanism.	44
Scheme 6. Illustrative mechanisms of re-polymerization of dimer decomposition products under basic and neutral conditions.....	46
Scheme 7. Possible reduction paths of the β -O-4 cleavage products in neutral water or water/EtOH.	61
Scheme 8. Reaction pathways of trace products in Entry 11 (Ni/C, Zn, EtOH).	64
Scheme 9. Mechanism of the vinyl ether (10) reduction. Path 1: The vinyl ether (10) is first hydrogenated to yield 24, which then undergoes metal catalyzed β -O-4 bond cleavage and reduction to yield 22. Path 2: Metal catalyzed β -O-4 bond cleavage and reduction occurs prior to hydrogenation to yield 25, which is then hydrogenated to 22..	74
Scheme 10. The paths of alkyl aryl ether cleavage and downstream reactions of immediate products.....	99
Scheme 11. Depolymerization of a sample lignin fragment via the elimination pathway. Elimination results in the cleavage of α -O-4 and β -O-4 ether bonds and the formation of carbonyl species. Carbon linkages and the 4-O-5 linkages remain intact.	100
Scheme 12. Depolymerization of a sample lignin fragment via the retro-aldol pathway. Only α -O-4 bonds are cleaved by the retro-aldol reaction that occurs in the presence of base. β -O-4 linkages are converted to vinyl ethers while β -1 linkages containing α and γ hydroxyl groups are converted to stilbene moieties.	104
Scheme 13. Homolytic cleavage mechanism of guaiacylglycerol- β -guaiacyl ether.	105
Scheme 14. Proposed mechanisms for path 4a: Ni-arene activation of C-O bond. Top: Nickel promotes elimination by weakening the β -O-4 through surface interaction with oxygen. Bottom: Nickel removes the α -H to induce β -elimination.	107

Scheme 15. Reaction intermediates leading from starting material, 4-propylguaiacol, to polyconjugated materials 6, 11, 12, and 17.	125
Scheme 16. Proposed synthesis scheme for a potential charge storage material.....	132

LIST OF TABLES

Table 1. Lignocellulosic ratios of potential biomass substrates	5
Table 2. Linkages in protolignin and processed lignin	10
Table 3. Mass spectral data of trimethylsilylated dimer and decomposition products	29
Table 4. Major decomposition products of dimer 3 under neutral and conditions.	33
Table 5. The calculated energies and relative probabilities of rotomers 1-9 for each diastereomeric pair	37
Table 6. The calculated activation energies and relative reaction rate constants of the elimination and hydrolysis transition states under basic conditions	40
Table 7. Stability tests of guaiacol and vanillin.	43
Table 8. Hydrothermal decomposition of dimer 3 under neutral and reductive conditions.	55
Table 9. “Other” products of hydrothermal decomposition of dimer 3 under reductive conditions.	57
Table 10. Hydrothermal decomposition of dimer 3 under basic and reductive conditions.	69
Table 11. Reductive delignification of pine sawdust with external reducing agent	90
Table 12. Reductive delignification of pine sawdust utilizing hydrogen generation from an alcohol solvent	109
Table 13. Characterization of biomass substrates	116
Table 14. Reductive delignification of agricultural waste products utilizing hydrogen generation from methanol	119

ABSTRACT

LIGNIN DEPOLYMERIZATION: MECHANISTIC ANALYSIS,
OPTIMIZATION AND APPLICATION

ERIC MICHAEL NAGEL

2018

Lignin is the most abundant aromatic biopolymer and is a potential source for phenolic chemical feedstocks. Lignin is composed of phenolic units connected by more than eight different linkages, the most common being β -O-4 which constitutes 50-60%. The hydrothermal decomposition of a guaiacol based β -O-4 lignin dimer was studied under neutral and basic conditions to elucidate the mechanism of β -O-4 bond cleavage and the formation of downstream products. Phenol-carbonyl condensation and vinyl-ether formation were shown to be the primary causes for low monomer yields under the tested conditions. Three Ni catalyst systems, Ni/C + H₂, Ni/C-Zn, and Ni/Zn, were investigated using the dimer model under a variety of conditions to counteract these processes. The role of each reagent was explored and monomer yields up to 80 C% were obtained.

These catalysts were used to investigate the intricacies of reductive depolymerization of raw biomass using pine sawdust as a substrate. Preservation of the cellulose matrix, lignin extraction and solubilization, and rate of hydrogen generation were identified to be the most important factors governing monomer yields. A quantitative monomer yield of 35 C% was realized using Ni/C + H₂ in ethanol with 4-propylguaiacol composing 32 C%. Ethanol and methanol solvents in the presence of Ni metal were identified as a hydrogen source for reductive depolymerization, allowing for

the omission of an external reducing agent. A monomer yield of 26 C% was obtained using only Ni/C and methanol. The lignin component of two agricultural waste crops, corn stover and sugarcane bagasse, and an energy crop, switchgrass, were effectively depolymerized using these conditions. Despite the successful depolymerization of lignin, the major product, 4-propylguaiacol, has few current applications outside substandard polymer composites. Therefore, new applications must be developed. To this end, 4-propylguaiacol was used in an attempt to synthesize a semi-conductive charge storage material for potential use in supercapacitors and battery cathodes.

CHAPTER 1: INTRODUCTION AND BACKGROUND

1.1 Overall significance

Global material and energy demands have increased dramatically over the past several decades and continue to do so at an unprecedented rate. Petrochemicals continue to satiate demand but the rate of crude oil production is dependent on both reserve discovery and the amount of recoverable oil remaining in a given reserve. Therefore, total depletion of world reserves is not the problem, but rather demand outpacing production as oil reserves approach their peak production limits. OPEC production is expected to peak in 2026 and accounts for an estimated 78% of the world's remaining conventional crude oil reserves.¹ Although unconventional oil sources such as tar sands and oil shales will help to mitigate this problem, it is possible that demand will begin to outstrip production resulting in market volatility and possible shortages in what has become a necessary economic and strategic resource. The combustion of petroleum fuels on the global scale has also been linked to anthropogenic climate change through CO₂ emission.²⁻³ If left unchecked, these atmospheric changes are predicted to result in increasingly adverse conditions for human civilization such as: increased frequency of inclement weather brought about by higher surface temperatures and cooler upper atmosphere temperatures,⁴ rising ocean levels due to the thawing of ice caps and glaciers,⁵ increasing desertification of lands,⁶⁻⁹ and dramatic changes to aquatic ecosystems due to acidification and higher surface temperatures.¹⁰⁻¹⁵

The development of biomass processing technologies could play an integral role in the solution of these problems. Plant based products ideally represent an unlimited source

of fuel and materials and can be viewed as carbon neutral as atmospheric CO₂ is ultimately the carbon source. Presently, no other technology exists that can convert atmospheric CO₂ into useable products more quickly, efficiently, and affordably than plants, and given that the foundation of modern society is agriculture, lignocellulosic biomass from plants represents a promising replacement for petroleum based products. Lignin in particular provides a unique opportunity as it is a natural phenolic polymer which accounts for 20-35 wt% in woody biomass (40-50 wt% in bark) and 10-20 wt% in agricultural stems.¹⁶ It has a higher specific heat content than the other two major biomass components, cellulose and hemicellulose.¹⁷⁻¹⁸ It is highly aromatic, and is therefore the most abundant aromatic biopolymer on the earth, making it a potential substitute for petroleum based chemical feedstocks if it can be efficiently depolymerized into its constituent monophenols.

Depolymerization is made more complex by the tendency for the products to undergo additional reactions, forming highly chemical resistant oligomers and polymers. Lignin depolymerization has been extensively conducted under pH neutral and alkaline conditions but there is little corroborative knowledge regarding the depolymerization and repolymerization mechanisms. Herein we present a detailed analysis of the hydrothermal decomposition of a lignin model compound under neutral and alkaline conditions. A decomposition mechanism that accounts for all detected chemical species, including vanillin, is established and the repolymerization process is expounded upon. Such knowledge is imperative for the development and optimization of systems for lignin depolymerization. Using this knowledge, three Ni-based catalytic systems are studied and optimized for monomer yield. The function of each catalyst component is identified and

the reaction mechanisms established for each unique reaction system, allowing for a more comprehensive design of lignin depolymerization catalysts for use with actual biomass substrates.

1.2 Lignocellulose

Plant cell walls contain the vast majority of photosynthetic carbon and so compose virtually all plant biomass. Cell walls are complex, heterogeneous structures consisting of one or more layers composed of varying amounts of cellulose, hemicelluloses, lignin, as well as lesser amounts of pectin, fats, and proteins. Figure 1 illustrates the layout of a typical vascular plant cell wall. The cell wall lies between the middle lamella, composed largely of pectin which acts to glue neighboring cells together, and the cell plasma membrane. Most vascular plants have both a primary and secondary wall. The primary wall is a thin, flexible, water permeable layer consisting of cellulose, hemicellulose, and pectin.¹⁹⁻²⁰ The secondary cell wall is responsible for many of the observed functions of plant cells and is produced after the primary wall is complete and the cell stops expanding. Differing considerably in composition from the primary wall, the secondary wall contains lignin and relatively few pectins and proteins which confers hydrophobicity, chemical resistance, rigidity, and mechanical strength. The hydrophobicity provided by lignin is essential for constraining water to vascular tissues, thereby allowing water transport throughout the plant. The increased durability and strength provided by lignin allow plants to overcome the mechanical burden placed on organisms by gravity, allowing for greater upward and outward growth before risking structural failure.¹⁹⁻²⁰ This function is most apparent in wood which is composed mostly of secondary cell wall with lignin concentrated heavily in compression wood.²¹

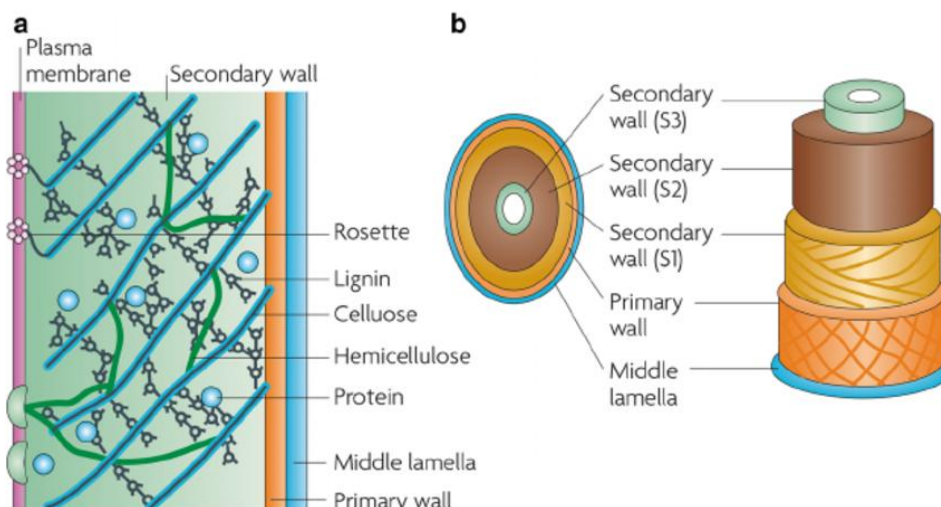


Figure 1. (a) Cross section of the secondary cell wall illustrating the organization of cellulose, hemicelluloses, and lignin. (b) Diagram of the cell wall illustrating the division into sections (S1-S3)²²

In addition to local variance, the ratio of the lignocellulose components can vary substantially across plant species likely due to environmental pressures during their evolution. Table 1 shows the relative percentages of each major component of lignocellulose found in a variety of general plant varieties and waste products. As can be seen in the table, cellulose and hemicelluloses account for about 75% of lignocellulosic biomass while lignin accounts for about 25%. The paper and pulp industry represents the single largest consumer of cellulosic materials with 131.2 million tonnes of delignified pulp produced worldwide in 2000.²³ Cellulose and hemicelluloses are polysaccharides and therefore also represent a source of fermentable sugars. These polymers can be broken down into their monomeric constituents by various hydrolysis processes. The resultant sugars can then be fermented to form bio-ethanol or further treated to produce specific chemicals. Whether the raw lignocellulose is pulped and converted to paper or transformed into biofuel or biochemicals, only the cellulosic components are utilized while lignin is removed as an unwanted waste product and burned to provide heat for

these processes. The pulp and paper industry alone was estimated to have produced about 70 million tonnes of lignin in 2011 of which only 2% was commercially utilized while the remainder was burned for heat at a value of \$80 per ton.²⁴ Lignin accounts for ~30% of non-fossil carbon and is the largest natural reservoir of solar energy, making the transformation of lignin into chemical feedstocks essential to combating global reliance on petrochemicals and climate change.²⁴ However, in order to successfully transform lignin, a complex amorphous polymer, into specific chemicals it is not only necessary to understand the chemical composition of lignin, but biomass as a whole.

Table 1. Lignocellulosic ratios of potential biomass substrates

Types of biomass	Lignocellulosic substrate	Cellulose (%)	Hemicellulose (%)	Lignin (%)
Agriculture waste	Corn cob	45	35	15
	Wheat straw	30	50	15
	Barley straw	33-40	20-35	8-17
	Corn stover	39-42	22-28	18-22
	Nut shell	25-30	25-30	30-40
Energy crops	Empty fruit bunch	41	24	21
	Switch grass	45	31	12
Forestry waste	Hardwood stems	40-55	24-40	18-25
	Softwood stems	45-50	25-30	25-35
	Leaves	15-20	80-85	0
Industrial waste	Waste papers from chemical pulp	60-70	10-20	5-10
	Organic compound from wastewater	8-15	0	0

At the molecular level, layered sheaths of microfibrils composed of crystalline cellulose make up the backbone of both the primary and secondary cell wall. Cellulose itself is composed of $\beta(1-4)$ linked D- glucopyranose units. The β -glycosidic linkage results in a relatively straight chain of D-glucopyranose units which allows extensive hydrogen bonding between chains, resulting in crystalline domains. The secondary cell wall can be subdivided into sections (S1, S2, S3, Figure 1) in which the cellulose microfibrils differ in direction.¹⁹ These microfibrils are embedded in a hemicellulose

polymer matrix which is interconnected to pectin in the primary cell wall or lignin in the secondary cell wall as seen in Figure 2.

Hemicellulose is heteropolymer composed of 5- and 6-carbon saccharides such as glucose, xylose, fructose, rhamnose, mannose, arabinose, and galactose linked by glycosidic bonds. Unlike cellulose, hemicellulose is composed of amorphous, short chains (500-3000 units) with carboxylic acid groups.²⁵ The extensive interpolymer crosslinking between the cellulose microfibrils and lignin chains through hemicellulose establishes the mechanical strength and rigidity of the plant cell wall. Hemicellulose is connected to cellulose via glycosidic linkages²⁵ and to lignin via ester linkages with hydroxycinnamic acids such as: coumaric acid, ferulic acid, and sinapinic acid.²⁶

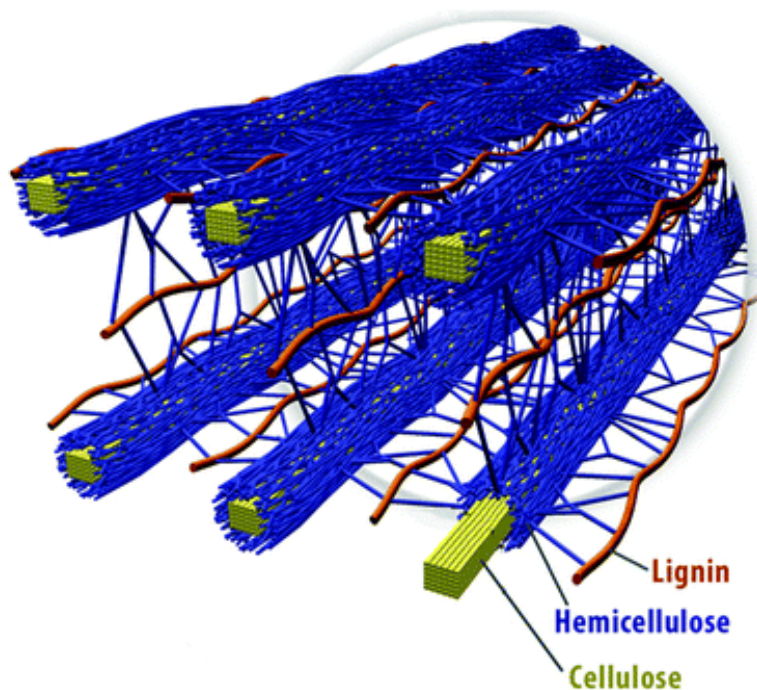


Figure 2. Molecular diagram of the secondary cell wall illustrating the structural relationship of the constituent biopolymers: Crystalline cellulose microfibrils are covalently attached to lignin through hemicellulose.

Lignin is an amorphous three-dimensional polymer consisting of methoxylated propyl phenol units derived from aromatic alcohols, commonly referred to as monolignols. There are three monolignols, distinguished by the degree of methoxylation of the aromatic ring at the 3 and 5 positions as shown in Figure 3. The monolignols, *p*-coumaryl alcohol, coniferyl alcohol, and sinapyl alcohol undergo enzyme assisted radical polymerization to form corresponding *p*-hydroxyphenyl (H), guaiacyl (G), and syringyl (S) units that are irregularly linked through a combination of carbon-carbon (C-C) and ether linkages.

The ratio of monomers and bonding varies considerably between species and even among individuals of a given species to a lesser degree. Generally, however, herbaceous plants contain mostly H units, softwoods almost entirely G units, and hardwoods mostly S units with 50-70% ether linkages and the remainder being C-C bonds. The percentage of ether bonds is strongly tied to the monomer ratio. A high amount of S units, such as in hardwood, results in fewer C-C bonds, as both the 3 and 5 positions of the ring are blocked. Lignin lacking S units, such as softwood lignin which consists of only G units, has considerable more C-C linkages and fewer ether linkages due to increased frequency of 5-5 and β -5 bonds. These C-C bonds are virtually inert in comparison to ether linkages and result in the crosslinking of lignin chains, making the delignification of herbaceous and softwood substrates particularly difficult.²⁷ Regardless, even S unit deficient lignin contains >50% ether linkages with the β -O-4 bond being the most prominent.²⁸ For this reason, the β -O-4 bond is considered the most important bond for the development of lignin depolymerization technologies.

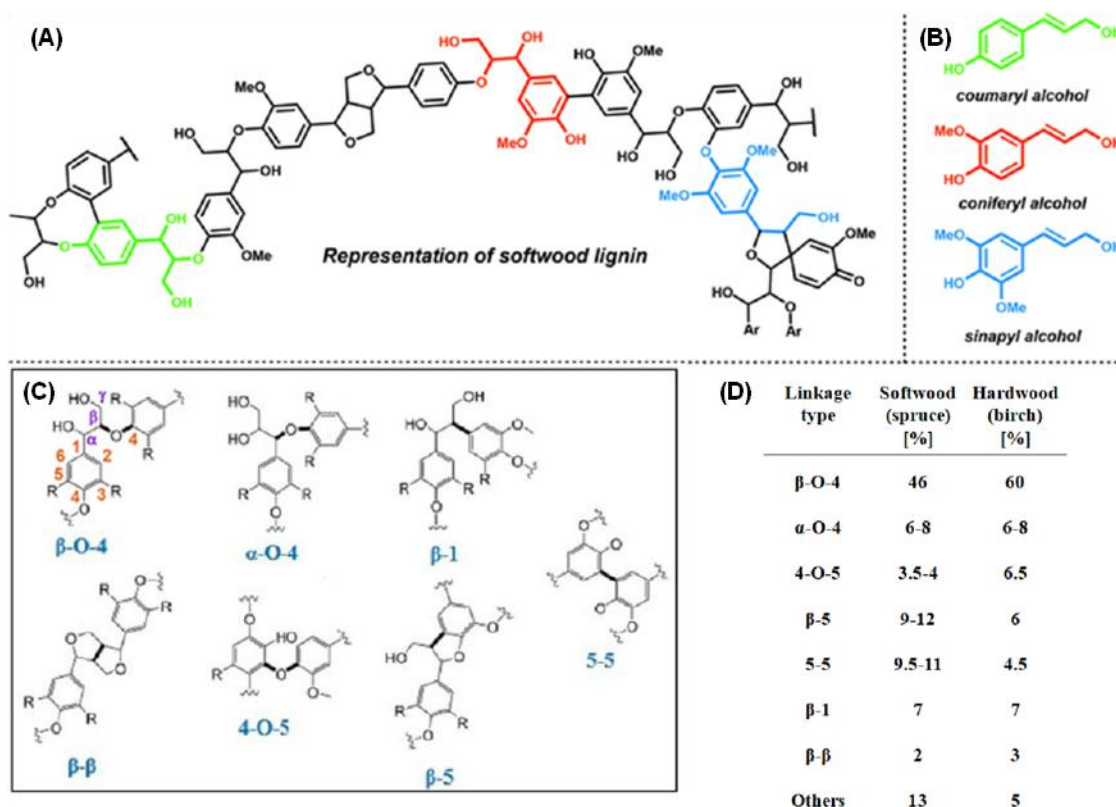


Figure 3. (A) Representative softwood lignin fragment, (B) Lignin monolignols, (C) lignin number convention, and (D) bond composition. Lignin is the result of enzyme catalyzed radical polymerization of up to three monolignols. The resultant structure is primarily linked by ether bonds but also contains an appreciable amount of C-C bonds, the percentage of which depends on the monomer ratios.

1.3 Lignin Depolymerization

1.3.1 Lignin sources and models

Lignin depolymerization from raw biomass is a relatively new field of research and is not accomplished on the industrial scale. Rather, lignocellulose is subjected to some form of pretreatment in order to separate the lignin component. Lignin separated by any such process is significantly chemically altered from the “protolignin” in biomass. Currently, the most industrial relevant delignification processes are the Kraft process, which accounts for over 90% of all produced pulp products,²³ and the sulfite process. These

methods, as well as niche processes, such as the soda process and organosolv process, work to solubilize the lignin component, allowing for filtration of the insoluble cellulose fibers.

The Kraft process treats physically processed biomass (chipped or milled) in a high pH solution of sodium sulfide at temperatures of 423-453K for several hours. The resulting mixture is filtered to separate the cellulose pulp. The filtrate contains soluble lignin fragments along with hemicellulose derived carbohydrates. These lignin fragments have a molecular weight of 1.5-5K g/mol and contain aliphatic thiols giving the isolated lignin a 1-3% sulfur content.²³⁻²⁴ The sulfite process treats similarly processed biomass in a lower pH solution (1-5) of sulfite and bisulfite at temperatures of 403-433K for several hours. Again, the mixture is filtered to separate the cellulose pulp, leaving the filtrate containing soluble lignin fragments along with hemicellulose derived carbohydrates. This method, however, results in highly water soluble 10-50K g/mol liginosulfonates with a 3-8% sulfur content.²³⁻²⁴

As evident by their unique physical properties, processed lignin is chemically inequivalent to protolignin. Table 2 illustrates the dramatic differences between linkages found softwood (pine, spruce) and hardwood (poplar, birch) protolignin and linkages found in Kraft lignin. A similar shift in linkages is observed in lignin recovered from the sulfite process.²⁹ The relative lack of remaining cleavable ether linkages and high molecular weight of these lignin species make them unattractive for depolymerization into monophenols. Because the dominant linkages present in these species are C-C bonds, monoaromatics can only be obtained through high temperature radical processes similar to hydrocracking with only limited success.²⁹ Therefore, Kraft and sulfite lignin are

neither suitable nor representative substrates for lignin depolymerization with the goal of monophenolic products. Even mild biomass pretreatments such as steam explosion and organosolv result in changes to the lignin structure that vary with time, temperature, and solvent, though the structure is closer to that of protolignin than Kraft or sulfite lignin.³⁰⁻

³¹ Therefore it is not representative to use any isolated lignin as a model for protolignin depolymerization.

Table 2. Linkages in protolignin and processed lignin

Lignin source	β -O-4	β -1	β - β	β -5	4-O-5	5-5
Poplar wood	57.8	2.1	2.1	1.8	0.7	0.7
Spruce wood	31.5	2.1	0.4	2.5	0.5	2.7
Pine kraft lignin	11.2	1.9	0.3	1.2	0.2	0.6
Birch kraft lignin	15.4	47	24.5	6.8	3.4	2.5

In order to study protolignin depolymerization without the complications of the cellulosic matrix and other cellular components, model compounds representative of α -O-4, β -O-4, and 4-O-5 ether bonds have been employed.³²⁻⁴⁴ Figure 4 illustrates the chemical structures of various model compounds studied in literature. These models range from biaryl structures lacking any functionalization beyond the single bond to chemical mimics of lignin dimer or trimer fragments. While simple models that feature only the bond being studied, such as compounds 1-3, can give some useful information, they are often not representative of the actual chemical reactivity of lignin due to missing functional groups and thus possible reaction sites. Due to their relatively low frequency in the native lignin structure, there is little interest in exploring α -O-4 and 4-O-5 ether cleavage processes in detail and thus no studies on more complex models. The prominence of the β -O-4 linkage, however, as prompted the synthesis of more complicated and representative dimer and trimer model compounds

such as 4-6. These models can experimental isolate the various reactions that occur at the β -O-4 bond by including or excluding phenols and methoxy groups, making model compounds the optimal tool to understanding lignin depolymerization chemistry before moving to biomass substrates.

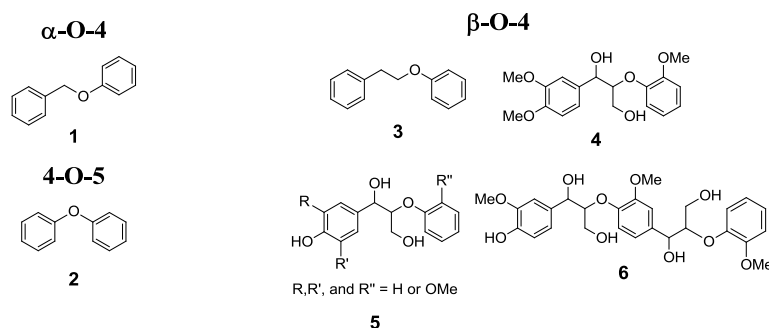


Figure 4. Common lignin model compounds. (1) Unfunctionalized α -O-4 dimer model. (2) Unfunctionalized 4-O-5 dimer model. (3) Unfunctionalized β -O-4 model dimer. (4) Nonphenolic β -O-4 model dimer. (5) Phenolic β -O-4 dimer model. (6) Phenolic β -O-4 trimer model.

1.3.2 Physicochemical and chemical methods

Physicochemical methods such as pyrolytic and hydrothermal degradation are the most attractive from an economic standpoint as they do not require the addition of any chemicals except for a cheap and often recyclable solvent. Pyrolysis, or heat induced bond cleavage, has been heavily studied and is achieved simply by heating the lignin sample under an inert atmosphere. Temperatures of 300-800°C are typically used and result in gaseous products, a complex bio-oil, and bio-char. The relative amounts and composition of the products is heavily dependent on reaction parameters, though the mechanism and thus challenges remain the same. The principal mechanism of pyrolysis is homolytic bond cleavage.⁴⁵ Therefore, the reaction proceeds through radical processes, which, without a hydrogen source (such as in hydrocracking – a related process) to quench the radicals, results in significant char formation (typically 30-50% based on dry

lignin weight).⁴⁶ High surface area, porous heterogeneous catalysts can be applied to significantly decrease char formation and increase the reaction selectivity for aromatic chemicals.⁴⁷⁻⁴⁸ These catalysts, however, are costly and rely heavily on surface morphology to function efficiently. Coking (char formation) still occurs and eventually is deposited into the catalyst pores, reducing efficiency after several runs.

Hydrothermal decomposition refers to processes in which lignin is decomposed in sub or supercritical water solutions. This method is particularly advantageous as water can exhibit a wide range of chemical and physical properties that vary from liquid-like to gas-like depending on the temperature and pressure. Supercritical water occurs above the critical point, 374°C and 218 atm (22MPa). Supercritical water can be advantageous in that it shows increased matrix permeation and can serve as an acid-base catalyst due to the increased autoprotolysis of water. Despite these apparent advantages, supercritical water has not been shown to effectively convert lignin into monophenolics. Although ether bonds are quickly degraded, large amounts of biochar are produced, indicating that condensation reactions are prominent.⁴⁹⁻⁵⁰

Subcritical water exists from the atmospheric boiling point, 100°C, to the critical temperature, 374°C, making it more versatile than super critical water. Subcritical water often is employed in conjunction with an acid or base catalyst. The lability of ether bonds in acid is well known, making acid catalyzed hydrothermal treatment one of the most thoroughly studied lignin depolymerization methods. Lignin model compounds have been used to uncover the underlying mechanisms of lignin “acidolysis.”⁵¹ Acid catalyzed decomposition of model compounds yielded an assortment of carbonyl products that are formed from carbocation intermediates. Both the carbonyl compounds and their

intermediates are reactive and readily participate in condensation reactions. This repolymerization process is visibly obvious upon treating a lignocellulose sample with strong acid to obtain Klason lignin as a brown precipitate.

The use of a base catalyst for lignin depolymerization has been applied in various solvent or solvent mixtures and has been found to suppress char formation and enhance production of liquid products. Despite its supposed success, there have been few studies on β -O-4 cleavage mechanisms under basic conditions. Therefore, there is little knowledge regarding the mechanism whereby base auspiciously alters product yields.

1.3.3 Oxidative methods

Lignin may be depolymerized via catalytic oxidative methods. These methods often feature a metal catalyst and an oxidizing agent, typically a peroxide. Oxidative methods cleave C-H or C-C bonds adjacent to C-O-C linkages producing vanillin and its analogues as primary products. Depending on the reaction conditions applied, further oxidation may occur, resulting ring opening and the production of carboxylic acids. Although high yields are realized for non-phenolic model compounds,⁵² these methods typically give low monophenol yields (<15%) when applied to phenolic models or lignin substrates.⁵³⁻⁵⁴ The formation of quinone structures and other carbonyl species results in subsequent condensation processes that greatly reduce the yield of monophenolics. The notable point of these methods is that the ether bond is not directly targeted; rather, benzylic carbons serve as the primary reaction site and result in ether bond cleavage as a secondary process. This makes oxidative methods particularly suited to the depolymerization of low ether bond content lignins such as Kraft lignin and Sulfite lignin.

1.3.4 Reductive methods

The near quantitative cleavage of the β -O-4 in model compounds has been achieved in the presence of a reducing agent and metal catalyst.^{37,39} It is likely that these catalysts reduce the reactive intermediates that are produced by β -O-4 cleavage, thus preventing the condensation reactions that lead to repolymerization. Although monomer yields are high, these methods are usually the most costly. A sacrificial reducing agent, such as hydrogen gas, formic acid, or hydrosilanes,³⁸ is needed along with a costly metal catalyst, rendering these methods financially unviable without means to recycle the reducing agent and catalyst.

1.3.5 Challenges and research objectives

Lignin has the potential to become a near inexhaustible source of aromatic chemicals if it can be efficiently depolymerized. There has been intense investigation towards the pursuit of this goal over the past decade, yet fundamental questions regarding the exact degradation pathway remain. The overall objectives of this study are 1) to investigate the reaction mechanisms governing lignin depolymerization and downstream pathways, 2) to apply this knowledge for the development of economic catalyst systems, and 3) to investigate the catalytic depolymerization of biomass substrates.

Most recent conversion studies are conducted under neutral or basic conditions due to the well established recalcitrant behavior of lignin under acidic conditions. However, there is a lack of understanding of lignin cleavage and condensation mechanisms under these conditions, preventing advancement of this potential technology. Uncovering these underlying mechanisms is the first objective of this study and is explored in Chapter 2, in

which a lignin model compound is employed to study the mechanisms governing bond cleavage of the most abundant bond in the lignin polymer structure (β -O-4), prevalent side reactions, and downstream processes. This knowledge is imperative for the development of economically plausible catalytic systems which are necessary to prevent the condensation processes that dramatically reduce monomer yields.

The development of non-noble metal catalytic systems for β -O-4 bond cleavage is the second objective and is the focus of Chapter 3. Three nickel-based catalytic systems are explored under a wide variety of conditions in order to maximize monomer yield, identify reduction pathways, identify the role of each catalyst component, and establish the effects of reaction parameters such as choice of solvent, addition of base, reaction time, and temperature. These results provide the necessary groundwork for the development of catalytic systems for lignin depolymerization from actual biomass substrates, which is the final objective and is explored in Chapter 4. Conclusions and a novel potential use for the monophenolic products obtained from lignin depolymerization are presented in Chapter 5.

CHAPTER 2: DETERMINATION OF THE HYDROTHERMAL DEGRADATION MECHANISM OF A LIGNIN DIMER UNDER NEUTRAL AND BASIC CONDITIONS

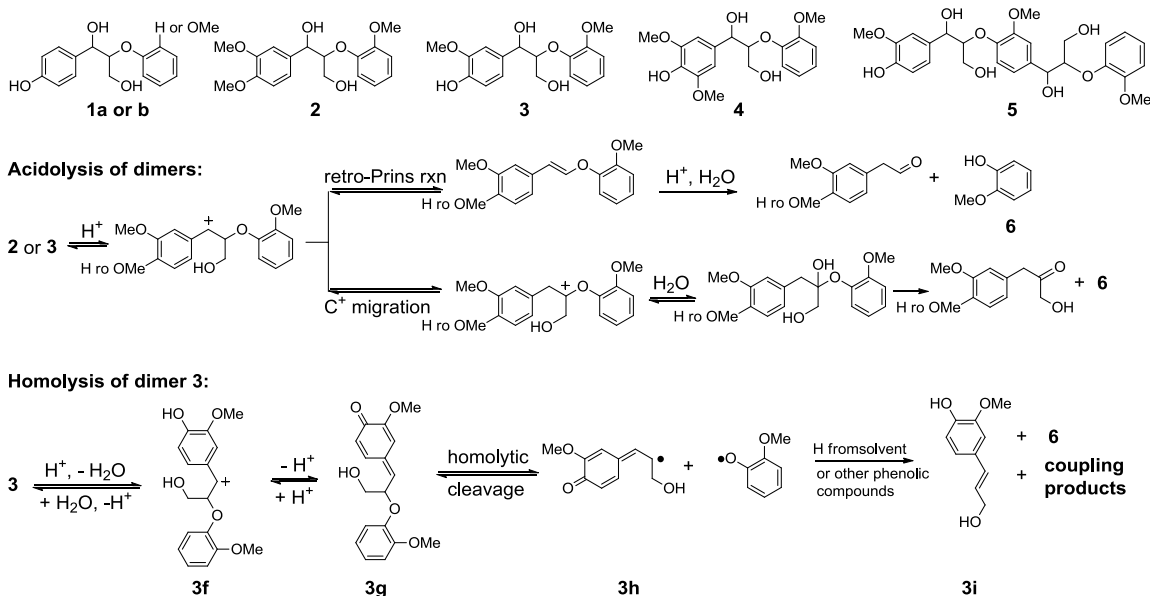
2.1 Introduction

Lignin is a natural phenolic polymer (600-15,000 kDa) which accounts for 20-35 wt% in woody biomass (40-50 wt% in bark) and 10-20 wt% in agricultural stems.⁵⁵ It has long been recognized as the major renewable source of aromatic chemicals such as phenols and aromatic hydrocarbons. In lignin, phenolic units are connected by more than eight different linkages, among them arylglycerol β -aryl ether (β -O-4) is the dominant linkage in both softwood and hardwood in most plants,⁵⁶⁻⁵⁷ consisting of approximately 50% of spruce linkages and 60% of birch and eucalyptus linkage,⁵⁸ and is the easiest to cleave. Understanding the β -O-4 bond cleavage and condensation chemistries is essential to the development of efficient catalytic systems and reaction conditions for efficient conversion of lignin to monomeric products.

Computational studies have been conducted by Beste et al. on the energies of bonds in the β -O-4 linkage,⁵⁹⁻⁶⁰ and the kinetics of their homolytic cleavage has been modeled by Faravelli et al. (for pyrolysis).⁶¹ Cleavage of the linkage has been intensively studied experimentally using model compounds such as 1³², 2,³²⁻³⁷ 3,³⁸⁻⁴⁰ 4,⁴¹ and 5⁴² (Fig. 1). Near quantitative cleavage has been achieved under very mild conditions (100 °C or lower) in transitional metal catalytic systems (homogeneous non-redox^{32-34,36,42}/oxidative,³⁵ and heterogeneous reductive^{37,39}), and under reductive conditions of hydrosilanes and Lewis acid ($B(C_6F_5)_3$).³⁸ However, most reaction systems involve noble or expensive metal catalysts,^{32-33,37,39} homogenous catalysts (hard to recycle),³⁵ expensive

organic ligands,^{32,36} expensive reagents,³⁸ and solvents³²⁻³³ other than water, methanol and ethanol. Development of inexpensive catalytic reaction systems for efficient β -O-4 cleavage and lignin decomposition into monomeric phenolics is still a daunting task and would benefit from better understanding of the cleavage mechanisms under various conditions particularly in aqueous or alcoholic reaction media and in presence of inexpensive catalysts such as inorganic base/acid.

β -O-4 cleavage is known to happen in aqueous or organic-water solution under acidic and basic conditions. Acid is typically used in various organosolv processes⁶²⁻⁶⁷ to help remove lignin from biomass by cleaving a fraction of the predominant aryl-ether linkages in lignin.⁶⁵⁻⁶⁷ Cleavage of aryl-ether lignin bonds has been observed after a few minutes in acidic pretreatment of biomass at temperatures around 170 °C.⁶⁵⁻⁷⁰ The mechanism of β -O-4 cleavage in model compounds under acidic conditions have been intensively studied by Lundquist et al.,⁷¹⁻⁷⁵ Yasuda et al.,⁷⁶⁻⁸² and Matsumoto et al. on two non-phenolic β -O-4 dimers using a range of acids including HBr, HCl, and H₂SO₄ in water-dioxane mixtures,⁸³⁻⁸⁷ and recently reviewed by Santos et al.²⁸ and Yokoyama.⁸⁸ As shown for the dimer **2** (Scheme 1- acidolysis),²⁸ acidolysis of β -O-4 dimers starts with the formation of α -carbon cation, followed by two paths: 1) loss of the γ -carbinol group as formaldehyde via cleavage of the β , γ carbon-carbon bond (a retro-Prins reaction⁸⁹) to form a vinyl ether (**2a**), which hydrolyzes to a β -aldehyde (**2b**) and guaiacol (**6**). 2) migration of cation from α -carbon to β -carbon, reaction of the β -carbon with water, followed by cleavage of the β -O-4 bond to form the Hibbert's ketone (**2e**) and guaiacol. The two pathways were also observed as main routes for β -O-4 cleavage of dimer **3** (Scheme 1).⁵¹



Scheme 1. Structures of some β -O-4 model compounds studied in the literature (top), and acidolysis (middle) and homolysis (bottom) mechanisms.

Under mild acidic conditions (e.g., 0.2 M HOAc aq. solution with 9% dioxane)^{34,90-91} or certain neutral conditions (1:1 dioxane:H₂O),³⁰ homolytic cleavage of phenolic β -O-4 bonds (Scheme 1– Homolysis of dimer **3**) is an important reaction in addition to the acidolysis paths shown above.³⁰ This reaction takes place via a homolysis of an intermediate quinone methide and gives coniferyl alcohol **3i** (for dimer **3**) as a characteristic product. **3i** was also formed as a major product (next to guaiacol) from treatment of **3** in supercritical MeOH.⁹²⁻⁹³ However, in neutral water both acidolysis and homolysis products were not detected for **3** and its two syringyl analogs.³⁴

Despite the usefulness of dilute inorganic acids in biomass pretreatment to remove lignin, acidic conditions are only rarely used for hydrothermal decomposition or solvolysis of lignin for biochemicals and fuel.⁹⁴⁻⁹⁵ This is because that repolymerization or condensation of lignin and decomposition products is well-known.^{51,96} and is a very serious problem in lignin hydrothermal treatments which typically require higher

temperatures and longer reactions time than used in delignification of biomass.⁶² Lignin depolymerization has been intensively studied under various basic conditions in various solvent or solvent mixtures including water⁹⁷⁻¹¹³ and water-alcohol mixture,¹¹⁴⁻¹¹⁶ as base has been found to suppress char formation and enhance production of liquid products.^{98,101} It has been observed that the optimal yield of low molecular weight lignin oils were obtained for low concentration of bases such 0.5% NaOH,⁹⁷ and 1.0M K₂CO₃.¹⁰³ Surprisingly, there are very few studies on β -O-4 cleavage mechanisms using model compounds under basic conditions.^{28,117}

Vanillin has been identified as a significant product in many hydrothermal treatments of lignin or lignocellulosic biomass under basic,^{97,99,104-107,109-110} neutral,^{98,102} and acidic conditions (pure HCOOH)¹¹⁸⁻¹¹⁹. However, this product is missing in the established mechanisms described above. No reaction path has been identified for its formation. In this work, the reactions of a lignin dimer, guaiacylglycerol- β -guaiacyl ether (**3**) under neutral and basic conditions are studied. The products of reactions under various conditions were carefully analyzed to construct β -O-4 cleavage pathways that have not been identified.

2.2 Experimental

2.2.1 Materials

2-methoxy 4-propylphenol, chloroform-d, sodium carbonate, and sodium bicarbonate were purchased from Sigma-Aldrich. Vanillin, 2-isopropylphenol, *tert*-butyldimethylsilyl chloride, and N,O-bis(trimethylsilyl)trifluoroacetamide were purchased from Acros Organics. Sodium hydroxide and HPLC grade acetonitrile were purchased from Fisher Scientific. Reagent grade dichloromethane and ethanol were purchased from Pharmco-

Aaper. All chemicals were used as received without further purification. The lignin model compound guaiacylglycerol-beta-guaiacyl ether was synthesized using a literature procedure.¹²⁰ Solvents used for dimer decomposition reactions were deoxygenated by percolating with N₂ gas for two hours.

2.2.1.1 Guaiacylglycerol synthesis

2.2.1.1.1. TBDMS protected coniferyl alcohol

Coniferyl alcohol (250 mg, 1.39 mmol), TBDMS chloride (460 mg, 3.05 mmol), and imidazole (236 mg, 3.47 mmol) were dissolved in anhydrous chloroform (10ml) and stirred for 48hr at room temperature under a nitrogen atmosphere. The solution was diluted with 20 mL hexane, filtered, and washed with water 7 times. 84% yield. Pale yellow oil. ¹H NMR chemical shifts: 0.103 (s, 6H), 0.120 (s, 6H), 0.923 (s, 9H), 0.950 (s, 9H), 3.825 (s, 3H), 4.336 (dd, J = 5.3, 1.5 Hz, 2H), 6.155 (dt, J = 15.6, 5.4 Hz, 1H), 6.510 (d, J = 15.6 Hz, 1H), 6.790 (d, J = 7.9 Hz, 1H), 6.842 (dd, J = 7.9, 1.9 Hz, 1H), 6.901 (d, J = 1.9 Hz, 1H).

2.2.1.1.2. TBDMS protected guaiacylglycerol

Potassium permanganate (241mg, 1.53 mmol) and Aliquat 336 (560 mg, 1.53 mmol) were combined in 20 mL of acetone and stirred for 2 hours at room temperature. The TBDMS-protected coniferyl alcohol was dissolved in 10 mL of acetone and cooled to 0°C. The KMnO₄/Aliquat 336 solution was then added over the course of 5 minutes then stirred for 10 hours at 0°C. Excess oxidant was then neutralized with sodium bisulfite, the mixture filtered, and acetone solvent removed under reduced pressure. The crude product was then extracted by DCM three times and dried over MgSO₄. DCM was removed under reduced pressure to give a pale yellow oil. The crude product was dissolved in

ethanol and 250 mg of 5% Pt/C was added under a nitrogen atmosphere. The flask was sealed then vacuumed and purged with hydrogen gas. This was repeated 3 times. The flask was then subjected to a constant 1 atm hydrogen atmosphere and stirred for 24 hours at room temperature. The mixture was filtered and the ethanol removed under reduced pressure. The crude product was dissolved in DCM, dried with MgSO₄, and filtered. DCM was removed under reduced pressure. The crude product, imidazole (236 mg, 3.47 mmol), and TBDMS chloride (460 mg, 3.05 mmol) were then dissolved in anhydrous chloroform under a nitrogen atmosphere and stirred at room temperature for 48 hours. The solution was diluted with 20 mL hexane, filtered, and washed with water 7 times. The product mixture was separated on a column with pure hexane and was obtained as a clear viscous oil (26% yield). ¹H NMR chemical shifts (in CHCl₃): -0.233 (s, 3H), -0.141 (s, 3H), -0.053 (s, 3H), 0.020 (s, 6H), 0.038 (s, 3H), 0.128 (s, 3H), 0.133 (s, 3H), 0.860 (s, 9H), 0.890 (s, 9H), 0.903 (s, 9H), 0.989 (s, 9H), 3.202 (dd, J = 10, 5.9, 1H), 3.623 (td, J = 5.7x2, 3, 1H), 3.699 (dd, J = 10, 5.5, 1H), 3.772 (s, 3H), 4.724 (d, J = 3, 1H), 6.715 (dd, J = 7.9, 1.9, 1H), 6.752 (d, J = 7.9, 1H), 6.925 (d, J = 1.9, 1H). ¹³C NMR chemical shifts (in CHCl₃): 55.27, 64.24, 74.06, 78.06, 111.30, 118.87, 120.02, 136.19, 143.60, 150.14.

2.2.2 Methods

2.2.2.1 Dimer decomposition reactions and workup

Dimer decomposition reactions were performed in a 21.9 mL stainless steel mini-reactor assembled from a Swagelok Tube Union (SS-1610-6) and two Swagelok plugs (SS-1610-P). The dimer was massed by attaching it to a stir bar which was then added into the reactor vessel. The unsealed reactor vessel was then brought inside a glovebox

equipped with a nitrogen atmosphere in which the base solution was introduced. The reactor vessel was then sealed under the nitrogen atmosphere. The reactor vessel was heated in a molten salt bath while stirring at 360 rpm. Reaction time was started when the reactor was within 5°C of the target temperature. The reactor was quickly cooled to room temperature in a water bath upon completion. The reaction mixture was filtered through filter paper and the reactor washed with water and dichloromethane to insure complete transfer of product oil. The filtrate was acidified to pH 2-3, and extracted with 15 mL of dichloromethane three times. In order to prevent the loss of any volatile products, the majority of solvent was removed on a rotovap under 350 mbar and with a low temperature water bath (50°C), and the residual solvent was removed under reduced pressure (10-20 mbar) at room temperature. Samples were spiked with 1 mg of 2-isopropylphenol as an internal standard and dissolved in about 2 mL of chloroform. Seven drops of sample were taken for GC-MS analysis and were derivatized by the addition of 7 drops of N,O-bis(trifluoromethylsilyl)acetamide. Samples were allowed to sit at room temperature for 20 minutes for derivatization to complete then diluted to about 0.5 mL with acetonitrile.

2.2.2.2 Guaiacylglycerol degradation

The TBDMS protected analogue was dissolved in 3 mL THF to which 8eq of tetrabutylammonium fluoride (50% aqueous solution) under a nitrogen atmosphere. The mixture was stirred for 16 hours at room temperature. THF was removed by vacuuming for 30 minutes at room temperature. 3 mL of 0.1M NaOH solution was added to the mixture, stirred briefly, then transferred to the reactor vessel. The reactor was sealed under a nitrogen atmosphere then placed in the preheated salt bath (175°C). The reaction

was stirred for 5 minutes after reaching 170°C then quickly quenched in a cold water bath. The same workup procedures as all other experiments were then followed.

2.2.2.3 Isolation of (Z)- and (E)-2-methoxy-4-(2-(2-methoxyphenoxy)vinyl)phenol

The dimer was degraded in accordance to the conditions described in Entry 5 in Table 4 and the work up procedures described above. The decomposition mixture (~45mg) was dissolved in 5 mL DCM along with 110 mg (0.73 mmol) TBDMSCl and 55 mg (0.80 mmol) imidazole and refluxed for 16 hours. The reaction mixture was filtered, washed with water 3 times, dried over MgSO₄, filtered, and the solvent removed under vacuum. The mixture was then separated on a column using hexane as eluent. *cis*, TBDMS-protected compound in CDCl₃ ¹H NMR chemical shifts: 7.532 (d, J=1.2Hz, 1H), 7.254 (s, 1H), 7.094 (dd, J=5.2, 1.2 Hz, 1H), 7.064 (dt, J=1.2, 5.2Hz, 1H), 7.061 (dd, J=5.6, 1.2Hz, 1H), 6.969 (dd, J=5.6, 1.2Hz, 1H), 6.934 (dt, J=1.2, 5.2Hz, 1H), 6.799 (d, J=5.2Hz, 1H), 6.527 (d, J=4.8Hz, 1H), 3.885 (s, 3H), 3.827 (s, 3H), 0.993 (s, 9H), 0.153 (s, 6H). ¹³C NMR chemical shifts: 150.56, 149.91, 146.63, 143.78, 140.69, 129.0, 123.71, 121.65, 120.90, 120.62, 116.75, 112.67, 112.56, 110.09, 55.98, 55.24, 25.75, -4.63.

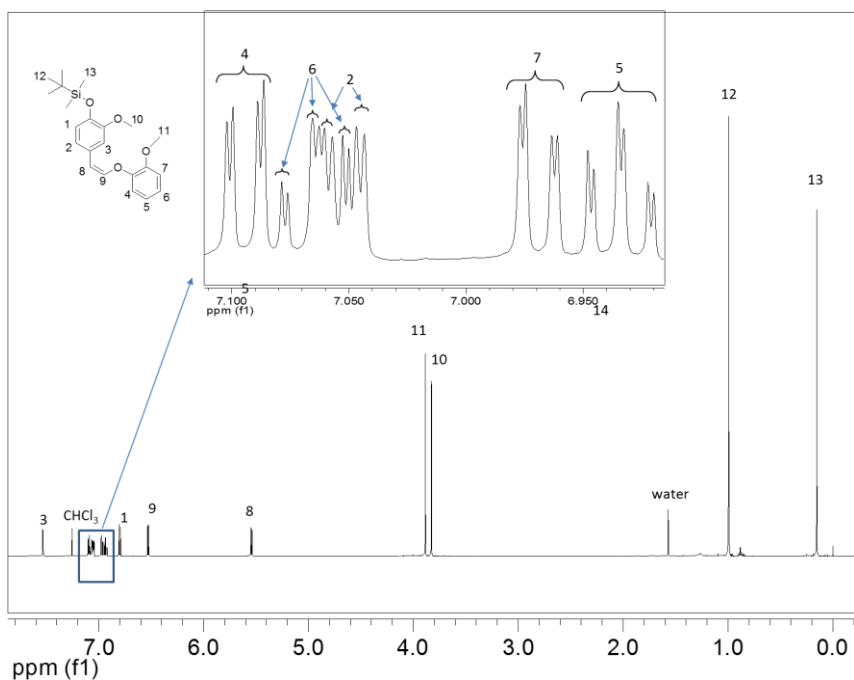


Figure 5. ^1H NMR spectrum of compound (Z)-2-methoxy-4-(2-(2-methoxyphenoxy)vinyl)phenol

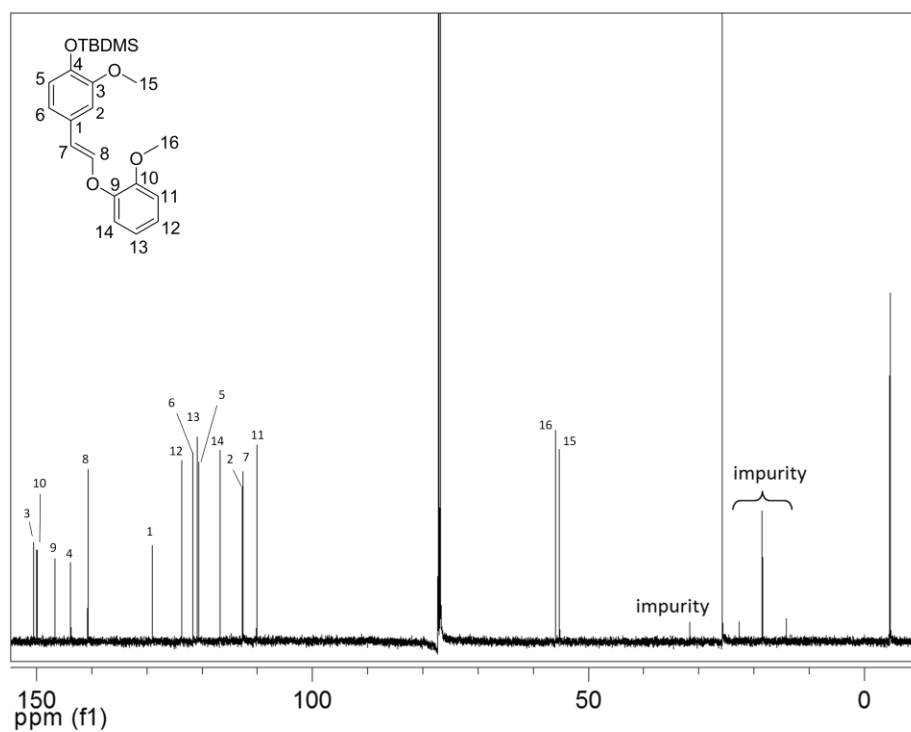


Figure 6. ^{13}C NMR spectrum of compound (Z)-2-methoxy-4-(2-(2-methoxyphenoxy)vinyl)phenol

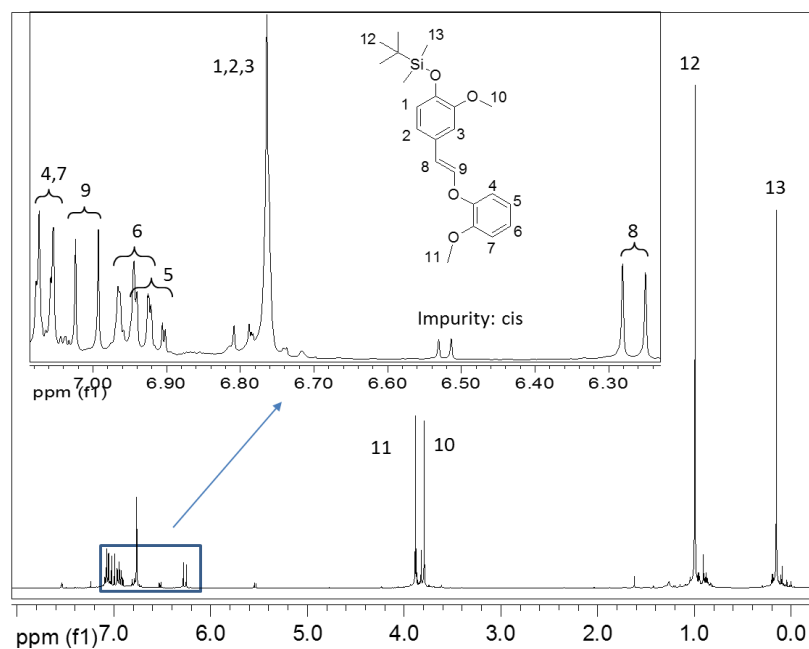


Figure 7. ^1H NMR spectrum of compound 9 (*trans*, TBDMS-protected).

2.2.2.4 Product characterization and quantification

2.2.2.4.1. Oil yield

The oil yield is simply a weight percentage of the dimer mass at the start of a reaction. It is calculated by dividing the weight of the post-workup products by the starting dimer mass.

2.2.2.4.2. GC-MS

The silylated derivatives of lignin model degradation products were characterized and quantified by GC/MS using a Shimadzu GCMS-QP2010 SE, which uses EI for mass selective detection. Hydrogen was used as the carrier gas. The GC flow rate was 0.92 mL/min through a Rxi-6Sil 30 m length \times 0.25 mm ID, 0.25 μm film thickness crossbonded 1,4-bis(dimethylsiloxy)phenylene dimethyl polysiloxane column. Quantification was done using a 240°C injection temperature and initial oven temperature

of 90°C with a split ratio of 10. The oven temperature was immediately increased after injection at a rate of 25°C/min to 140°C at which point the temperature increase was slowed to 4°C/min to 149°C to insure adequate separation of guaiacol and the internal standard. Upon reaching 149°C, the temperature was increased at 25°C/min to 240°C, held for two minutes then further increased at 25°C/min to 250°C and held for 10 minutes to insure complete product elution.

Mass spectra were recorded in TIC mode (mass range 75-450 m/z) with the exception of guaiacylglycerol analysis which was performed in SIM mode using ion and fragment masses observed in dimer degradation experiments. Products were identified using the mass spectroscopy NIST database when available. Products not found in the NIST database were identified by NMR, standards and/or mass fragmentation patterns (Table 3). The mass of each product was calculated by integration of the corresponding TIC peak, comparing the area to that of the internal standard, and multiplying by the response factor and the product molecular weight. Response factors of the products relative to the internal standard (2-isopropylphenol) were obtained by calibration with commercial or synthesized standards (See Table 3) or obtained by ECN-based calculations.¹²¹

When standards were available, the response factor was established by preparing up to five solutions near the approximate concentration of products that would be produced from dimer degradation and reaction workup. As an example, standards of guaiacol and 4-propylguaiacol of 1mg, 2.2mg, 5.8mg, 16.4mg, and 34mg/~3mL ACN with 1mg 2-isopropylphenol were prepared. Each standard was derivatized with N,O-bis(trifluoromethyl silyl)acetamide and run in triplicate using the same temperature

program described above, stopping once 240°C was reached. The theoretical amount of analyte was calculated by comparing the area of the analyte peak to that of the internal standard (2-isopropylphenol). The response factor is the known amount of analyte divided by calculated amount. The response factor was found to be constant across the tested range (1.070 ± 0.032 for guaiacol and 1.089 ± 0.033 for 4-propylguaiacol). A similar process was performed for vanillin and the dimer model compound.

Due to a lack of purified material, standards of 2-methoxy-4-(2-(2-methoxyphenoxy)vinyl)phenol could not be reliably prepared. Instead 1mg of internal standard was added to the product mixture of entry 5 in Table 4. An NMR sample was taken of the product mixture and the molar ratio of the internal standard to both the (Z) and (E) isomers calculated by comparing the integration of the isopropyl quintet (~3.0 ppm) of the internal standard to the characteristic HC=CH peaks of the vinyl ether. GC-MS of the sample was performed in triplicate. The response factor was calculated by dividing the molar ratio of vinyl ether to internal standard established using NMR by the calculated molar ratio of vinyl ether to internal standard found by GC-MS.

If a standard was not available for a product observed in the GC-MS chromatogram, a response factor was assigned using an estimated carbon number (ECN) method.¹²¹ In the context of this method, silicon was considered to be synonymous with carbon. This method provided response factors comparable to those established using standards for compounds with simple functional groups (0.96 vs 1.09 for 4-propylguaiacol, 1.29 vs 1.28 for vanillin) making it useful in the scope of this study.

The product yield is reported as a carbon yield and is defined as followed:

$$\text{yield (C\%)} = \frac{m_{\text{product}} \times \text{wt\%}C_{\text{product}}}{m_{\text{dimer}} \times \text{wt\%}C_{\text{dimer}}} \times 100 \quad \text{Equation 1}$$

$$\text{wt\%}C_{\text{product}} = \#C_{\text{product}} \times \frac{MW_C}{MW_{\text{product}}} \quad \text{Equation 2}$$

$$\text{wt\%}C_{\text{dimer}} = \#C_{\text{dimer}} \times \frac{MW_C}{MW_{\text{dimer}}} \quad \text{Equation 3}$$

The wt%C of the product and dimer is simply the percent of the mass that can be attributed to carbon. Thus it is the number of carbons multiplied by the molar mass of carbon (12.011 amu) divided by the molar mass of the product or dimer. The yield (C%) is then the mass of the product multiplied by its wt% carbon over the mass of the dimer multiplied by its wt% carbon.

Table 3. Mass spectral data of trimethylsilylated dimer and decomposition products

Compound	Standard ^a	Response Factor ^b	M+ Fragments (relative intensity)							
1	Yes	1.07	196 (24)	181 (34)	167 (14)	166 (100)	151 (24)	136 (16)		
2	No	1.07	210 (33)	196 (6)	195 (20)	181 (17)	180 (100)	179 (11)	166 (7)	165 (8)
3	No	1.08	224 (40)	209 (43)	195 (16)	194 (100)	179 (62)	149 (10)		
4	No	1.08	222 (28)	207 (19)	193 (13)	192 (100)	177 (9)	162 (10)		
5	Yes	1.09	238 (49)	223 (32)	210 (18)	209 (100)	208 (66)	180 (11)	179 (60)	149 (13)
6	No	0.98	236 (30)	221 (10)	209 (10)	208 (11)	207 (16)	206 (100)	205 (24)	179 (10)
7	Yes	1.28	224 (33)	210 (8)	209 (53)	195 (16)	194 (100)	193 (43)		
8	No	0.98	236 (48)	221 (13)	209 (5)	208 (5)	207 (18)	206 (100)	205 (25)	
9	No	1.10	238 (54)	224 (30)	223 (83)	209 (20)	208 (64)	194 (35)	193 (100)	
10	No	0.93	252 (14)	211 (5)	210 (15)	209 (100)	193 (5)	179 (23)	149 (8)	
11	No	0.97	252 (21)	224 (19)	223 (100)	209 (20)	207 (11)	193 (21)		
12	No	1.20	312 (48)	298 (25)	297 (100)	282 (27)	267 (67)	253 (56)	223 (55)	193 (22)
13	Yes	0.76	326 (32)	311 (12)	236 (28)	221 (17)	210 (13)	209 (16)	207 (20)	206 (100)
14	Yes	-	299 (8)	298 (21)	297 (100)	223 (8)	194 (6)			
15	No	0.47	346 (12)	225 (5)	224 (19)	223 (100)	209 (7)	207 (7)	193 (19)	192 (22)
16	Yes	0.48	344 (100)	315 (16)	314 (23)	285 (28)	284 (18)	211 (37)	209 (21)	179 (22)
17	Yes	0.63	299 (10)	298 (27)	297 (100)	223 (3)	209 (4)	181 (5)	166 (5)	

^aCommercial or synthesized compound was used as the standard to determine the GC-MS response factor. ^bResponse multiplier compared to a molar equivalent of trimethylsilylated 2-isopropylphenol.

2.2.2.4.3. GPC

Samples were investigated by gel permeation chromatograph using an Agilent 1100 series HPLC system with ChemStation B.04.03 and GPC Data Analysis B.01.02, equipped with two serial GPC columns (PL1110-6500: PLGel 5 μ m MIXED-C 7.5 x 300

mm). Guaiacol, 2-methoxy-4-propylphenol, (*E*)-2-methoxy-4-(2-(2-methoxyphenoxy)vinyl)phenol, and guaiacylglycerol- β -guaiacyl ether, 5K PS, and 9k PS were used as standards to generate a calibration curve in order to approximate the molecular weight and abundance of oligomeric and polymeric reaction components. Freshly distilled tetrahydrofuran was used as the solvent. The flow rate was 1 mL/min and elution was monitored using a UV-Vis detector at 290nm.

2.2.2.4.4. NMR

NMR spectra were recorded on a Bruker Avance 600 MHz nuclear magnetic resonance spectrometer using chloroform-*d* at 20°C-25°C. The ^1H experiments (Bruker pulse sequence “zg30”; proton) had the following parameters: spectral width of 20 ppm, acquisition time (AQ) of 2.65 s, 16 or 128 scans with a 1.0 s interscan delay (D1). ^{13}C experiments (Bruker pulse sequence “zgpg30”; proton decoupled ^{13}C) had the following parameters: spectral width of 240 ppm using 32768 data points for an AQ of 0.91 s, 1024 scans with a 1.0 s interscan delay (D1).

2.2.2.4.5. DFT modeling and calculations

2.2.2.4.5.i. Minimized rotamer models

Models were drawn in Chem3D in the approximate position for each rotamer then imported into Gauss View 5.0. Each model was minimized and the thermochemistry calculated (opt freq) using DFT B3LYP with the 6-311G+(d,p) basis set and PCM model (default in Gaussian) of a water solvent. Tight convergence criteria and an ultrafine integration grid were imposed to ensure accuracy. The ΔG (electronic + thermal free energy) values for each rotamer were used in further calculations and can be found in

Table 5. Rotamer 1 was used as an arbitrary basis of comparison for the other rotamers. The relative differences in energy were used to calculate the Boltzmann distribution of the rotamers for each diastereomeric pair according to Equation 4.

$$p_i = \frac{e^{-\varepsilon_i/kT}}{\sum_{j=1}^M e^{-\varepsilon_j/kT}} \quad \text{Equation 4}$$

2.2.2.4.5.ii. Transition state models

The minimized model of Rotamer 9 (S,R) was used as the basis for the γ -elimination and hydrolysis transition states while Rotamer 4 (S,R) was used as the basis for the α -elimination transition state. A free hydroxyl (OH⁻) was added to the model and set at about 6 Å from the idealized reaction site, the hydrogen on the alpha or gamma carbon in the case of elimination or beta carbon in the case of substitution. Using the opt=modredundant function, the hydroxyl group was moved stepwise by 0.2 Å towards the reaction site with the energy being taken at each step. This calculation was performed using DFT B3LYP with the 6-31G(d) basis set. The saddle point was selected and the transition state optimized using DFT B3LYP with the 6-311G+(d,p) basis set with the PCM model (default in Gaussian) of a water solvent. Tight convergence criteria, an ultrafine integration grid and the calculation of force constants at every iteration were used to insure accuracy. After optimization, a freq calculation was performed in order to compare ΔG values. The activation energy was calculated as the transition state energy minus the sum of the separate minimized energy of the dimer and hydroxide anion. The relative reaction rates were calculated according the Arrhenius equation (Equation 5). The term A represents the frequency of collisions in the correct orientation for the

reaction to occur. Therefore the ratio A_1/A_2 is the ratio of rotamers in the necessary orientation for a reaction to occur.

$$\frac{k_1}{k_2} = \frac{A_1}{A_2} e^{\frac{E_{a2} - E_{a1}}{kT}} \quad \text{Equation 5}$$

2.3 Results and Discussion

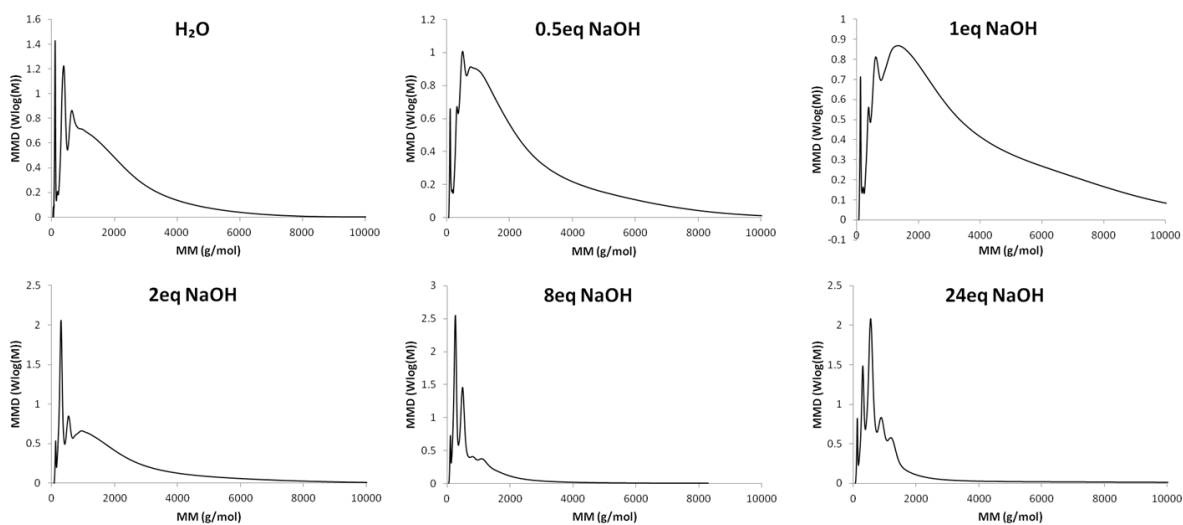
2.3.1 Reactions and Data

Table 4 summarizes the results of a series of reactions of β -O-4 model dimer **3** in water under neutral (Entry 1) and basic (Entries 2-10) conditions. Entries 2-6 investigate the effect of the increasing amount of NaOH from 0.5 to 24 eq of the dimer. At 24 equivalent, the concentration is 5 wt% NaOH, a concentration commonly used in lignin decomposition studies.^{110,107,88} Entries 7-9 investigate the use of carbonate bases at various concentrations. Entry 10 investigates the effect of the less basic bicarbonate species. Entry 11 investigates the effect of a lower polarity solvent (EtOH). GPC results of entries 1-7 (neutral and hydroxide bases) are shown in Figure 8, and those of entries 8-11 (carbonate bases) are shown in Figure 9.

Table 4. Major decomposition products of dimer 3 under neutral and conditions.

Entry	Base	Product Yields (C%)							Total Identified	Oil (wt%)
		6	7	8	9	3i	10	3		
1	H ₂ O	20.83	0.17	-	-	0.07	-	13.12	34.20	67
2	0.5eq NaOH	15.30	0.04	0.05	-	-	21.67	0.78	37.84	92
3	1eq NaOH	13.53	0.02	0.03	Trace	-	18.50	0.41	32.49	67
4	2eq NaOH	23.07	0.04	0.02	Trace	-	39.53	0.04	62.70	90
5	8eq NaOH	13.98	0.06	0.03	0.01	-	58.75	0.08	72.90	87
6	24eq NaOH	14.99	0.10	0.07	0.02	-	45.39	0.83	61.21	73
7	0.5eq Na ₂ CO ₃	11.10	0.11	0.24	-	0.03	8.58	1.20	21.26	90
8	1eq Na ₂ CO ₃	10.97	0.10	0.14	Trace	-	11.08	0.46	22.75	87
9	2eq Na ₂ CO ₃	7.47	0.06	0.14	Trace	-	11.50	0.18	19.35	96
10	2eq NaHCO ₃	6.61	0.09	0.15	Trace	-	11.10	0.33	18.28	89
11	Ethanol*	2.7	-	-	-	0.2	-	82.0	84.9	89

50mg of dimer **3**, 3 mL of solvent (water, except in entry 11), N₂ atmosphere, and 175 °C for 15 min except entry 11 which was run for 1h.

**Figure 8.** Mass distribution of products in DCM oil obtained from hydrothermal decomposition using hydroxide bases.

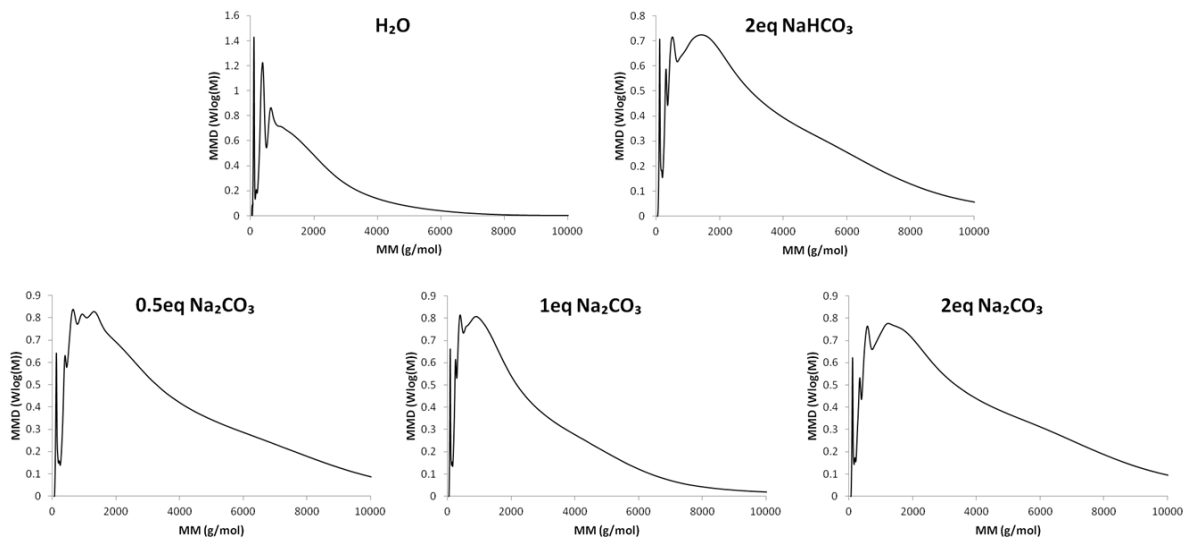


Figure 9. Mass distribution of products in DCM oil obtained from hydrothermal decomposition using carbonate bases.

2.3.2 β -O-4 bond cleavage mechanisms under neutral and basic conditions

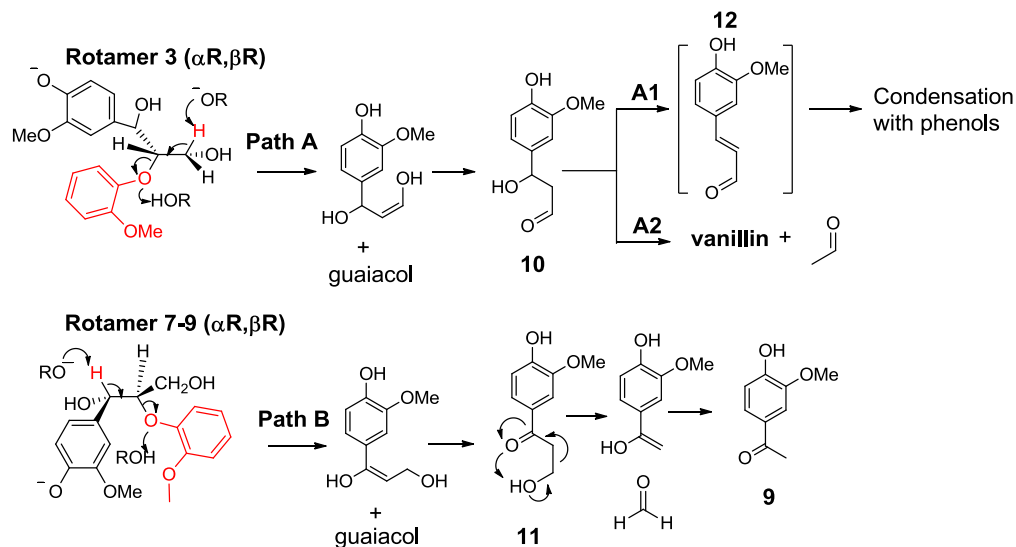
From entry 1 to 4, the amount of NaOH was increased from zero to 2 molar eq. of the dimer. The GC eluable fraction of each entry contained similar products, including guaiacol as the major product and vanillin, vanillyl alcohol, and acetovanillone as trace products. No decomposition products containing the 3-carbon chain were detected. Mechanisms are proposed in Scheme 2 to account for the formation of formation of guaiacol, vanillin, acetovanillone (**9**).

The first steps of the mechanisms shown are bimolecular elimination reactions (E2). An E2 reaction requires an anti conformation of an H on one carbon and a leaving group (in this case, guaiacyl) on a neighbouring carbon. Dimer **3** has two stereocenters, C_α and C_β , and thus 4 stereoisomers. Each stereoisomer has 9 rotamers with 3 for rotation around each of the two C-C bonds in the side chain. Scheme 3 shows Newman projections of all rotamers for a pair of diastereomers along with the relative probability for each rotamer. Rotamers that can undergo elimination across the β - γ bond (rotamers $_{\beta-\gamma}$) are highlighted

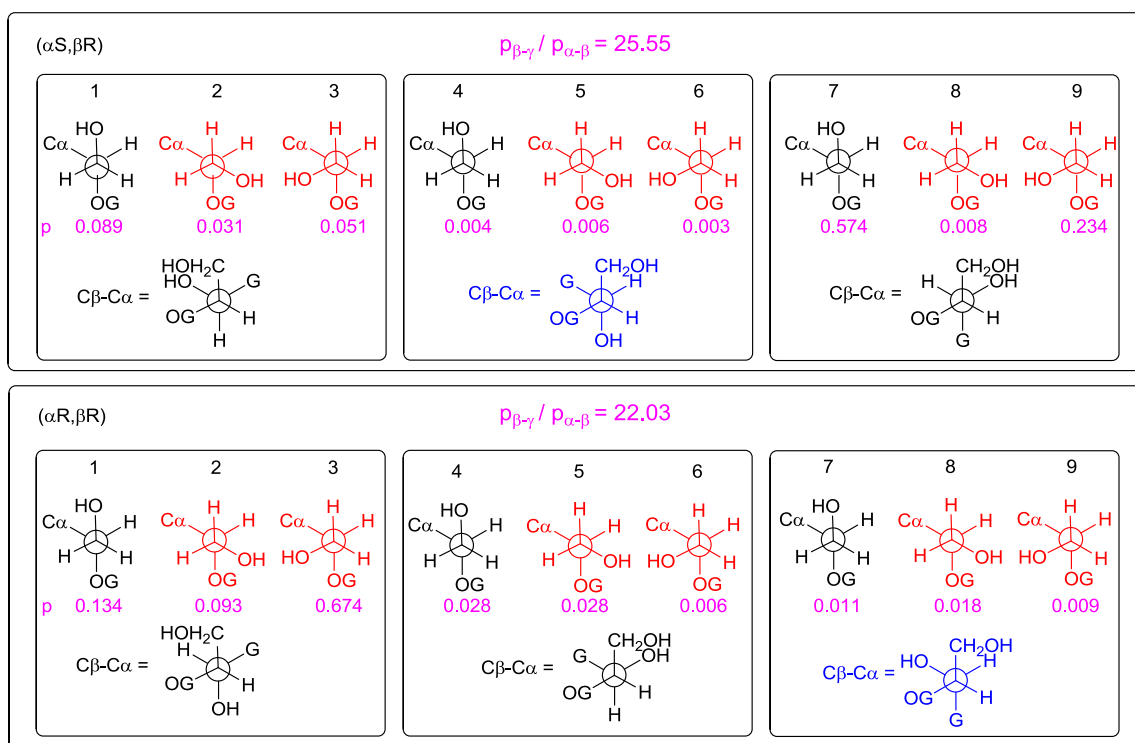
in red. Rotamers that can undergo elimination across the α - β bond (rotamers $_{\alpha-\beta}$) have the Newman projection of the C $_{\alpha}$ -C $_{\beta}$ bond highlighted in blue. The mechanisms in Scheme 2 are shown for rotamers 3 and 7-9. The dimer undergoes an elimination reaction at the β,γ -carbons (path **A**) to give an enol product which can tautomerize into an aldehyde product (**11**). Elimination reactions may also happen on the α - and β -carbons (path **B**) to form an α -ketone **12** which undergoes a retro-aldol reaction to give **9** and formaldehyde. The much higher abundance of vanillin (**7**) than **9** across all entries suggests that path **A** is much more competitive than path **B**.

The relative reaction rates of path A and path B are affected mainly by the relative stability of the anti conformer among all rotamers of each stereoisomer and difference in activation energy of the E2 reactions in the two paths. The total probability for rotamers $_{\beta-\gamma}$ is expected to be much greater than for rotamers $_{\alpha-\beta}$ for both modeled stereoisomers. This can be rationalized by the fact that rotamers $_{\alpha-\beta}$ necessitate that the two phenyl rings be in the gauche position, creating steric strain. Additionally, there are twice as many rotamers $_{\beta-\gamma}$ as rotamers $_{\alpha-\beta}$.

To quantify the effect of steric hindrance, the relative energies of the conformers were calculated by DFT using B3LYP/6-311+G** with a water solvent PCM. Since enantiomers will have the same energy in any given conformation as they are simply mirror images so only (R,R) and (R,S) isomers are calculated. The probabilities of each enantiomeric pair for each rotamer were calculated at reaction temperature using the Boltzmann distribution and are shown in Scheme 3 and Table 5. The high probability of rotamers $_{\beta-\gamma}$ vs rotamers $_{\alpha-\beta}$ supports the empirical evidence in Table 4.



Scheme 2. β -O-4 bond cleavage mechanism and downstream reactions under neutral and basic conditions.



Scheme 3. Newman projections and relative probabilities of all rotamers for $\alpha S, \beta R$ and $\alpha R, \beta R$ stereoisomers. Rotamers that can undergo elimination across the β - γ bond are highlighted in red. Rotamers that can undergo elimination across the α - β bond have the Newman projection of the C_α - C_β bond highlighted in blue.

Table 5. The calculated energies and relative probabilities of rotamers 1-9 for each diastereomeric pair

Rotamer (S,R/R,S)	Energy (kJ/mol)	ΔE (kJ/mol)	p
Rotamer 1	-2916192.333	0.000	0.089
Rotamer 2	-2916188.474	3.859	0.031
Rotamer 3	-2916190.267	2.066	0.051
Rotamer 4	-2916180.755	11.578	0.004
Rotamer 5	-2916182.364	9.969	0.006
Rotamer 6	-2916179.694	12.639	0.003
Rotamer 7	-2916199.296	-6.963	0.574
Rotamer 8	-2916183.176	9.158	0.008
Rotamer 9	-2916195.957	-3.623	0.234

Rotamer (R,R/S,S)	Energy (kJ/mol)	ΔE (kJ/mol)	p
Rotamer 1	-2916195.797	0.000	0.134
Rotamer 2	-2916194.434	1.363	0.093
Rotamer 3	-2916201.825	-6.028	0.674
Rotamer 4	-2916189.952	5.844	0.028
Rotamer 5	-2916189.942	5.855	0.028
Rotamer 6	-2916184.415	11.382	0.006
Rotamer 7	-2916186.465	9.331	0.011
Rotamer 8	-2916188.348	7.449	0.018
Rotamer 9	-2916185.541	10.255	0.009

As far as we know, the mechanisms in Scheme 2 are new for β -O-4 cleavage under neutral and basic conditions, and path **A** is the first mechanism that accounts for vanillin formation in hydrothermal reactions of lignin or lignin model compounds. Under the neutral solution (Entry 1), a strong base is not available, elimination reactions of rotamers 1 and 2 involve the cooperation of a Lewis base (e.g., solvent) and a Lewis acid (e.g., a phenolic proton) as illustrated in the first step of the path A. Since no acidolysis and few homolysis (see 3.3.3.4 for discussion) products were detected, the newly proposed path **A** and path **B** are likely the primary source for guaiacol.

Another possibility is that β -O-4 cleavage occurs via hydrolysis to yield guaiacylglycerol as shown in Scheme 4. Guaiacylglycerol can then undergo dehydration to form hydroxyketone products, including **11** and **12**, which quickly decompose. However, neither guaiacylglycerol nor any of the hydroxyketone dehydration products were observed in any experiment. Additionally, when a sample of guaiacylglycerol was subjected to the same conditions as entry 4, a unique product profile containing an abundance of vanillic acid was observed (Figure 10). Finally, the transition state energies, activation energies, and relative rate constants for both elimination mechanisms and the hydrolysis mechanism were calculated for the (R,S)/(S,R) diastereomeric pair under basic conditions (Table 6). It was found that among the 3 pathways, the rate constant of hydrolysis vs alpha and gamma elimination is 0.005 and 0.012, respectively. Therefore, it is unlikely that hydrolysis poses a significant pathway under basic conditions. Interestingly, the relative rate of gamma elimination to alpha elimination was estimated to be only 2.34. This is due to the difference in activation energy of the E2 reactions in the two paths which is mainly caused by the relative acidity of H atoms on C $_{\alpha}$ and C $_{\gamma}$. According to the

results shown in Table 4, the relative reaction rate is expected to be closer to 5-7. This difference can likely be attributed to differences in the calculated activation energy vs the activation energy of the actual system. The calculated activation energy is for that of an isolated dimer molecule in the gas phase with solvent modeled as a continuous polarization field. In reality, there are likely considerable solvent interactions that may work to negate the theoretical differences in activation energy.

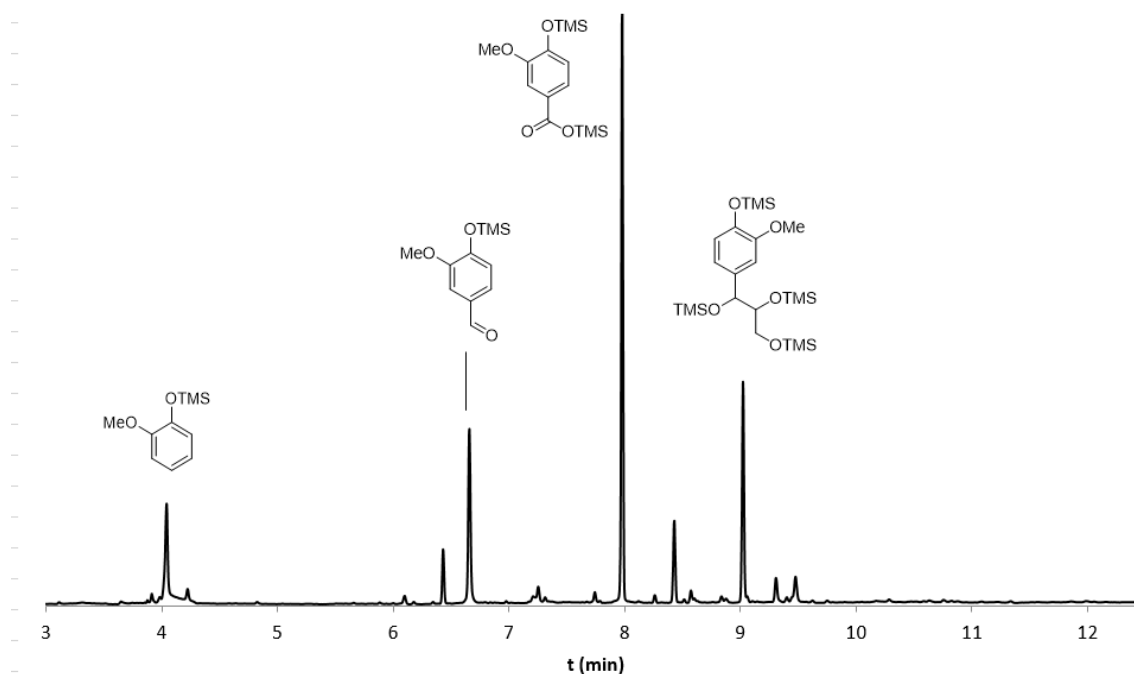
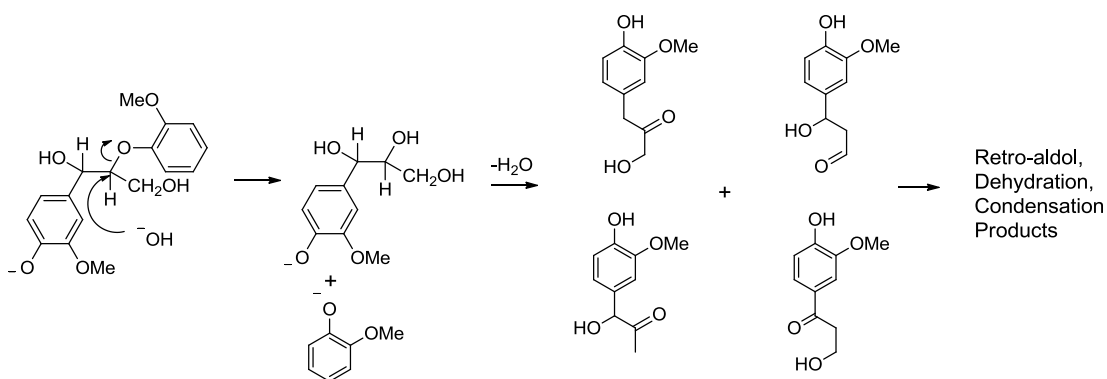


Figure 10. GC-MS chromatogram of guaiacylglycerol degradation in 0.1M NaOH. 8 eq of tetrabutylammonium fluoride was also present prior to the reaction as the hydroxy groups of guaiacylglycerol were protected by TBDMS.

Table 6. The calculated activation energies and relative reaction rate constants of the elimination and hydrolysis transition states under basic conditions

Transition State	E_a (kJ/mol)	k/k_g	k/k_a	k/k_s
γ -elimination	101.307	1.000	2.340	190.714
α -elimination	92.667	0.427	1.000	84.519
Intermolecular S_N2	122.900	0.005	0.012	1.000



Scheme 4. β -O-4 hydrolysis (intermolecular substitution) mechanism under basic conditions and fate of guaiacylglycerol

Condensation is always a competing process and involves phenolics and carbonyl species. The fact that the yield of guaiacol is much lower than its theoretical yield of 41.2 C% suggests that condensation is the most prevalent competing process in Entries 1-11 of Table 4. It is of interest to find whether any amount of the dimer survive the 15-minute reactions. GC-MS analysis revealed <2 C% of the dimer in the products under basic conditions, meaning the dimer was largely consumed by condensation. Neutral water results in a significant portion of the dimer (>10 C%) surviving the reaction. This could be attributed to elimination being slowed by the low hydroxide concentration, hydrolysis becoming a more prominent mechanism, decreased solubility in neutral water, or a combination of these factors.

The oil yield of Entry 1 is among the lowest of all entries while the molecular weight is smaller than other entries except the most basic ones (Entries 5 & 6), which is unusual, as low MW products are more extractable by DCM and thus should have higher yield. This inconsistency was likely caused by the poor solubility of the dimer in neutral water. The undissolved dimer condensed much faster than the dimer molecules in solution and form DCM-insoluble biochar, which is not reflected in the GPC curve.

When NaOH was used, the dimer could be deprotonated and dissolved in water quickly. At high NaOH concentrations (entries 5 and 6), condensation reactions were further suppressed as evident by the much-reduced polymer formation (Figure 8). However, the guaiacol yield did not increase, implying that additional decomposition paths emerged and competed with β -O-4 cleavage. Indeed, a vinyl ether, 1-(4-hydroxy-3-methoxybenzene)-2-(2-methoxyphenoxy) ethene (**10**), appears when even a small amount of base is added as evident by Entries 2 and 7. The yield of **10** increased dramatically as the amount of NaOH was increased from 2 eq to 24 eq. Further discussion on **10** is conducted in 3.1.4.

2.3.3 The fate of the major β -O-4 cleavage product **11**

Guaiacol is produced from β -O-4 bond cleavage, and is a major product under all conditions in Table 4. Therefore, the other major β -O-4 cleavage product **11** should also be produced in similar quantity. Since **11** was never detected, it must quickly be converted into other products. Three paths are proposed for its conversion as shown in Scheme 2: **A1** - condensation with phenolic species (discussed further in 3.1.5), **A2** - a retro-aldol reaction to vanillin and acetaldehyde, and **A3** - dehydration to the conjugated aldehyde **12**. Although **13** could not be observed by GC-MS, it is well established that

dehydration of aldol products to produce conjugated aldehydes or ketones proceeds readily.

In path **A2**, the intramolecular H-bonding between –OH and the carbonyl oxygen facilitated the reaction by providing a convenient path to vinyl alcohol (the precursor of acetaldehyde). However, when the solution was made basic, the retro-aldol process was disfavored due to dehydration to the conjugated aldehyde **13**. Increasing the base concentration results in higher vanillin yields indicating that deprotonation of the α -OH may prevent dehydration and thus favor the retro aldol process. In the deprotonated molecule, the proton is replaced by Na^+ , which is solvated and has weaker interaction with the carbonyl oxygen and thus reduces the driving force for the retro-aldol reaction compared to the intramolecular mechanism. The vanillin yields were always much lower than the guaiacol yields by two to three orders of magnitude. Since no significant amount of downstream small molecule products of vanillin were found, the low vanillin yields could be attributed to two reasons: 1) path **A2** was not competitive in all conditions, and 2) vanillin was mostly condensed. To determine the major reason for low vanillin yields, test reactions of guaiacol and vanillin were conducted under various conditions. Vanillin was recovered nearly quantitatively under a strongly basic and neutral conditions (Entries 2 and 4, Table 7) and was recovered in 54% yield under a weakly basic condition (Entry 3, Table 7) – a condition most favorable for condensation of aldehydes (See 2.3.5 for more discussion). So, the major reason for low vanillin yields is that path **A2** is not competitive in all conditions tested.

Table 7. Stability tests of guaiacol and vanillin.

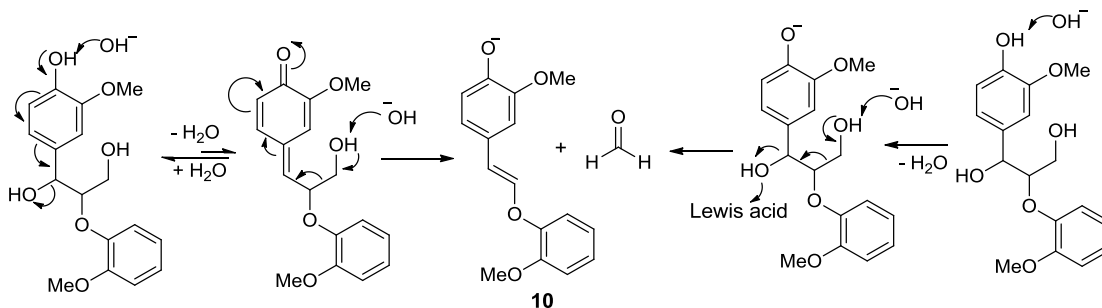
Entry	Catalyst	Solvent	%guaiacol recovered	%vanillin recovered	Wt% recovered
1	-	24 eq NaOH	N/A	>95 ^a	100
2	-	8 eq NaOH	74	94	89
3	-	0.5 eq NaOH	68	54	59
4	-	water	84	>90	89
5	Ni/C	water	82	87	? ^b
6	Ni/C - Zn	water	83	0 ^c	81
7	Ni/C	8 eq NaOH	52	92	82

Reaction conditions: 175 °C, N₂, 2h. ^aDetermined by ¹H NMR. ^bNo evidence of any reaction. Not even a color change. ^c Vanillin was reduced to 2-methoxy-4-methylphenol in 90 mol%.

2.3.4 Formation of vinyl ether **10** under strongly basic conditions

Starting from the first basic entry (Entry 2), vinyl ether **10** was produced as a mixture of *trans* and *cis* isomers. ¹H NMR spectra of the mixture and separated isomers are shown in Figure 5-Figure 7. GM-MS spectrum of Entry 4 products is shown in Figure 11 with the peaks of the two isomers labeled. The yield of **10** ranges from 18.50 to 58.75% as NaOH was increased from 2 to 24 eq. Scheme 5 shows two possible paths to the vinyl ether. The left path has been presented for the same model compound in the review article of Santos et al.²⁸ It is a two-step process in which a quinone methide is formed after deprotonation of the phenol moiety and elimination of the α -OH, followed by a retro-aldol reaction (initiated by deprotonating the γ -OH), which releases formaldehyde, restores aromaticity to the ring and forms the vinyl ether. The path on the right, which involves a coupled retro-aldol and E2 reaction, cannot be ruled out as a similar vinyl ether could be produced from dimer **2**, which has a OMe group (instead of a free OH) and

thus cannot be converted into a quinone methide intermediate.¹²²



Scheme 5. Possible formation mechanisms for the vinyl ether (10). Left: deprotonation of the phenol results in the formation of quinone methide and elimination of the α -OH followed by deprotonation of the γ -OH, resulting in β - γ cleavage and the release of formaldehyde. Right: deprotonation of the γ -OH results in the ejection of the α -OH by an E2 or E1cb mechanism.

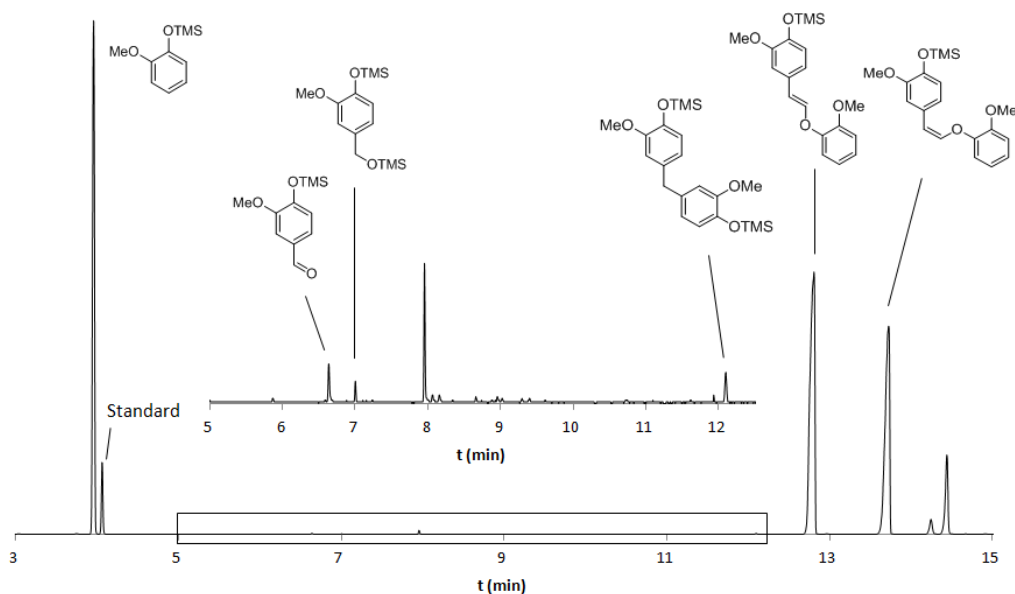


Figure 11. GC-MS chromatogram of the products of Entry 5 (Table 4). The y-axis is the signal intensity of the MS detector and the x-axis is the retention time in minutes. The internal standard is 2-isopropylphenol.

2.3.5 Condensation of dimer decomposition products to biochar

It has been established in 3.1.3 that most of the key β -O-4 bond cleavage product aldehyde **11** ended in condensation. The minor/trace aldehyde products, formaldehyde and acetaldehyde, are less sterically hindered and are expected to be even more reactive for condensation reactions. They can all react with phenolic species such as the dimer,

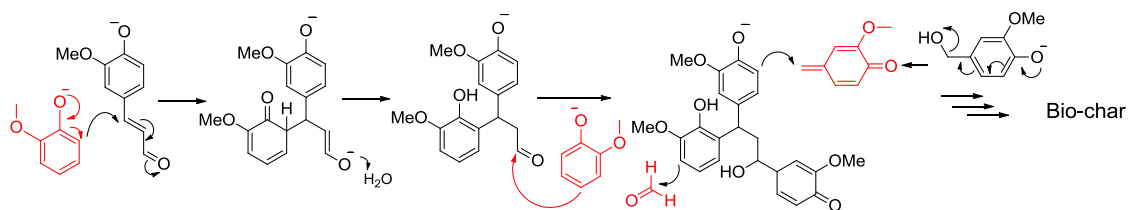
guaiacol, the vinyl ether (**10**) and condensation products. The vanillic alcohol **8** observed in the reaction mixtures is the product of such a reaction between guaiacol and formaldehyde as evident by the lack of vanillic acid, indicating that it is not produced by disproportionation of **7**. The condensation between vanillic alcohol and another guaiacol unit can also be observed (Figure 11). Condensation of these species leads to the formation of polymers and even insoluble crosslinked resins (biochar). These condensation reactions are irreversible and pH dependent. It is noted that the yields of vanillin and vanillic acid both show a minimum in Entry 3 (1 eq NaOH) of Table 4. These results are consistent with the optimal pH for the preparation of industrial phenolic resins (resoles and novolacs), known to be between 9 and 11, and reported lignin derived resins.¹²³⁻¹²⁴. At this pH level, an optimal balance exists between the concentrations of phenolic anion (a nucleophile) and phenols (Lewis acids for activating aldehydes). Gel permeation chromatography (GPC) (Figure 8) was performed to show the molecular weight distribution of DCM soluble products of reactions that used different amount of hydroxide bases. Indeed, Entry 3 (1 eq NaOH) does show the heaviest high MW peaks. As the amount of NaOH was increased, the high MW peaks and tail decrease consistently all the way to Entry 6 (24 eq NaOH).

Based on these observations, two illustrative mechanisms are shown in Scheme 6 for basic conditions and neutral/weakly acidic conditions, where guaiacol is used as a representative of all phenolic species for the sake of simplicity (knowing that the concentration of guaiacol is only a fraction of all other phenolic species). The mechanisms appear to be complicated, but only involve one type of reaction - nucleophilic addition of phenolic anions to two kinds of electrophiles -aliphatic

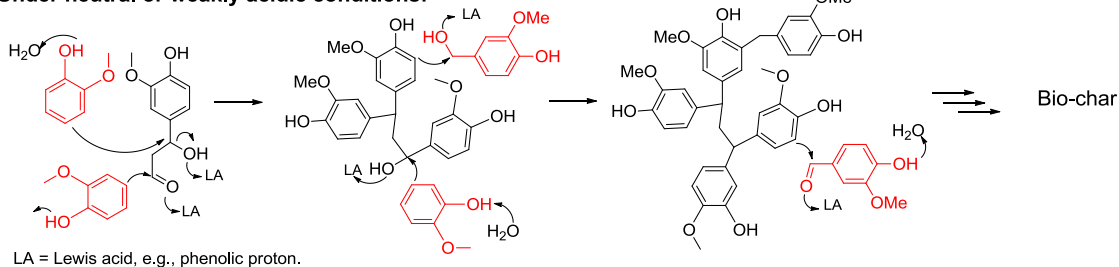
aldehydes and quinone methide.¹²⁵ The major differences between the mechanisms are that Lewis acids are employed under neutral/weakly acidic conditions to activate carbonyl groups and that vanillin (and similar compounds such as **12**) are not effectively involved in the condensation under basic conditions.

The GPC results for carbonate bases entries are shown in Figure 8. The differences among the GPC curves are less significant as seen in Figure 8. This is due to weak basicity of carbonates. Sodium bicarbonate has a pK_a almost equivalent to phenol, meaning a pH of 10 will be achieved somewhere between 1 and 2eq Na_2CO_3 .

Under basic conditions:



Under neutral or weakly acidic conditions:



Scheme 6. Illustrative mechanisms of re-polymerization of dimer decomposition products under basic and neutral conditions.

2.4 Conclusions

According to the results in Table 4 and above discussions, simple base catalyzed hydrothermal treatment of lignin is not an effective process for lignin depolymerization. While weakly basic conditions do result in higher oil yields and appear to be quite efficient at cleaving the β -O-4 bond, there is no simple way to control the condensation reactions that readily take place under the same conditions. Strongly basic conditions

appear to inhibit these side reactions to a certain extent but produce unwanted vinyl ethers while leaving the β -O-4 intact. Therefore, it is likely that a solution that eliminates or deactivates either the phenol or carbonyl groups is needed for hydrothermal lignin depolymerization to be viable.

CHAPTER 3: LIGNIN DIMER DECOMPOSITION UNDER REDUCTIVE CONDITIONS

3.1 Introduction

Condensation processes have been identified as the primary reason for low monophenol yields following β -O-4 bond cleavage. Several potential solutions have been investigated to stop unwanted condensation processes, namely phenol oxidation, phenol capping, and carbonyl reduction. Metal catalysts have been employed to achieve oxidative conditions, which can oxidize phenolics to quinones, hindering the identified condensation pathway. These conditions, however, often feature specialized ligands and solvent systems and can fail to cleave the β -O-4 bond entirely, resulting in a more oxidized side chain and low monomer yields.^{35, 41, 126} Phenol may be deactivated by the addition of boric acid which caps the hydroxyl group, thus reducing its nucleophilicity. Notable increases in oil production were observed during hydrothermal lignin depolymerization in the presence of boric acid but only when a boric acid was used in excess. Char production was not impeded by boric acid but instead promoted at all concentrations, indicating that phenolic capping is not adequate to prevent condensation processes.^{116, 127} The shortcomings of these methods suggest that the phenolic moiety cannot be readily deactivated, leaving carbonyl reduction as a more favorable approach.

Reductive hydrothermal treatment has been implemented in lignin depolymerization through a diverse array of systems with accordingly variable results.¹²⁸ Due to the complexity of the lignin polymer and diversity in solvents, reducing agents, metal catalysts, time, temperature, and the multitude of other additives it is difficult to draw a definite conclusion on the mechanism and role of reduction within the lignin

depolymerization process. Few studies have been performed on lignin model compound substrates under reductive conditions. Molinari et al. reported the use of a TiN-Ni nanocomposite as a hydrogenolysis catalyst that was able to cleave α -O-4, β -O-4, and 4-O-5 ether bonds of the tested model compounds in ethanol and 12 bar of H₂, yielding the monomeric constituents in high yield although aromaticity was lost in many cases.¹²⁹ Zhang et al. investigated aqueous Ni-M bimetallic systems under 5-12 bar H₂ and reported that Ni₈₅Ru₁₅, Ni₈₅Rh₁₅, and Ni₈₅Pd₁₅ were able to cleave α -O-4 and β -O-4 bonds in near quantitative yield and 4-O-5 bonds in about 10% yield with a much higher selectivity towards the aromatic products than any monometallic catalyst.¹³⁰ The near quantitative cleavage of guaiacylglycerol- β -guaiacyl ether to yield guaiacol and 2-methoxy-4-propylphenol was achieved in methanol in the presence of a synergistic Zn²⁺-Pd/C catalyst with 20 bar H₂.³⁹ Galkin et al. demonstrated a unique method to selectively degrade dimer model compounds into their corresponding aryl ketone or alkane over Pd/C in a water-ethanol solvent system, using ammonium formate as a hydrogen source.¹³¹ The increased yields presented in these studies allude to effectiveness of reductive conditions in preventing condensation processes; however, the use of noble metal catalysts in many cases limits their value for practical application.

Herein we present the study of 3 Nickel catalyst systems (Ni/C + Zn, Ni/C + H₂, and Ni/Zn) for the reductive cleavage of a β -O-4 model dimer under neutral and basic conditions. Nickel is a low cost alternative to noble metal catalysts such as Pt as Pd that has the potential for easy recycling by magnetic separation. The function of each catalyst component is identified and the reaction mechanisms established for each unique reaction condition.

3.2 Experimental

3.2.1 Materials

Activated carbon (100 mesh, 161551, BET surface area previously reported as 853 m²/g.¹³²), zinc dust (<10 μm, 209988, BET surface area estimated to be 0.9 m²/g as judged from the specific surface area of Fe and Zn dust of similar size¹³³⁻¹³⁴), 2-methoxy 4-propylphenol, hydrazine hydrate, chloroform-d, sodium carbonate, sodium bicarbonate, potassium carbonate, and potassium hydroxide were purchased from Sigma-Aldrich. Nano zinc (75-125 nm) was purchased from Strem Chemicals Inc. Nickel(II) acetate tetrahydrate and 2-methoxyphenol were purchased from Alfa Aesar. Vanillin, 2-isopropylphenol, and N,O-bis(trimethylsilyl)trifluoroacetamide were purchased from Acros Organics. Sodium hydroxide and HPLC grade acetonitrile were purchased from Fisher Scientific. Reagent grade dichloromethane and ethanol were purchased from Pharmco-Aaper. All chemicals were used as received without further purification. The lignin model compound guaiacylglycerol-beta-guaiacyl ether was synthesized using a literature procedure.¹²⁰

3.2.1.1 Preparation of 10% Nickel/Carbon Catalyst

The carbon supported nickel catalyst was prepared by a literature method.¹³⁵ Nickel(II) acetate tetrahydrate (4.24g) was dissolved in 14 mL of deionized water to which 9.00 g of activated carbon was added. The water was evaporated while manually stirring the mixture at 110-120°C. The Ni(II) loaded on carbon was then reduced in 40 mL of water using 6.0 g of hydrazine hydrate and 1.75 g NaOH while stirring for 20 minutes at room

temperature. The reaction was completed by heating to 85 °C and stirring for 10 minutes. The mixture was then filtered and dried at 80 °C under vacuum.

3.2.1.2 Preparation of Ni/Zn Catalyst

Ni/Zn was prepared *in situ* for each individual trial by the reductive deposition of nickel from a 3mL solution of nickel acetate tetrahydrate (42.4mg) onto the zinc (100 mg) surface prior to the reaction.

3.2.2 Methods

3.2.2.1 Reductive dimer decomposition

Reactions were performed in a 21.9 mL stainless steel mini-reactor assembled from a Swagelock Tube Union (SS-1610-6) and two Swagelok plugs (SS-1610-P). The reactor volume was measured as 21.9mL with the volume of the stirring bar (0.9 mL) and the solvent (3 mL) leaving 18 mL. At 4 atm and RT, the amount of H₂ filled into the reactor was calculated to be 3.39 mmol assuming H₂ is an ideal gas and its solubility in the solvent (water or ethanol) is negligible. Therefore, for the 50 mg (0.156 mmol) of dimer used in every test, 0.468 mmol of H₂ or Zn is needed to reduce the dimer into a guaiacol and 4-propylguaiacol.

The dimer was massed by attaching it to a stir bar which was then added into the reactor vessel. The unsealed reactor vessel was then brought inside a glovebox equipped with a nitrogen atmosphere in which the base solution and any other additives were introduced. The reactor vessel was then sealed under the nitrogen atmosphere. If a hydrogen atmosphere was used, the reactor was then vacuumed and refilled to 1 atm H₂ three times then H₂ added until the desired pressure. The reactor vessel was heated in a

molten salt bath while stirring at 360 rpm. Reaction time was started when the reactor was within 5°C of the target temperature. The reactor was quickly cooled to room temperature in a water bath upon completion.

The reaction mixture was filtered through filter paper and the reactor washed with water and dichloromethane to insure complete transfer of product oil. If ethanol was used as solvent, the reactor was washed with ethanol and the solvent was removed on a rotovap (100mbar, 50°C) immediately after filtration. The filtrate was acidified to pH 2-3, and extracted with 15 mL of dichloromethane three times. In order to prevent the loss of any volatile products, the majority of solvent was removed on a rotovap under 350 mbar and with a low temperature water bath (50°C), and the residual solvent was removed under reduced pressure (10-20 mbar) at room temperature. Samples were spiked with 1 mg of 2-isopropylphenol as an internal standard and dissolved in about 2 mL of chloroform. Seven drops of sample were taken for GC-MS analysis and were derivatized by the addition of 7 drops of N,O-bis(trimethylsilyl)acetamide. Samples were allowed to sit at room temperature for 20 minutes for derivatization to complete then diluted to about 0.5 mL with acetonitrile.

3.2.2.2 Characterization and quantification

The silylated derivatives of lignin model degradation products were characterized and quantified by using the same methods described in 2.2.2.4.

3.2.2.3 NMR

NMR spectra were recorded on a Bruker Avance 600 MHz nuclear magnetic resonance spectrometer using chloroform-d at 20°C-25°C. The ¹H experiments (Bruker

pulse sequence “zg30”; proton) had the following parameters: spectral width of 20 ppm, acquisition time (AQ) of 2.65 s, 16 or 128 scans with a 1.0 s interscan delay (D1). ^{13}C experiments (Bruker pulse sequence “zgpg30”; proton decoupled ^{13}C) had the following parameters: spectral width of 240 ppm using 32768 data points for an AQ of 0.91 s, 1024 scans with a 1.0 s interscan delay (D1).

3.3 Results and Discussion

3.3.1 Three reductive systems Ni/C + H₂, Ni/C + Zn, Ni/Zn and the main reduction path

Herein we investigate the effect of Ni/C + H₂ and two Ni/Zn bimetallic systems on the decomposition of dimer **3**. Ni/C is not considered a strong hydrogenation catalyst and has not been used intensively for reductive conversion of lignin model compounds or biomass. In the two bimetallic systems, nickel metal is expected to act as a catalyst while zinc metal is expected to function as a reducing agent (either by generating H₂ or through electron transfer to Ni) and to generate a Lewis acid oxide (ZnO) which continues to serve as the support for Ni. Ni/Zn microparticles were synthesized *in situ* by reducing Ni²⁺ onto the surface of 6-9 micron Zn dust. A comparative study of the effectiveness of the three systems allowed us to explore the roles of each component and co-operation of the components in the cleavage of the lignin dimer and reduction of the dimer degradation intermediate products. For all systems, different conditions (solvent, base, absence of Ni or Zn) were tested to identify optimal condition, maximize monomer yield, and provide evidence for mechanism determination. The results of all tests are shown in Table 8 (neutral conditions) and Table 10 (basic conditions). Minor and uncommon

products, which are listed collectively as “other products” in these two tables, are shown in Table 9 with a yield for each of the “other products”.

The success of the systems at reducing condensation and retention of the carbon atoms of the side chain is immediately evident by the increase of monomer yield from about 23.13 C% in Table 1 to 78.1 C% (Entry 13A in Table 8) and the abundance of products 4-propylguaiacol and 4-(3-hydroxypropyl)guaiacol from reduction of **11**. Despite the very different yield and product distribution, retention of aromaticity in products was observed in all cases, demonstrating the selectivity of the three systems.

The results and discussions will be presented in three subsections below. First, three baseline tests, which were to identify the functions of individual metal and effect of solvent on cleavage and condensation of the dimer, will be presented in 3.3.2. Reductive decomposition of the dimer will be presented in the sections 3.3.3 and 3.3.4 for neutral and basic conditions, respectively.

Table 8. Hydrothermal decomposition of dimer **3** under neutral and reductive conditions.

Product Yields (C%)										
Entry	Rxn Conditions ^a	6	22	16	15	Other	Total ^c	3	Zn%	Oil yield (wt%)
1	Zn, H ₂ O	18.0	0	0	0	0	18.0	0	0	75.4
2	Ni/C, H ₂ O	18.2	0	0	0	0	18.2	0	n/a	28.1
3	Ni/C, 4atm H ₂ , H ₂ O	29.1	0.3	8.9	38.7	0	77.0	0	n/a	70.9
4	Ni/C, 1atm H ₂ , H ₂ O	28.0	0.4	11.8	26.4	0.3	66.9	0	n/a	73.4
5	Ni/C, EtOH	17.9	0	0	0	0.5	18.4	4.6	n/a	64.4
6	Ni/Zn, H ₂ O	23.7	0.1	13.6	14.6	0.1	52.2	0	0	80.3
7	Ni/nano Zn ^b , H ₂ O	32.8	1.3	20.0	13.6	0.4	68.2	0	0	83.6
8	Ni/C, Zn, H ₂ O	21.5	0.7	3.5	33.5	0.1	59.4	0	0	60.9
9	Ni/C, Zn, EtOH:H ₂ O (1:1)	26.8	0.1	11.3	27.8	0.2	66.3	0	0	64.2
10	Ni/C, Zn, EtOH:H ₂ O (9:1)	28.8	0.1	19.3	28.9	0.2	77.3	0	<5	75.3
11	Ni/C, Zn, EtOH	25.4	0.7	15.1	0.8	1.6	43.6	0	35	63.8
12A	Ni/Zn, EtOH:H ₂ O (9:1)	20.9	0.1	3.4	16.1	2.3	42.8	30.1	12	92.6
12B	Zn, EtOH:H ₂ O (9:1)	12.7	0	0	0	0	12.7	29.9	0	85.1

^a50 mg (0.156 mmol) of dimer **3**, 3 mL of solvent, 100mg Ni/C when used, 100 mg (1.53 mmol) of 6-10 μm Zn metal when used, 50 mg (8 eq to **3**, 1.64 w/w%) NaOH when used, 175 °C unless otherwise noted. ^b30-150 nm.

^cTotal yield of identified monomeric products. See Table 9 for other identified products.

3.3.2 The functions of individual metals and effect of solvent on cleavage and condensation under neutral conditions

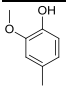
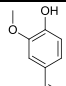
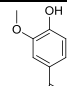
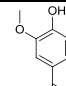
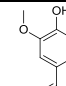
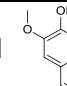
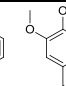
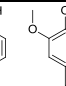
Decomposition of the dimer **3** was conducted under neutral conditions in three entries, Zn + H₂O (Entry 1), Ni/C + H₂O (Entry 2), and Ni/C + EtOH (Entry 5), to investigate the function of individual metals and the effect of EtOH on dimer composition. The following common observations were made. First, reduction products of the cleavage product (**11**) were absent, indicating that Zn and Ni/C alone do not reduce carbonyl products and EtOH does not act as a H₂ source. Second, β -O-4 cleavage of the dimer was catalyzed by ZnO and Ni/C as evident by the low amount of surviving dimer in Entry 5 (4.6 C%) compared to Entry 11 in Table 4 (82 C%). Third, **12** (the β -O-4 cleavage Path B product) and **9** (cleavage product of **12**) were not detected. Since **12** and **9** are aromatic ketones and are more resistant to condensation than aldehydes **11** and vanillin,

respectively, their absence is an indication that Path B of β -O-4 bond cleavage is even less significant when Ni/C or ZnO is present. This is an expected result of cleavage happening on the catalyst surface where thermal motion is restricted, further reducing the participation of the higher energy rotamer in β -O-4 cleavage (Path B).

Vanillin, a cleavage product of **11**, was not detected in Entries 1 and 2, while 0.17 C% of vanillin was found in Entry 1 of Table 4 (no catalyst, neutral H₂O). Since vanillin is quite stable in presence of guaiacol (Entries 4, 5, Table 7, even when Ni/C was used), condensation of **11** must be greatly catalyzed by ZnO (from Zn) and Ni/C, leaving no chance for **11** to cleave into vanillin (path A2, Scheme 2). However, in Entry 5 (Ni/C + EtOH), 0.5 C% of vanillin was detected (Table 9). Presumably, EtOH better solvated **11**, reducing its interaction with the surfaces, and thus slowed its condensation and allowed its cleavage to happen to form a small amount of vanillin.

There are some differences among the results of the three entries. First, the oil yield of Ni/C + H₂O (Entry 2) is much lower than that of Entry 1 (Zn, water; 28.1 vs 75.4 wt%), suggesting that Ni/C promotes condensation reactions under neutral conditions to produce DCM insoluble char, likely by providing a large surface area for oligomers to meet and react. Second, from Entry 2 (Ni/C + H₂O) to Entry 5 (Ni/C + EtOH), the amount of surviving dimer increased from 0 to 4.63 % and the oil yield increased from 28.13 wt% to 64.4 wt%, suggesting that both cleavage of the dimer and condensation of the dimer and cleavage products were slowed in EtOH. Likely, the better solubility in EtOH kept the dimer and oligomers dispersed in solution and reduced their interactions with the Ni/C surface and thus slowed cleavage and condensation reactions.

Table 9. “Other” products of hydrothermal decomposition of dimer **3** under reductive conditions.

Entry	Rxn Conditions ^a	Product Yields (C%)								Total
										
1	Zn, H ₂ O	0	0	0	0	0	0	0	0	
2	Ni/C, H ₂ O	0	0	0	0	0	0	0	0	
3	Ni/C, 4atm H ₂ , H ₂ O	0	0	0	0	0	0	0	0	
4	Ni/C, 1atm H ₂ , H ₂ O	0.2	0	0.1	0	0	0	0	0.3	
5	Ni/C, EtOH	0	0.5	0	0	0	0	0	0.5	
6	Ni/Zn, H ₂ O	0.1	0	0	0	0	0	0	0.1	
7	Ni/nano Zn ^b , H ₂ O	0.2	0	0.1	0	0	0	0	0.4	
8	Ni/C, Zn, H ₂ O	0.1	0	0	0	0	0	0	0.1	
9	Ni/C, Zn, EtOH:H ₂ O (1:1)	0.2	0	0	0	0	0	0	0.2	
10	Ni/C, Zn, EtOH:H ₂ O (9:1)	0.2	0	0	0	0	0	0	0.2	
11	Ni/C, Zn, EtOH	0	0.5	0	0	0	0.2	1.0	1.6	
12A	Ni/Zn, EtOH:H ₂ O (9:1)	0.1	0	0	0	0	0.1	2.1	2.3	
12B	Zn, EtOH:H ₂ O (9:1)	0	0	0	0	0	0	0	0	
13A	Ni/Zn, NaOH	0.1	0	0	0	0	0	0	0.1	
13B	Ni/Zn, NaOH, 30 min	0.1	0.1	0	0	0.1	0	0	0.3	
14A	Ni/C, NaOH	0	0.4	0	0	0.2	0	0	0.6	
14B	Zn, NaOH	0.1	0.1	0	0	0.2	0	0	0.4	
14C	Ni/C, Zn, NaOH	0.2	0	0	0.8	0	0	0	1.7	
14D	Ni/C, Zn, NaOH, 10 min	0.1	0.4	0	0.2	0	0	0	0.6	
15A	Ni/C, 1atm H ₂ , NaOH	0.2	0	0	0.1	0	0	0	0.3	
15B	Ni/C, 1atm H ₂ , NaOH, 10 min	0.1	0.2	0	0.1	0	0	0	0.4	
15C	Ni/C, 1atm H ₂ , NaOH, 170°C, 5 min	Trace	0.1	0	0	0.3	0	0.1	0.5	
15D	Ni/C, 1atm H ₂ , NaOH, 125°C, 13 min	0	0	0	0	0	0	0	0	

^a50 mg (0.156 mmol) of dimer **3**, 3 mL of solvent, 100 mg (1.53 mmol) of 6-10 μm Zn metal when used, 50 mg (8 eq to **3**, 1.64 w/w%) NaOH when used, 175 °C unless otherwise noted. ^b30-150nm.

3.3.3 Reduction under neutral conditions

3.3.3.1 Reduction in aqueous solutions

Ni/C + H₂ (Entries 3 & 4): When H₂ gas (4 atm at RT, 3.39 mmol) was added to the reaction system (Entry 3, Ni/C), a good monomer yield (77.0 C%) was obtained. When the pressure of H₂ was reduced to 1 atm (0.848 mmol, Entry 4), the monomer yield was reduced to 66.9 C%, largely due to the drop in the combined yield of **16** & **15** – a consequence of slowed reduction of **11**. Surprisingly, the yield of 4-propylguaiacol (**16**)

actually increased from 8.93 C% to 11.82 C%. This may be explained by the more acidic surface of Ni at a low H₂ pressure, which promotes the reduction of the γ -OH of **15** and condensation of the same group with guaiacol (which reduced monomer yield). Since the yield increase for **16** (by 2.9%, or 32.5% relative) is much greater than the yield decrease for guaiacol (1.18% or 4.05% relative), the promotion for reduction of the γ -OH of **15** is stronger than that for condensation.

Ni/Zn (Entries 6 & 7): With Ni/Zn, a moderate yield of monomers (52.2 C%) was obtained despite that the amount of Zn used could produce 1.53mmol of H₂, more than that of 1 atm H₂ (0.848 mmol). When nano zinc (Ni/Zn nano, Entry 7) was used, the monomer yield was increased to 68.2 C% and a yield increase is seen for all monomeric products. Presumably, the larger surface area of Ni facilitated the reduction and hence reduced condensation. A more significant change is that the yield of 4-ethylguaiacol (**22**) was increased from 0.11 C% to 1.34 C% (by 1118%), making it the highest yield of **22** under all neutral conditions. Since **22** is a reduction product of the vinyl ether, dimer to vinyl ether (**10**) conversion, which rarely happens under non-basic conditions, must be promoted by the electron-rich (hence, basic) Ni surface. Ni/Zn may deprotonate the phenol moiety of the dimer, forming a phenolic anion, facilitating the dimer's conversion into **10** according the mechanism shown in Scheme 5. From Entry 4 (Ni/C, 1 atm H₂) to entry 7 (Ni/Zn nano), the most significant change is that the **16/15** ratio was increased from 0.447 to 1.465. Apparently, the coexistence of ZnO (a Lewis acid oxide) with Ni promoted the reduction of the γ -OH of **15**. This is in line with the similar observation for Entry 4 vs Entry 3 that has been discussed for Ni/C + H₂ – lower H₂ pressure favors reduction of the γ -OH of **15**.

Ni/C + Zn (Entry 8): Compared to Entry 4 (Ni/C, 1 atm H₂), the yield of Entry 8 is smaller by 7.5%, mainly due to the low yield of guaiacol (21.5 C%), which is the lowest among all Ni-based reductive entries of neutral conditions. Since both Ni/C and Zn promote β -O-4 cleavage, the lower yield of guaiacol must be due to its consumption in condensation reactions with carbonyl compounds, primarily **11**, which can consume more than one molar equivalent of guaiacol as shown in Scheme 6 for neutral conditions. Since the only difference between Entry 8 and Entry 4, that can negatively affect the yield of guaiacol, is the presence of ZnO in Entry 8, it is reasonable to believe that ZnO also catalyzes condensation reactions. The ratio of **16/15** (0.104) is also the lowest among these entries. This can be explained by the stronger interaction of **15** with ZnO, reducing its chance for further reduction on Ni surface.

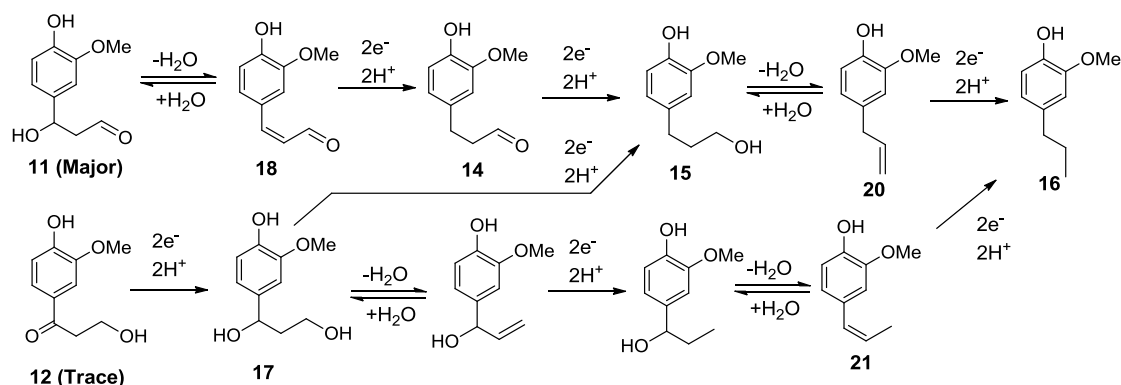
One common observation in all entries in this subsection is that neither vanillin nor its reduction product, 2-methoxy-4-methylphenol, were detected. There are three possible explanations: 1) cleavage of **11** to vanillin, which is known to happen under neutral conditions (Entry 1, Table 4), did not happen because the reduction and condensation of **11** was very fast. 2) Vanillin was formed, but was decomposed in condensation reactions. 3) Vanillin was formed and reduced to 2-methoxy-4-methylphenol which was 100% consumed in condensation reactions. To determine which scenario is true, entry 8 reaction was repeated with the dimer replaced by a mixture of guaiacol and vanillin. The result (Entry 6, Table 7) shows that vanillin was completely reduced to 2-methoxy-4-methylphenol which was extracted in 90% yield. So, in the above neutral reductive treatment of the dimer, vanillin was simply not formed. In other

words, the reduction and condensation of **11** was much faster than the retro-aldol reaction (path **A2**) of **11**.

3.3.3.2 Reduction pathway

Under neutral conditions, cleavage of β -O-4 predominantly follows path A as shown in Scheme 2. Only two major GC-eluable products (**16** & **15**) were obtained from the reduction of the major β -O-4 cleavage product **11**. Based on the structures of **16** & **15**, a probable reduction path for **11** in neutral conditions is a combination of dehydration and reduction steps as proposed in Scheme 7. Reduction of the major cleavage product **11** may start with dehydration to give compound **18**, reductive removal of α -OH to give compound **14**, or with reduction of the aldehyde group to give **17**. The following two observations support the loss of the α -OH: 1) **17** was not detected under any condition in Table 8-Table 10 (even basic conditions in entries 13-16, where **17** is more stable), and 2) **14** was observed under certain conditions (~0.1 C% in Entry 11, <<0.1 C% in Entries 3, 9, and 10). The absence of coniferyl aldehyde **18** and coniferyl alcohol **3i** in all cases suggests that reduction of the α -OH is also faster than its elimination. **14** is reduced to **15**, which is quite stable, and was only partially reduced to **16**.

As discussed in 3.3.2, the minor β -O-4 cleavage path B was likely further suppressed in the presence of Zn or Ni. **12** (the path B product) was not detected even under a selected basic condition (entry 14, Ni/C Zn, 8 eq NaOH, Figure 12) when **12** is more stable. This suggests that **12** was either not formed or was reduced quickly. The reduction of **12** should follow the pathway proposed in Scheme 7, which also leads to the same products **15** and **16**.



Scheme 7. Possible reduction paths of the β -O-4 cleavage products in neutral water or water/EtOH.

In many neutral reductive entries (4, 6-10, 12A), vanillin reduction product, 4-methylguaiacol, was found in a small amount (Table 9). The intermediate reduction product, 4-hydroxymethylguaiacol, was not detected. This observation indicates that reduction of the α -OH in 4-hydroxymethylguaiacol is fast, lending further support for the earlier reduction of the α -OH groups in the mechanism in Scheme 7.

3.3.3.3 The effect of ethanol

From Entry 8 to Entry 9 (Ni/C + Zn used in both), water was replaced by a 1:1 (vol) mixture of EtOH and H₂O. The monomer yield was increased from 59.3 C% to 65.9% (by 6.6 C%) with the most significant increase contributed by guaiacol (5.24 C%), and only 2.14 C% by **16** and **15** combined. The increase can be explained by slowed condensation of **11** and **15** on the surfaces (most likely surface of ZnO) due to their better solvation in the mixture solvent. Since condensation of **11** involves multiple molar equivalents of guaiacol (Scheme 6), slower condensation should result in a larger increase in guaiacol yield. When the EtOH:H₂O ratio was increased to 9:1 (entry 10), the monomer yield was further increased to 77.3 C% (by 11.4 C%). Interestingly, the yield increase now came mostly from the gain in **16** & **15** (9.1 C%) vs 2.0 C% from the gain in

guaiacol. Apparently, the adhesion of guaiacol to the surface(s) and hence the participation of guaiacol in condensation were already substantially reduced in Entry 9; further improvement in solvation mainly reduces the adhesion of **11** to the surfaces.

From Entry 8 to Entries 9 and 10, the most significant change is the increase in **16/15** ratio from 0.105 to 0.407 and 0.669, and may be explained as follows: **15** was adsorbed on the ZnO surface, instead of the Ni/C surface (due to the lack of H-bonding capability) when water was used as the solvent. EtOH solvated **15** and thus increased its concentration in the solution and its chance to contact with Ni surface where it could be reduced by electron transfer (with activation the γ -OH by a Lewis acid, eg. a proton in or from a solvent molecule).

The use of pure EtOH did not result in a better monomeric product yield. The yield of Entry 11 (Ni/C, Zn, EtOH) dropped by 34.9 C% to only 42.4 C%. Interestingly, the drop in overall yield was mostly caused by the drastic drop in the yield of **15** from 28.9 C% (entry 10) to 0.78 C%. Apparently, the zinc oxidation product ($\text{Zn}(\text{OEt})_2$), a soluble Lewis acid, can interact with the γ -OH of **15** and promote the reduction of **15** to **16**. The same interaction also promotes the electrophilic attack of **15** on phenolics. The lower combined yield of **15** and **16** may be partially due to slower reduction of **11** since Zn consumption/ H_2 production was slow in this entry. Also, it is noted that the yield of “other” monomeric products (Figure 12) is the highest among all entries in Table 8 that utilize Ni/C. Some of these products such as **20** (4-allylguaiacol) and **21** (4-(1-propenyl)guaiacol) were transformed from **14** and **15** under the unique condition of Entry 11 via reactions proposed in Scheme 8. Hydrogenation of **21** is likely very fast (see 3.3.7 for discussion on hydrogenation of **25**, a homologue of **21**), providing an additional and

more efficient reduction path to **16**. This explains the low ratio of **21/20** and the all-entries high ratio of **16/15**. The four identified carbonyl compounds (**7**, **9**, **14** and **23**), which were not found in other neutral condition entries, survived (in trace amount) in this entry because they were likely formed as a vinyl ethyl ether (in the case of **23**) or partially protected as acetal or ketal species. These species would be hydrolyzed back to carbonyl compounds upon acid treatment during the reaction workup.

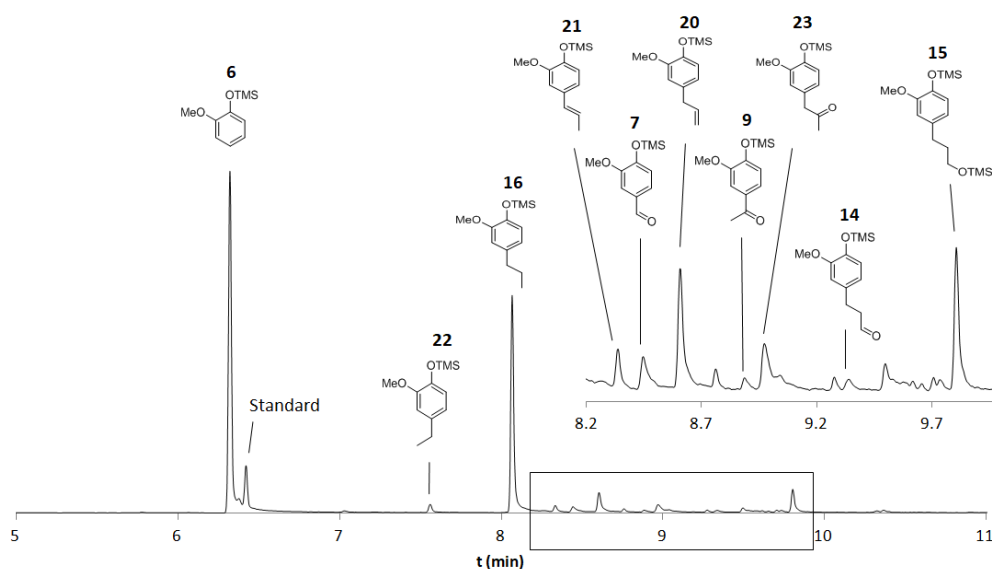
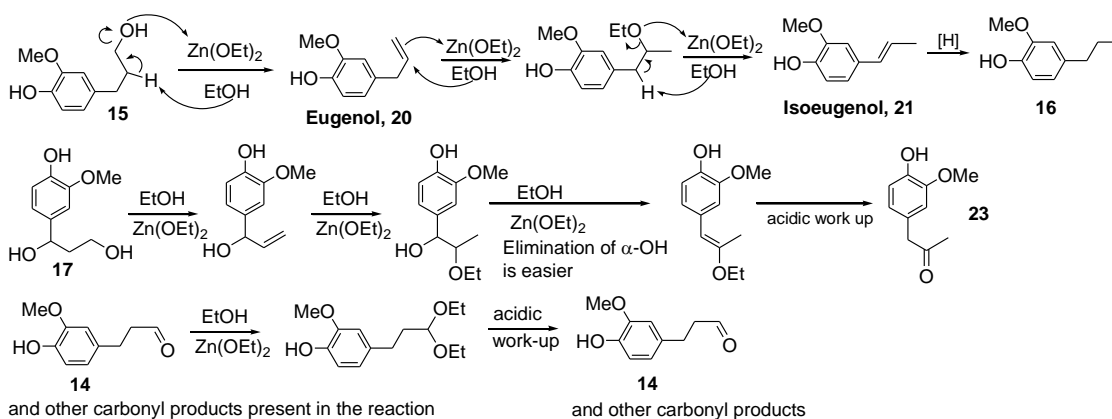


Figure 12. GC-MS chromatogram of decomposition products of β -O-4 dimer under reducing conditions in ethanol (Entry 11, Ni/C, Zn, EtOH). The y-axis is the signal intensity of the MS detector and the x-axis is the retention time in minutes. The internal standard is 2-isopropylphenol.



Scheme 8. Reaction pathways of trace products in Entry 11 (Ni/C, Zn, EtOH).

9:1 EtOH:H₂O was also used as solvent for Ni/Zn in Entry 12A. Surprisingly, the monomer yield dropped from 52.2 C% in Entry 6 (Ni/Zn, H₂O) to 42.8 C%, and 30 % of the dimer survived to the end. Interestingly, the dimer was not detected in Entry 6, as well as all other 2h entries (except 14B) that use water as the solvent. It is believed that water, a poor solvent for the dimer, forced the dimer to interact more with Ni and ZnO surface, thus speeding up the β -O-4 cleavage. When EtOH, a better solvent for the dimer, was used, the dimer was fully solvated and thus cleaved slower. Similar to 12A, 30% of the dimer also survived in Entry 12B (Zn, EtOH:H₂O (9:1)). When Ni/C was used, dimer cleavage or condensation was faster likely due to its large surface area. For examples, only 4.6% of the dimer survived Entry 5 (Ni/C + EtOH) and no dimer **3** was detected in Entry 11 (Ni/C, Zn, EtOH); the latter case, acidic Zn(OEt)₂ likely further sped up cleavage or condensation.

3.3.3.4 Homolytic β -O-4 cleavage in ethanol

Under non-reductive conditions, coniferyl alcohol **3i** is an indicator of homolytic cleavage (Scheme 1). This compound has been shown to have a degradation $t_{1/2}$ of about 1h at 180 °C in 1:1 dioxane:H₂O buffered at pH 7.⁷¹ In the aqueous reaction media at 175

°C in Table 4, stability of **3i** should be similar in entry 1 (neutral) and better in basic condition entries. If **3i** was formed in a small amount (say 0.5 C%), it could be easily detected. In the aqueous entries (regardless of the amount of base added), **3i** was not detected, therefore, homolytic cleavage does not happen in water – a highly polar solvent. On the other hand, **3i** was detected in Entry 11 of Table 4 (EtOH, no catalyst), suggesting that the homolytic cleavage happened in EtOH. However, this process is much slower than the eliminative cleavage in water even if the formation of all the guaiacol in Entry 13 is accredited to homolytic cleavage, since the amount of dimer consumed and guaiacol formed in Entry 11 (Table 4) are only 18% and 2.7 C%, respectively, as compared to 100% and 11.2 C% in Entry 1 (Table 1). Since the amount of **3i** detected was only 0.2 C%, about 1/13 of the abundance of guaiacol, homolytic cleavage is likely less competitive than eliminative cleavage even in EtOH.

Compound **3i** was not detected in Entry 5 of Table 8 (Ni/C, EtOH), indicating that Ni/C must cleave the β -O-4 bond via elimination reactions before the homolytic cleavage can occur. Compounds **20** and **21** may be produced from **3i** by reduction, and therefore, serve as a possible indication of homolytic cleavage of **3**. Absence of these two compounds in Entry 10 (Table 9) provides further evidence that homolytic cleavage was completely suppressed when Ni/C was present. With the above understanding, **20** and **21** in Entry 11 (Ni/C, Zn, EtOH) must be derived from **15** per the mechanism in Scheme 8.

In Entry 12A (Ni/Zn, 9:1 EtOH:H₂O), **20** and **21** are likely reduction products of **3i** because conversion of **15** to these two compounds did not happen in 9:1 EtOH:H₂O when Ni/C was present (Entry 10). In other words, homolytic cleavage of **3** occurred in

9:1 EtOH:H₂O when Ni/C was absent. However, this cleavage was minor compared to the eliminative cleavage described in Scheme 2 since the combined yield of **20** and **21** (2.2 C%) or the combined yield of **16**, **20** and **21** (5.6 C%, considering that **16** was only produced from **20** and **21**) are much smaller than the yield of **15** (16.1 C%) which is a product of reduction of **11** and **12**, not **3i**, as **3i** can be easily reduced to **20** or **21** via the α -carbon cation intermediate. In the case of Entry 12B (Zn, 9:1 EtOH:H₂O) where a reduction condition was absent, **3i** (if produced) could not be converted into more stable molecules (**20** and **21**). The lack of **20** and **21** in this entry suggests that **3i** was consumed in condensation reactions, which could be catalyzed by ZnO, and/or homolytic cleavage became even less competitive in the presence of ZnO.

3.3.4 Reduction under basic conditions

Under basic conditions, the dimer was converted to the vinyl ether **10** (Entry 5 of Table 4) in high yield in the absence of any catalyst via a mechanism shown in Scheme 5. To investigate the effect of catalysts on dimer decomposition and reduction under basic conditions, reactions were run in aqueous solution of 8 molar equivalent NaOH in the presence of Ni/Zn, Ni/C + Zn and Ni/C + 1 atm of H₂. The results are given in Table 10 and are discussed in detail in the paragraphs below.

Ni/Zn + H₂O + 8 eq NaOH (Entry 13A): The best monomer yield (78.1 C%) was achieved in entry 13A. The yield of the vinyl ether-derived product **22** is the highest among all entries and is 1.7 times the yield of **22** that could be derived from the yield of **10** (45.69 C%) in Entry 5 of Table 4 (same basic condition, but without Ni/Zn). Clearly, the retro-aldol reaction to the vinyl ether (Scheme 5) was greatly promoted by Ni/Zn. Presumably, the electron rich Ni surface can interact strongly with the quinone methide,

thus promoting its formation and hence the vinyl ether production. The yield of **22** is 81.8% of the theoretical yield. The remainder of dimer (18.2%) was at least partially cleaved to **11**. However, **11** was not detected and only trace amounts of its reduction products are found (0.1% of 4-methylguaiacol and 0.2% of 4-propylguaiacol). Apparently, reduction of **11** under the basic condition is not as competitive as its condensation. Knowing that reduction of **11** is effective on Ni/Zn under neutral conditions (e.g., Entry 6, Table 8), the low reduction activity may be attributed to the inability of the dianionic form of **11** to adsorb on the electron-rich Ni/Zn surface.

Ni/C + 8 eq NaOH (Entry 14A) and Zn + 8 eq NaOH (Entry 14B): These two reactions were performed to examine the roles of Ni/C and Zn (ZnO) in decomposition of the dimer. Entry 14A (Ni/C) shows that formation of **10** (only 0.2 C%) was reduced by a factor of 29.4 times as compared to Entry 5 of Table 4 when Ni/C was not used. So, Ni/C catalyzes β -O-4 cleavage of the dimer in both neutral and basic conditions. Interestingly, ZnO formed from Zn was found to promote formation of **10** in Entry 14B (Zn only), where 39.4 C% of **10** was produced. However, the suppression of formation of **10** by Ni/C is much stronger than the promotion by ZnO.

Ni/C + Zn + H₂O + 8 eq NaOH (Entry 14C): When Ni/Zn was replaced with Ni/C + Zn, the monomer yield dropped dramatically from 78.1 C% to 32.1 C%, and the yield of **22** dropped from 40.5 C% to 13.3 C%. The 73.4% drop in the yield of **22** is the consequence of the promotion of β -O-4 cleavage by Ni/C which is evident in Entry 14A. Despite the preference for β -O-4 cleavage, there is only 2.6 % (**15** + **16**) products from reduction of the cleavage product **11**. Apparently, reduction of carbonyl compounds

under the basic condition is slow relative to condensation. Indeed, carbonyl compounds including aldehyde **14** are found in the product (**Figure 13**).

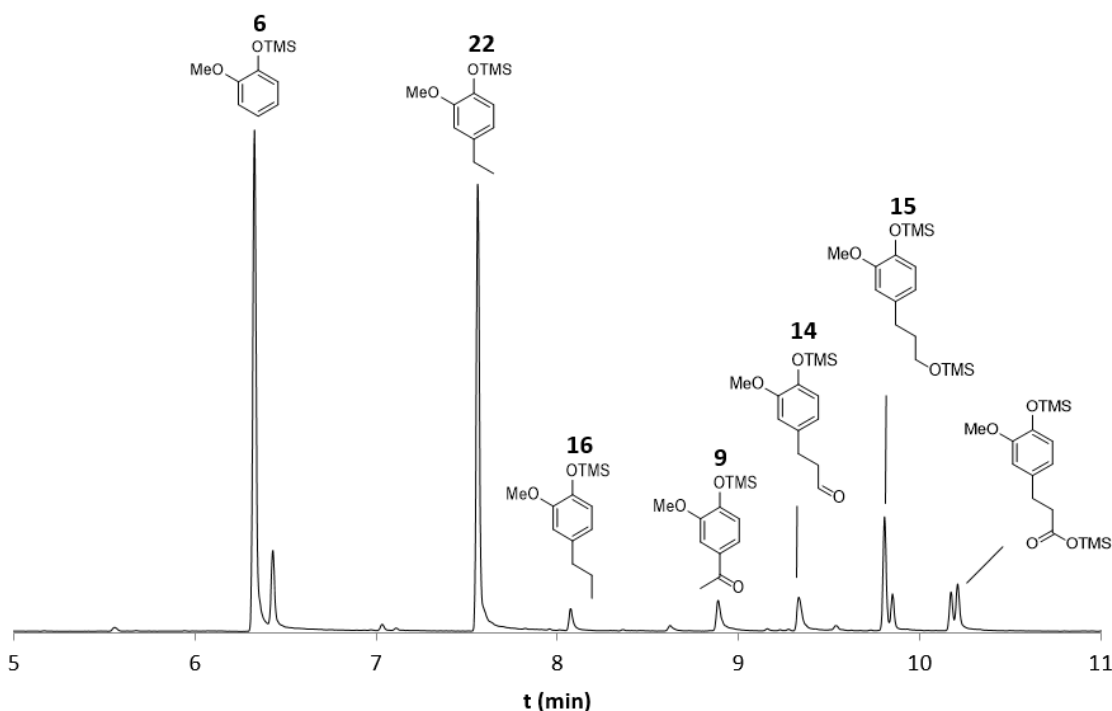


Figure 13. GC-MS chromatogram of decomposition products of β -O-4 dimer under reducing conditions in basic water (entry 14A: Ni/C + Zn + 8 eq NaOH + water). The y-axis is the signal intensity of the MS detector and the x-axis is the retention time in minutes. The internal standard is 2-isopropylphenol.

Ni/C + 1 atm H₂ + H₂O + 8 eq NaOH (Entry 15A): When Zn in Entry 14C was replaced with 1 atm of H₂ (Entry 15A), the product distribution is similar, and the monomer yield is only slightly lower (30.3 % vs 32.1 C%). A detailed comparison of yields of individual products may provide a better understanding of the roles of Zn and the effect of H₂ pressure on product distribution. The yield of guaiacol actually increased from 14.5 C% to 16.3 C%, this could be an indication of ZnO catalyzed condensation and guaiacol was more involved in the condensation on the surface than in solution (a situation also observed in Entry 8 - Ni/C + Zn, no NaOH). The yield of **22** dropped slightly from 13.3 C% to 12.9 C%, and combined yield of **15** and **16** dropped from 2.6 C%

to 0.8 C%, which can be explained by the lower amount H₂ in Entry 15A (0.848 mmol) vs 1.53 mmol in Entry 14C (from Zn + water) and thus slower reduction in Entry 15A which affects the yield of **15** and **16** more than **22** as the reduction path to **22** does not involve carbonyl formation. The lower amount of H₂ in 15A also led to the quicker reduction of **15** and hence a higher ratio of **16/15**. (1.7 vs 0.53 in 15A). The similar correlation of the ration with H₂ pressure was also observed from Entries 3 and 4.

Table 10. Hydrothermal decomposition of dimer 3 under basic and reductive conditions.

Entry	Rxn Conditions ^a	6	22	16	15	Other	Total ^b	3	10	24	25	Zn%	Oil yield (wt%)
13A	Ni/Zn, NaOH	37.3	40.5	0.2	0	0.1	78.1	0	3.2	2.1	0	29	73.6 ^c
13B	Ni/Zn, NaOH, 30 min	19.9	22.5	0.2	0	0.2	42.9	0.4	25.1	1.4	0.1	73	74.0
14A	Ni/C, NaOH	20.1	0	0	0	0.6	20.7	0	0.2	0	0.2	n/a	28.0
14B	Zn, NaOH	10.1	0.1	0	0	0.4	10.6	0.3	39.4	0	0.2	0	73.0
14C	Ni/C, Zn, NaOH	14.5	13.3	0.9	1.7	1.7	32.1	0	0	0.9	0	<5	66.1
14D	Ni/C, Zn, NaOH, 10 min	20.3	6.9	0.4	1.8	0.6	30.0	0.6	0.9	0.4	0	nd	35.1
15A	Ni/C, 1atm H ₂ , NaOH	16.3	12.9	0.5	0.3	0.3	30.3	0	0	0.1	0	n/a	49.4
15B	Ni/C, 1atm H ₂ , NaOH, 10 min	24.9	14.6	0.3	0.2	0.4	40.4	0	0	2.7	0	n/a	50.8
15C	Ni/C, 1atm H ₂ , NaOH, 170°C, 5 min	10.2	0.4	0	0	0.5	11.1	27.0	8.5	Trace	0.3	n/a	55.8
15D	Ni/C, 1atm H ₂ , NaOH, 125°C, 13 min	1.3	0	0	0	0	1.3	68.6	0	0	0	n/a	75.4

^aSee the footnote of Table 8. ^bTotal yield of identified monomeric products. ^cIt is possible that the oil wt% yield is smaller than C% yield when the monomer yield is high because two oxygen atoms are lost, which accounts for ~10% of the weight of the dimer.

3.3.5 Vanillin formation and reduction

In all basic condition entries (except 15D), vanillin and/or its reduction product 4-methylguaiacol were produced in small amounts (0.5 C% or less). In all 2h runs (13A, 14C, and 15A), vanillin was completely reduced. However, its immediate reduction product, 4-hydroxymethylguaiacol, was never detected, and the abundances of 4-

methylguaiacol in those 2h entries are smaller than the combined abundances of 4-methylguaiacol and vanillin in the runs of shorter time (13B, 14D, 15C). Clearly, a substantial portion of 4-hydroxymethylguaiacol formed was lost to condensation. This observation supports the involvement of 4-hydroxymethylguaiacol in the condensation mechanism under the basic conditions depicted in Scheme 6.

3.3.6 ZnO formation under basic conditions

Entry 14A reaction was repeated in absence of Ni/C and the dimer **3**. After the reaction, the white solid was collected by filtration. After being dried in vacuum at RT overnight, 90.0 mg of white powder was obtained. Vacuuming at 185 °C for 5h only reduced the mass to 89.1mg (a loss of 1 wt%). Yield of ZnO (based on 100 mg of Zn dust used) is 71.6%. Since Zn(OH)₂ decomposes to ZnO at 125 °C with a reduction in MW by 19.1%, the content of Zn(OH)₂ in the solid formed is only 5%. If vacuuming at RT did not remove all the physically absorbed water, then, the content of Zn(OH)₂ is less than 5%.

3.3.7 Reduction mechanism of the vinyl ether (compound **10**)

Based on the identification of intermediate reduction products of **10** (Table 10) and the discussion below, a mechanism of the reduction of **10** to **22** is proposed in Scheme 9. Compound **24** – the hydrogenation product of **10**, was found in small percentages (2.1, 0.9, 0.4 C%) in Entries 13A, 14C and 15A, as well as in shorter runs (1.4 C% in 13B-30 min, and 0.4 C% in 14D-10 min). To better track the formation of **10** and **24**, Entry 15A was repeated under different temperature and time (entries 15B-D). Observations are summarized below:

First, conversion of the dimer to **10** did not happen at 125 °C over the course of 13 min (15D), and **24** was not formed either; however, 31.4% of the dimer was lost mainly via condensation since the only monomeric product formed is guaiacol at a very low yield of 1.3 C%. Second, at 170 °C for 10 min (15C), an additional 41.6 C% of the dimer was lost while 9 C% of **10** and 10.2 C% of guaiacol were formed. Obviously, both β -O-4 cleavage and the retro-aldol reaction to form **10** occurred. However, no trace of **11**, **15** and **16** were found, indicating that condensation of **11** was extremely fast. Only 0.4 C% of **22** (the final reduction product of **10**) and a trace amount (0.04 C%) of **24** were formed. Third, when the reaction was run at just 5 degrees higher (175 °C) for only 10m (15B), **10** disappeared, and **22** and **24** increased to 14.6 C% and 2.7 C%. A separate reaction at this temperature for 2h (Entry 15A) caused **24** to drop to 0.4 C%.

The above observations suggest that **24** is an intermediate hydrogenation product of **10** as shown in the first step of Path 1 in Scheme 9. Additionally, it is apparent that the reaction of **24** is much slower than the reaction of **10** (since it took only 10 min at 175 °C for **10** to disappear, while a trace amount of **24** survived even after 2h). **25** may appear to be a downstream product of **24** as it may be formed from **24** by elimination. However, there is a lack of correlation between the abundances of these two species. Since no other species were identified as a possible intermediate product of **24**, the following reduction mechanism is proposed. **24** is split into a guaiacol anion and 4-guaiacyl ethyl radical following electron transfer from Ni/Zn or Ni/H₂. This radical can be directly reduced by single electron or hydrogen transfer from the catalyst surface or alternatively, abstract a hydrogen from a phenolic species, forming a relatively stable radical (phenolic or benzylic) which would then be reduced on the catalyst surface.

As shown in the mechanism, the elimination reaction of **24** is believed to be assisted by metal cations (Lewis acids). If a noble metal catalyst is used, which is a better hydrogenation catalyst for the C=C bond but has no cation on the metal surface or in solution to serve as a Lewis acid, the intermediate **24** may be observed in a greater abundance. A 2-h test reaction was performed at 150 °C under otherwise similar conditions of Entry 15A using Pd/C instead of Ni/C. The ^1H NMR spectrum of the product oil (Figure 14) indeed shows that a significant amount of **24** (43% of **22**) was present, much higher than the abundance of **24** in Entry 15b product (18.5% of **22**), while **10** was 100% gone. So, the result of this test supports the proposed involvement of metal cations in the elimination reaction of **24**.

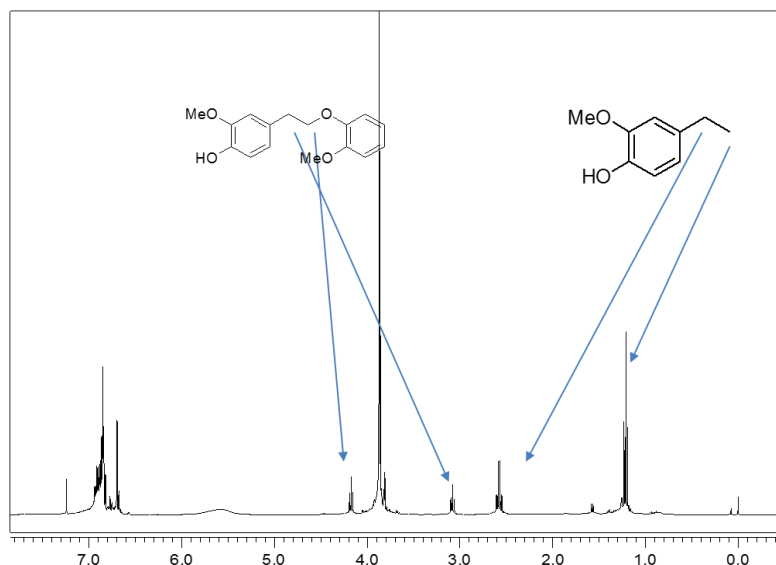


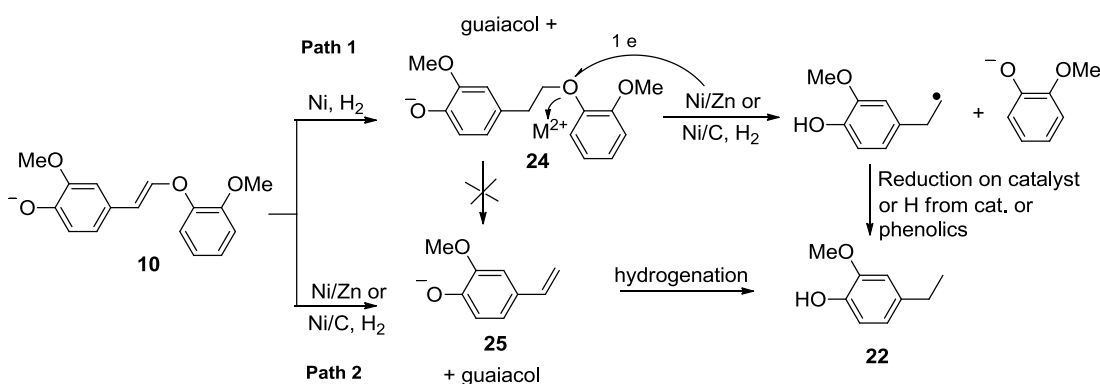
Figure 14. ^1H NMR spectrum of the product of dimer hydrothermal decomposition catalyzed by Pd/C. An appreciable amount of vinyl ether reduction product (**24**) is observed when Pd/C is used. Pd/C functions as a much better hydrogenation catalyst than Ni/C.

A careful examination of the GC-MS data revealed **25** as another immediate product of **10** (Path 2, Scheme 9). This compound was very elusive in the basic condition reactions where both the catalyst Ni and a reducing agent (Zn or H_2) were present. In these reactions, **25** could only be captured in a trace amount (<0.3 C%) when **10** was still

present in a significant amount (Entries 13B and 15C) and disappeared (or was not detectable) when **10** was mostly or completely consumed. This suggests that hydrogenation of **25** was very fast, much faster than the reduction of **24** which survived to the end when **10** was long gone. The most likely chemistry for **10** to lose the guaiacyl moiety is C-O bond splitting after accepting an electron from metal (much like the reaction between alkyl or vinyl halides and active metals). It is also a two-step radical process similar to that shown in Path 1 for reduction of **24**. By comparing the abundances of **10** and **25** in Entries 13B and 15C, one can see that abundance of **25** in Entry 13B is only $\frac{1}{4}$ of that in 15C even though the abundance of **10** is 3 times as high as in 15C. This can be explained by different kinetics in 13B (as compared to that in 15C): faster hydrogenation of **25**, or slower reduction of **10** to **25**, or both. Since the effective catalyst for the majority of the reaction period in this entry was Ni/ZnO, and ZnO is a Lewis acid substrate, slower reduction of **10** is more likely to be the true reason for the low abundance of **25** in 13B. Paths 1 and 2 are competing processes. Based on the higher abundances of **25** over **24** in 15C and that hydrogenation of **25** is much faster than reduction of **24**, Path 2 must be dominant by far in 15C with Ni/C as the catalyst. When Ni/ZnO is the catalyst, it is hard to determine which path is more competitive.

25 was also found at an abundance of 0.206 C% in 14A (Ni/C, NaOH) and 0.158 C% in 14B (Zn, NaOH) where either a reducing agent or a catalyst was not added. It is believed that **25** was formed via the same path (Path 2). In 14A, Ni metal supplied the electrons, however, no H₂ was present to hydrogenate **25** to **22**. In 14C, Zn provided the electrons to reduce **10** to **25**, but could not catalyze the hydrogenation; the trace amount

(0.1 C%) of **22** found in this entry was likely produced by hydrogenation catalyzed by the Ni in the reactor which is made of stainless steel 316.



Scheme 9. Mechanism of the vinyl ether (**10**) reduction. Path 1: The vinyl ether (**10**) is first hydrogenated to yield **24**, which then undergoes metal catalyzed β-O-4 bond cleavage and reduction to yield **22**. Path 2: Metal catalyzed β-O-4 bond cleavage and reduction occurs prior to hydrogenation to yield **25**, which is then hydrogenated to **22**.

3.4 Conclusions

Hydrothermal decomposition of a guaiacol-based lignin dimer has been studied under neutral and basic conditions for production of monomeric phenolic products. While neutral and weakly basic conditions appear to readily cleave the β-O-4 bond, the immediate products as well as resultant downstream products are largely consumed in subsequent condensation reactions, resulting in low monomer recovery. Strongly basic conditions appear to inhibit these side reactions to a certain extent but produce unwanted vinyl ethers while leaving the β-O-4 bond intact.

The above results suggested that a neutral and reductive system would allow for effective β-O-4 bond cleavage, minimization of condensation reactions, and a great enhancement in monomer yield. Ni/C + H₂ and two Ni/Zn bimetallic systems (Ni/C + Zn and Ni/Zn) were used for β-O-4 bond cleavage and carbonyl reduction. Under neutral conditions, the β-O-4 cleavage is catalyzed by nickel metal and dominates the dimer

decomposition. The reduction rate of the γ -aldehyde (**11**) determines the yield of monomeric products. In neutral water, Ni/C with H₂ gave the highest yields. When H₂ was replaced with Zn, where Zn provide more H₂ than 1 atm of H₂, a lower yield was obtained due to faster condensation of **11** catalyzed by the ZnO surface. Switching the solvent from water to mixtures of water and ethanol brought significant increases in monomer yield with a maximum of 77.3 C% at a EtOH:H₂O ratio of 9:1. Ethanol solvates the intermediate **11** better, thus reducing its condensation on ZnO. However, use of pure EtOH caused the yield to drop dramatically as the soluble acidic Zn(OEt)₂ catalyzed condensation in the solution. Ni/Zn performed worse in both neutral water and 9:1 EtOH:H₂O due to incomplete β -O-4 cleavage of the dimer and slow reduction of **11** as a result of limited surface area as evident by the markedly higher yield observed when nano Ni/Zn was used in neutral water. A mechanism for reduction of **11** is proposed based on intermediates found in GC-MS analysis, which is composed of fast reduction of the α -OH, slower reduction of γ -aldehyde, and further slower reduction of the γ -OH. Although homolytic β -O-4 cleavage can occur in pure ethanol and 9:1 EtOH:H₂O, it is not competitive with eliminative β -O-4 cleavage due to the comparatively slow reaction rate.

Under basic conditions, the vinyl ether was formed and converted to the final reduction product 4-ethylguaiacol in all three reduction systems. The best monomer yield (78.1 C%) among all conditions was obtained for Ni/Zn + H₂O + 8 equivalent NaOH. In this case, Ni/Zn greatly promoted the vinyl ether (**10**) formation and products from the β -O-4 bond cleavage reaction were detected only in trace quantities. When Ni/Zn was replaced with Ni/C + Zn or Ni/C + 1 atm H₂, β -O-4 bond cleavage became competitive

with vinyl ether formation on the Ni surface. Monomer yield dropped dramatically as reduction of the β -O-4 cleavage product (**11**) on Ni/C is less competitive than its condensation, which could happen on surfaces and in solution. Two mechanisms for the reduction of the vinyl ether are proposed. The first path involves hydrogenation of the C=C bond, followed by the reductive cleavage of the C-O bond to yield a 4-guaiacylethyl radical and guaiacol anion. The radical can then be directly reduced on the catalyst surface or abstract a hydrogen from a phenolic species to produce a relatively stable radical that would then be reduced on the catalyst surface. The second path involves a similar radical-mediated reductive cleavage of the vinyl ether C-O bond to yield 4-vinylguaiacol and guaiacol. 4-vinylguaiacol is then hydrogenated to 4-ethylguaiacol. Reactions utilizing Ni/C as a catalyst appear to follow path 2 while it is unclear which mechanism is favored by Ni/Zn. Because no carbonyl intermediate is involved and radical species are stabilized by an abundance of phenolics, high yields can be obtained as in the case of Ni/Zn + NaOH.

To conclude, β -O-4 bond cleavage processes under different conditions have been analyzed in detail, reaction paths (mechanisms) are proposed and rationalized to account for the product distributions of reactions under various conditions. Under strongly basic conditions, Ni/Zn system provided the best monomer yield; while under neutral conditions, Ni/C + Zn + 9:1 EtOH:H₂O and Ni/C + 4 atm H₂ + H₂O performed the best and afforded yields only slightly lower the highest yield. Therefore, Ni-based catalytic systems present a versatile and effective option for the decomposition of lignin based β -O-4 dimers into monomeric products.

CHAPTER 4: SELECTIVE DEPOLYMERIZATION OF LIGNIN IN A RAW BIOMASS SUBSTRATE

4.1 Introduction

Lignin depolymerization into its aromatic, monomeric constituents under mild conditions has been a heavily investigated approach for its valorization. Previously reported methods include hydrothermal, pyrolysis, oxidation, and reduction. Hydrothermal and pyrolysis are the most desirable methods as they do not require the use of catalysts and may instead employ the use of relatively cheap and abundant reagents. Hydrothermal reactions utilizing hydroxide or carbonate bases have been shown to cleavage C-O-C linkages to produce phenolic monomers but in yields <10%.¹³⁶⁻¹³⁸ Simple pyrolysis has been shown to yield similar results.^{46, 139} Oxidative methods cleave C-H or C-C bonds adjacent to C-O-C linkages producing vanillin and its analogues in yields <15%.⁵³⁻⁵⁴ Low yields in all cases are likely a result of the formation of reactive carbonyl species that quickly repolymerize into oligomers.¹⁴⁰ This problem can be alleviated to an extent by capping hydroxyl groups with boric acid or adding phenol as a sacrificial condensation reagent.^{116, 141} These practices are impractical, however, given the value of the sacrificial reagents.

Reductive depolymerization looks to be a significantly more viable alternative in that it directly addresses the issue of repolymerization without necessitating the use of valuable chemicals. Hydrogenolysis and hydrogenation have been shown to selectively cleave ether linkages to give monomeric phenolics. Kou *et al.* have demonstrated monomer yields as high as 46% by degrading birch sawdust in the presence of noble metal catalysts (Rh, Pd, and Pt) on carbon and 4MPa H₂.¹⁴² Similarly, Van den Bosch *et*

al. reported the highly selective conversion of the lignin in birch sawdust to 4-*n*-propylsyringol and 4-*n*-propylguaiacol in 50% yield while retaining >78% of cellulosic material as a pulp using Ru on carbon and 3 MPa H₂.¹⁴³ Abu-Omar *et al.* reported similar selective depolymerization results using a synergistic bimetallic system consisting of Zn²⁺ and Pd on carbon with 3.4 MPa H₂.¹⁴⁴ Despite producing excellent results, the use of noble metals and external hydrogen gas still possess a significant burden in terms of both sustainability and cost. Galkin *et al.* obtained high yields of 4-(prop-1-enyl) guaiacol and 4-(prop-1-enyl) syringol from birch sawdust using Pd on carbon in an ethanol-water solvent and claim endogenous formic acid as the hydrogen source.¹⁴⁵ Song *et al.* reported ≈50% yields of 4-*n*-propylsyringol and 4-*n*-propylguaiacol from birch sawdust using cheaper and more abundant Ni on carbon and methanol as both the solvent and hydrogen source.¹⁴⁶ Both methods avoid the use of gaseous H₂ and/or noble metal catalysts while maintaining selective lignin depolymerization, allowing for easy separation of the solublized lignin and insoluble cellulosic products.

Despite the considerable number of studies reported, there is little consensus on the actual mechanism of how reductive depolymerization of lignin from raw biomass occurs and the factors that allow for a successful catalytic system. Due to the differences in solvent, reaction temperature, reaction time, and catalyst selection there is little consistency in the mechanistic interpretation of reductive depolymerization and factors that lend to its efficacy. Many papers name hydrogenolysis as the process whereby either the lignin polymer or fragmented lignin oligomers are reductively cleaved to monophenols; however, this is only one facet of the depolymerization process.^{142-143, 145-}

¹⁴⁷ Because hydrogenolysis is often achieved using heterogenous catalysts, it is necessary

for lignin to be dissolved before appreciable interaction with the catalyst can occur. Dissolution of lignin is not a simple phase change and involves numerous reactions. In addition to being freed from hemicellulose and extraction from the cellulose matrix, it must be fragmented to achieve solubility in most solvents. This process is known to affect the chemical composition of lignin but has never been studied in the context of the reductive depolymerization system. Herein we investigate a nickel based reductive lignin depolymerization system with and without the use of external reducing agents with the goal of maximizing monomer yields and product selectivity through the establishment of a more comprehensive depolymerization mechanism. Almost all studies use hardwood sawdust or organosolv lignin as a substrate due its less recalcitrant behaviour compared to softwood and grass derived substrates. However, an optimal feedstock should be both fast growing and have additional incentive for cultivation, rendering the utilization of hardwoods rather impractical outside of unutilized mill residues. In this regard, grasses or agriculture waste products such as corn stover are favorable candidates for use in an envisioned “biorefinery” in which lignin is selectively depolymerized into phenolic chemicals and the remaining cellulosic component can be separated and fermented into cellulosic ethanol or upgraded to chemicals such as furfural and γ -valeroactone. Pine sawdust was chosen as the primary substrate due to its structure being more comparable to optimal feedstocks and the added benefit of simplified analysis due to the exclusion of hydroxyphenyl and syringyl monolignols. Corn stover, sugarcane bagasse, and switchgrass (*Panicum virgatum*) were subject to the most promising reaction conditions.

4.2 Experimental

4.2.1 Materials

Activated carbon (100 mesh, 161551, BET surface area previously reported as 853 m²/g.¹³²), zinc dust (<10 μm, 209988, BET surface area estimated to be 0.9 m²/g as judged from the specific surface area of Fe and Zn dust of similar size¹³³⁻¹³⁴), 2-methoxy 4-propylphenol, hydrazine hydrate, and chloroform-d were purchased from Sigma-Aldrich. Nickel(II) acetate tetrahydrate and 2-methoxyphenol were purchased from Alfa Aesar. Vanillin, 2-isopropylphenol, and N,O-bis(trimethylsilyl)trifluoroacetamide were purchased from Acros Organics. Sodium hydroxide, HPLC grade acetonitrile, 12.1N hydrochloric acid, and sulfuric acid were purchased from Fisher Scientific. Reagent grade dichloromethane, methanol, and ethanol were purchased from Pharmco-Aaper. All chemicals were used as received without further purification. 10% Ni/C was prepared according to section 3.2.1.1. Ni/Zn was prepared according to section 3.2.1.2. Corn stover, sugarcane bagasse, and switchgrass (*Panicum viragatum*) were obtained from the South Dakota State University Department of Agricultural Engineering.

4.2.2 Methods

4.2.2.1 Biomass Characterization

4.2.2.1.1. Klason Lignin Content

Product yields are based on the amount of acid insoluble lignin (Klason lignin). The Klason lignin content of each biomass substrate was determined based on a literature method.¹⁴⁸ The biomass samples were ground using a standard kitchen blender to particles ranging in size from 10-100 mesh. Each sample underwent Soxtec extraction to

remove extractives such as resins, fats, waxes, and terpenoids that would otherwise not be removed and thus erroneously counted as Klason lignin. Soxtec extraction was accomplished by extracting each pre-massed sample with a 2:1 toluene:ethanol mixture overnight (~16h). The samples were washed with ethanol then dried in a vacuum oven at 333K and <10 mbar. The weight of each sample was recorded and transferred to a flask along with 15mL of 72wt% H₂SO₄ solution per 1g of extracted lignocellulose. The mixture was stirred at room temperature for 2 hours then diluted with DI water until a 3wt% H₂SO₄ solution was obtained. The mixtures were refluxed for 4 hours. The Klason lignin was observed as a brown precipitate. The mixtures were filtered, washed with DI water to remove residual acid, and dried in a vacuum oven at 333K and <10 mbar. The wt% of Klason lignin was determined by comparing the lignin weight to the weight of the extracted lignocellulose and correcting for the lost extractives.

4.2.2.1.2. Monomer Ratios (H/G/S)

The relative abundance of H, G, and S phenolic units in each lignocellulose substrate was determined by HSQC NMR of the lignin oil obtained from the following depolymerization reactions: Entry 12 Table 12 and Entries 1-3 Table 14. The chloroform peak was used as an internal reference (δ_C 77.2, δ_H 7.26 ppm). The HSQC experiments (Bruker pulse sequence “hsqcetgpsi2”; phase-sensitive ge-2D HSQC using PEP with gradients in back-inept) had the following parameters: spectral width of 12 ppm in F2 (¹H dimension) using 1024 data points for an acquisition time (AQ) of 72 ms, 165 ppm in F1 (¹³C dimension) using 256 increments (AQ of 5.1 ms), 2 scans with a 1.5s interscan delay (D1). The monophenolic composition was determined by integration of carbon-hydrogen correlation signals corresponding to the 2 and 6 positions of hydroxylphenyl (H_{2,6}) (δ_C

128.8, δ_{H} 7.00 ppm), the 2 and 6 positions of syringyl ($\text{S}_{2,6}$) (δ_{C} 104.9, δ_{H} 6.38 ppm), and the 2 position of guaiacyl (G_2) (δ_{C} 114.1, δ_{H} 6.79 ppm) units. The G_2 integration was multiplied by 2 in order to compare on a molar basis with the $\text{H}_{2,6}$ and $\text{S}_{2,6}$ signals. These chemical shifts are congruent with the signals previously identified in deuterated DMSO and DMSO/pyridine^{143, 149} (differences can reasonably be attributed to solvent) as well as those predicted by Chemdraw Ultra 12.0.

4.2.2.2 Biomass Decomposition Reactions

Reactions were performed in a 21.9 mL stainless steel mini-reactor assembled from a Swagelock Tube Union (SS-1610-6) and two Swagelok plugs (SS-1610-P). The reactor volume was measured as 21.9 mL with the volume of the stirring bar (0.9 mL) and the solvent (4 mL) leaving 17 mL. The biomass was ground using a standard kitchen blender to particles ranging in size from 10-100 mesh and used without any additional pretreatment. 400 mg of biomass was used in each reaction. The unsealed reactor vessel was then brought inside a glovebox equipped with a nitrogen atmosphere in which solvent and any other additives were introduced. The reactor vessel was then sealed under the nitrogen atmosphere. If a hydrogen atmosphere was used, the reactor was then vacuumed and refilled to 1 atm H_2 three times then H_2 added until the desired pressure. The reactor vessel was heated in a molten salt bath while stirring at 450 rpm. Reaction time was started when the reactor was within 5°C of the target temperature. The reactor was quickly cooled to room temperature in a water bath upon completion.

The reaction mixture was filtered through filter paper and the reactor washed with water and dichloromethane to insure complete transfer of product oil. If methanol or ethanol were used as solvent, the reactor was washed with corresponding alcohol and the

solvent was removed on a rotovap (100mbar, 50°C) immediately after filtration. The filtrate was acidified to pH 2-3, and extracted with 15 mL of dichloromethane three times. In order to prevent the loss of any volatile products, the majority of solvent was removed on a rotovap under 350 mbar and with a low temperature water bath (50°C), and the residual solvent was removed under reduced pressure (10-20 mbar) at room temperature. Pine sawdust samples were spiked with 1 mg of 2-isopropylphenol as an internal standard and dissolved in about 2 mL of chloroform. Seven drops of sample were taken for GC-MS analysis and were derivatized by the addition of 7 drops of N,O-bis(trimethylsilyl)acetamide. Samples were allowed to sit at room temperature for 20 minutes for derivatization to complete then diluted to about 0.5 mL with acetonitrile. Product quantification of samples from other biomass sources was accomplished using a standard addition method. Samples were first analyzed without an internal standard, then spiked with 1mg of guaiacol as an internal standard (2-isopropylphenol cannot be used due to the co-elution of 2-isopropylphenol and 4-propylphenol) and analyzed again.

4.2.2.3 Product characterization and quantification

4.2.2.3.1. Oil yield

The oil yield is a weight percentage of the biomass present at the start of a reaction. It is calculated by dividing the weight of the post-workup products by the initial mass of the biomass.

4.2.2.3.2. GC-MS

The silylated derivatives of lignin model degradation products were characterized and quantified by GC/MS using a Shimadzu GCMS-QP2010 SE, which uses EI for mass

selective detection. Hydrogen was used as the carrier gas. The GC flow rate was 0.92 mL/min through a Rxi-6Sil 30 m length \times 0.25 mm ID, 0.25 μ m film thickness crossbonded 1,4-bis(dimethylsiloxy)phenylene dimethyl polysiloxane column. A 240°C injection temperature and initial oven temperature of 60°C was used with a split ratio of 10. The oven temperature was immediately increased after injection at a rate of 15°C/min to 120°C at which point the temperature was held for 30 seconds. The temperature was then increased at 25°C/min to 240°C and held for 17 minutes to insure complete product elution.

Mass spectra were recorded in TIC mode. Products were identified using the mass spectroscopy NIST database when available. Products not found in the NIST database were identified by NMR, standards and/or mass fragmentation patterns (Table 3). The mass of each product was calculated by integration of the corresponding TIC peak, comparing the area to that of the internal standard, and multiplying by the response factor and the product molecular weight. The internal standard for pine sawdust decomposition runs was 2-isopropylphenol. The internal standard for runs using other biomass was guaiacol because 2-isopropylphenol co-elutes with the decomposition product, 4-propylphenol. In the latter case, a sample was run prior to the addition of internal standard to account for the small amount of guaiacol produced during the reaction. Response factors of the products were obtained by calibration with commercial or synthesized standards (See Table 3) or obtained by ECN-based calculations.¹²¹

When standards were available, the response factor was established by preparing up to five solutions near the approximate concentration of products that would be produced from dimer degradation and reaction workup. Each standard was derivatized with N,O-

bis(trifluoromethyl silyl)acetamide and run in triplicate using the same temperature program described above, stopping once 240°C was reached. The theoretical amount of analyte was calculated by comparing the area of the analyte peak to that of the internal standard. The response factor is the known amount of analyte divided by calculated amount. The response factor was found to be constant across the tested range (1.070±0.032 for guaiacol and 1.089±0.033 for 4-propylguaiacol). Response factors for a guaiacol standard were obtained by converting the response factors found relative to the 2-isopropylphenol standard. This was accomplished by dividing the response factor of a given analyte vs 2-isopropylphenol by the response factor of guaiacol vs 2-isopropylphenol.

Due to a lack of purified material, multiple standards of 2-methoxy-4-(2-(2-methoxyphenoxy)vinyl)phenol could not be reliably prepared. Instead 1mg of internal standard was added to the product mixture of entry 5 in Table 4. An NMR sample was taken of the product mixture and the molar ratio of the internal standard to both the (Z) and (E) isomers calculated by comparing the integration of the isopropyl quintet (~3.0 ppm) of the internal standard to the characteristic HC=CH peaks of the vinyl ether. GC-MS of the sample was performed in triplicate. The response factor was calculated by dividing the molar ratio of vinyl ether to internal standard established using NMR by the calculated molar ratio of vinyl ether to internal standard found by GC-MS.

A similar procedure was performed to calculate the response factor for 4-(3-hydroxypropyl)-2-methoxyphenol. A relatively pure sample of this compound was obtained by combining the product mixtures of entries 3-4 and 8-10 from Table 8 and separating using column chromatography. Approximately 12mg of pure 4-(3-

hydroxypropyl)-2-methoxyphenol was spiked with 1mg of internal standard (2-isopropylphenol) and a proton NMR was taken. The molar ratio was calculated by comparing the integration of the isopropyl quintet (~3.0 ppm) of the internal standard to the benzoic protons of the analyte (divided by 2 to account for the 2:1 proton ratio). GC-MS of the sample was performed in triplicate. The response factor was calculated by dividing the molar ratio of vinyl ether to internal standard established using NMR by the calculated molar ratio of vinyl ether to internal standard found by GC-MS.

If a standard was not available for a product observed in the GC-MS chromatogram, a response factor was assigned using an estimated carbon number (ECN) method. In the context of this method, silicon was considered to be synonymous with carbon. This method provided response factors comparable to those established using standards for compounds with simple functional groups (0.96 ECN vs 1.09 actual for 4-propylguaiacol, 0.74 ECN vs 0.75 actual for 4-(3-hydroxypropyl)-2-methoxyphenol) but breaks down for small aromatics (1.27 ECN vs 1.07 actual for guaiacol). It can be assumed that syringol and 4-propylsyringol will ionize similarly to their guaiacol counterparts as the only structural difference is the presence of a methoxy group on the ring. Therefore, in order to help mitigate these errors for syringol and 4-propylsyringol, the ECN value was adjusted by multiplying the ECN response factor by the actual response factor of guaiacol or 4-propylguaiacol, respectively, over the ECN response factor.

The product yield is reported as a carbon yield and is defined as followed:

$$\% \text{ yield (C\%)} = \frac{\sum(m_{\text{product}} \times \text{wt\%}C_{\text{product}})}{m_{\text{lignocellulose}} \times \text{wt\%}C_{\text{lignin}} \times \text{wt\%}C_{\text{lignin}}} \times 100 \quad \text{Equation 6}$$

$$\text{wt\%}C_{\text{product}} = \#C_{\text{product}} \times \frac{MW_C}{MW_{\text{product}}} \quad \text{Equation 7}$$

$$\text{wt\%}C_{\text{lignin}} = \#C_{\text{lignin monomer}} \times \frac{MW_C}{MW_{\text{lignin monomer}}} \quad \text{Equation 8}$$

The wt%C of the product and lignin monomer is the percent of the mass that can be attributed to carbon; thus it is the number of carbons multiplied by the molar mass of carbon (12.011 amu) divided by the molar mass of the product or lignin monomer. The molecular weight of the lignin monomer is the average molecular weight of the three monolignols (*p*-coumaryl alcohol, coniferyl alcohol, and sinapyl alcohol) based on the distribution of H, G, and S units in the lignocellulose sample as determined by HSQC. The yield (C%) is then the mass of the product multiplied by its wt% carbon over the mass of the lignin monomer multiplied by its wt% carbon.

4.2.2.3.3. Maximum theoretical monomer yield

It is useful to consider the theoretical maximum monomer yield that can be obtained from a given substrate, as it is one of the only ways to compare the effectiveness of a depolymerization method between substrates. The maximum theoretical monomer yield is essentially dependent solely on the ether bond content of the lignin polymer. Although lignin is in reality a cross-linked 3-D polymer, an estimate can be made using a linear polymer chain model in which any given monomer is linked to 2 other monomer units by either a C-C bond or ether bond. Therefore, the probability that each linkage will be an ether bond is equal to the fraction of ether bonds in the given substrate. In order for a monomer to be obtained, both linkages must be ether bonds; therefore the maximum

monomer yield is the square of the fraction of ether bonds. The ether bond content of pine lignin is typically around 55-60%,²⁸ meaning the theoretical maximum monomer yield is 30-36%.

4.2.2.3.4. GPC

Samples were investigated by gel permeation chromatograph using an Agilent 1100 series HPLC system with ChemStation B.04.03 and GPC Data Analysis B.01.02, equipped with two serial GPC columns (PL1110-6500: PLGel 5 μ m MIXED-C 7.5 x 300 mm). Guaiacol, 2-methoxy-4-propylphenol, (*E*)-2-methoxy-4-(2-(2-methoxyphenoxy)vinyl)phenol, and guaiacylglycerol- β -guaiacyl ether, 5K PS, and 9k PS were used as standards to generate a calibration curve in order to approximate the molecular weight and abundance of oligomeric and polymeric reaction components. Freshly distilled tetrahydrofuran was used as the solvent. The flow rate was 1 mL/min and elution was monitored using a UV-Vis detector at 290nm.

4.2.2.4 Zinc oxide synthesis

Zinc oxide was synthesized by placing 3g of Zn dust (6-10 μ m) along with 5mL water and a stir bar in the reactor vessel and heating to 180°C for 6 hours while stirring at 360 rpm. The reactor was cooled to room temperature and slowly vented. The resulting dispersion was filtered, washed with DI water, and dried overnight at 140°C in air to afford a cream white powder.

4.3 Results and discussion

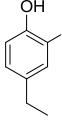
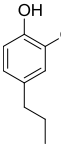
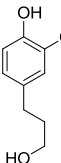
4.3.1 Lignin depolymerization in pine sawdust with external reducing agent (H₂ or Zn)

4.3.1.1 Effects of reaction conditions

Table 11 summarize the results of a series of reductive depolymerization reactions using Zn metal or H₂ as a reducing agent and a nickel catalyst. Previous work on a lignin dimer using the same catalytic system established the roles of each system component. Nickel was shown to catalyze β-O-4 bond cleavage and hydrogenate carbonyl species and olefins. Zinc was shown to act as a source of time released H₂ and ZnO and was unable to actuate reduction in the absence of nickel. The product yields are given as a carbon percent of the lignin component. The oil yield is given as a weight percent of the raw biomass used in the reaction. It should be noted that because the biomass is not Soxhlet extracted, a portion of the total extractable material (13.21% wt) dependant on the reaction conditions will be present in the product oil, rendering direct comparison of oil yields between different solvents and temperature invalid. Entries 1-12 study the Ni/C and Zn metal system. Entries 1-2 investigate the possibility of utilizing water as a solvent using Zn and H₂, respectively. Entries 3-4 investigate the effects of alkaline solution with Zn and H₂, respectively. Entry 5 utilizes a Ni/Zn catalyst in 4% NaOH that had previously been shown to be effective in a dimer decomposition study under strongly alkaline conditions. Entries 6-7 investigate the use of Zn with pure ethanol and methanol as reaction solvents, respectively. Entry 8 serves as a comparison by using H₂ with pure ethanol. Entries 9-14 examine the effect of the 1:1 water-alcohol solvent system with entries 9-10 using the standard 6 hour reaction time at 200°C. Entries 11-12 examine the

effect of extended reaction time and entries 13-14 study the effect of higher reaction temperature within the 1:1 solvent system. Pine sawdust was used in all runs due to its previously noted resistance to depolymerization and simplified analysis. 4-*n*-propylguaiacol (PG), 4-*n*-propanolguaiacol, and 4-*n*-ethylguaiacol compose the bulk of the identified monophenols in the product mixtures. Syringol derivatives were never observed, indicating that it likely composes <1% of aryl lignin moieties.

Table 11. Reductive delignification of pine sawdust with external reducing agent

Entry	Conditions ^a	Temp (°C)	t (h)	Product Yields (C%)					
							Other	Total	Oil Yield (% wt)
1	Ni/C, Zn, H ₂ O	200	6	0.2	5.4	0.7	0.3	6.6	14.5
2	Ni/C, 4atm H ₂ , H ₂ O	200	6	0.2	15.8	2.7	1.0	19.7	24.9
3	Ni/C, Zn, 4% NaOH	200	6	2.7	0.6	0.5	1.0	4.8	32.5
4	Ni/C, 4atm H ₂ , 4% NaOH	200	6	4.3	0.6	2.2	1.1	8.3	22.8
5	Ni/Zn, 4% NaOH	200	6	2.6	0.4	0.7	0.4	4.2	26.9
6	Ni/C, Zn, EtOH	200	6	0.2	10.0	0.6	1.0	11.8	9.8
7	Ni/C, Zn, MeOH	200	6	0.2	10.2	0.5	1.2	12.2	10.1
8	Ni/C, 4atm H ₂ , EtOH	200	6	0.2	32.0	1.4	1.3	34.8	30.8
9	Ni/C, Zn, 1:1 EtOH/H ₂ O	200	6	0.4	20.7	1.6	0.4	23.1	21.0
10	Ni/C, Zn, 1:1 MeOH/H ₂ O	200	6	0.3	13.8	1.0	1.4	16.4	16.8
11	Ni/C, Zn, 1:1 EtOH/H ₂ O	200	18	-	21.7	1.9	0.6	24.3	26.0
12	Ni/C, Zn, 1:1 MeOH/H ₂ O	200	18	0.3	16.8	1.1	0.8	19.0	17.0
13	Ni/C, Zn, 1:1 EtOH/H ₂ O	220	6	0.5	24.4	2.2	0.9	28.0	31.0
14	Ni/C, Zn, 1:1 MeOH/H ₂ O	220	6	0.5	23.0	1.7	0.8	26.0	28.5
15	Pd/C, Zn, 1:1 EtOH/H ₂ O	200	6	0.3	20.0	5.8	0.8	27.0	23.3
16	Pd/C, Zn, 1:1 MeOH/H ₂ O	200	6	0.3	23.3	6.2	0.9	30.7	19.8

^a400 mg pine sawdust, 4 mL of solvent, 14mg of Ni (59.3mg Ni(OAc)₂ or 140mg 10% Ni/C), 200 mg (3.06 mmol) of 6-10 μm Zn metal when used, 163mg (4 w/w%) NaOH when used, 140mg 10% Pd/C when used.

It is a fundamental concept of organic chemistry that reaction mechanisms and chemical kinetics, and thus product selection, are highly dependent on the polarity and proticity/aproticity of the solvent. Within the context of lignin depolymerization from raw biomass, solvent choice is of great importance in that it affects not only the efficacy and

mechanism of depolymerization, but also the extraction of lignin from the cellulose matrix and the degradation or preservation of cellulose. Solvents used in this study were limited to water (neutral and 4% NaOH), ethanol, and methanol. In terms of both sustainability and economic viability, water is the foremost choice for use on an industrial scale.

The use of neutral water with Zn (entry 1) resulted in a low monomer yield of 6.4C% with PG comprising 5.4C% while H₂ (entry 2) resulted in a 19.2C% yield with PG comprising 15.8C%. It was noted in both cases that the wood chips did not retain their shape and reduced sugar alcohols were observed in the GC-MS (Figure 15), indicating that the hemicellulose and/or cellulose component was hydrolysed to some extent. The significant difference in yield between entries 1 and 2 can be attributed to the rate of lignin depolymerization relative to the rate at which H₂ is generated. In entry 2, the entirety of the reducing agent (H₂) is immediately available whereas in entry 1 it must be generated over time. The low yield of entry 1 implies that lignin depolymerization occurs faster than H₂ can be produced resulting in condensation of reactive intermediates and thus product loss.

The yields of entries 1 and 2 can be further rationalized by considering that the solubility of large lignin fragments in water is likely quite low even at elevated temperatures, which may cause fragments to aggregate into micelles instead of dispersing into solution. This is undesirable because it increases the proximity of the reactive lignin intermediates, increasing the rate of condensation. This problem is intensified when H₂ is limited due to the high surface area of the catalyst and its affinity towards lignin species, which serves to promote aggregation and thus condensation. It is also possible that the

release of soluble sugars over the course of the reaction contribute to the low monophenol yield observed for entry 1. The sugars could compete with lignin intermediates for the limited amount of H₂ as it is produced from the reaction of Zn and water. Conversely, when an abundance of H₂ is present as in entry 1, there is sufficient reducing agent for both the lignin degradation products and released saccharides. However, far fewer reduced sugar alcohols are observed in the chromatogram of entry 1 than entry 2 (Figure 15). Indeed, it appears that reduced sugar alcohols and monophenol products exhibit a direct relationship when aqueous conditions are applied. Several studies on the enzymatic hydrolysis of cellulose have reported delignification as the most important factor governing the process.¹⁵⁰⁻¹⁵¹ It is expected that lignin would function similarly under our conditions, denying the catalyst and solvent access to the cellulose and slowing hydrolysis. Therefore, a higher degree of delignification results in increased hydrolysis of cellulose which produces soluble sugars that can compete for reduction. This self-limiting behaviour poses an intrinsic problem to using water as solvent for valorizing lignin directly from raw biomass.

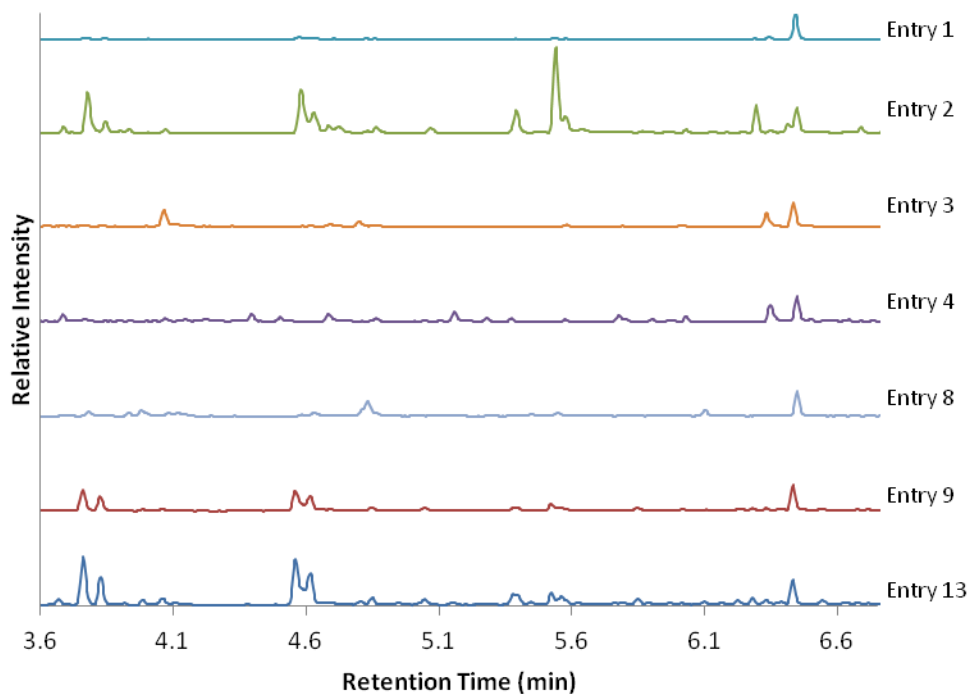


Figure 15. GC-MS chromatograms of 6h methanol entries from Table 11 depicting the amount of hemicelluloses/cellulose derived alcohols relative to the concentration of internal standard. Each chromatogram is normalized to the internal standard (peak at 6.42 minutes). Other peaks represent the abundance of 5 or 6 aliphatic carbon chains containing one or two hydroxyl groups. The lack of aromatic moieties indicates that these alcohols must be derived from polysaccharides.

Alkaline water is often used for the hydrothermal treatment of lignin and has been shown to increase oil yields.^{101, 152} The benefits of alkaline solution can be attributed to slowed condensation of carbonyl intermediates with phenols due to the pH dependant nature of the reaction as well as the increased solubility of phenols in basic water and thus better dispersion. However, lower monomer yields were obtained for both systems (5.7C% and 8.8C% for entries 3 and 4, respectively) compared to their neutral water counterparts. Initially it was thought that strongly alkaline conditions greatly increase the rate of cellulose hydrolysis as very little organic material was recovered on the filter. However, when the solution was acidified, a white pulpy precipitate was formed. Additionally, very little reduced alcohol sugars were present in the extracted samples

regardless of the chosen reducing agent as shown in Figure 15. This implies that cellulose was not hydrolyzed but rather converted to another polymorph. This is consistent with the cellulose hydrolysis – delignification relationship previously described.

Under basic conditions, lignin depolymerization is extremely limited. This is because the lignin depolymerization mechanism is different under basic conditions as evident by the selection for 4-ethylguaiacol (**2**) which is only produced in trace amounts in neutral water. Under basic conditions, β -O-4 cleavage is suppressed and a retro-aldol process becomes dominant, forming pi bonds between α and β carbons along the polymer backbone through the release of formaldehyde. In the case of β -O-4 bonds, the vinyl ether can then be reductively cleaved to form **2**. This final step is likely quite difficult as the unsaturated lignin polymer or oligomer is likely more resistant to hydrolysis and elimination reactions than the original lignin, resulting in slower degradation of the lignin polymer fragments.

Using a lignin dimer model, we previously demonstrated that nickel reductively deposited on zinc (Ni/Zn) was a superior catalyst to Ni/C in alkaline water due to its relative ineffectiveness at cleaving the β -O-4 bond, thereby making vinyl ether formation and subsequent reductive cleavage the dominant pathway. The advantage to this strategy is that reactive intermediates are entirely avoided, thus preventing repolymerization. The use of this catalyst (entry 5) resulted in a 6.3C% yield with **2** comprising 2.6C%, which is very similar to that of entry 3. Given that low yields are observed in all cases and that reduced alcohol sugars are nearly absent from the product mixtures, it must be that reduction of the unsaturated polymer chain is extremely limited. It is interesting to note that despite the low monomer yields, large oil yields were obtained for all reactions

conducted under basic conditions, which is indicative of lignin fragmentation and the absence of repolymerization. The use of alkaline water is obviously a poor choice for single pot lignin valorization but given its ability to prevent condensation reactions it may be useful in a two step process in which lignin is first allowed to undergo the retro-aldol reaction then reduced in a better solvent such as ethanol.

Ethanol and methanol are cheap renewable commodity chemicals that could reasonably be used as solvent for lignin valorization processes. Alcohols can better solubilize lignin than neutral water and cannot hydrolyze cellulose, leading to a more selective reaction system. The replacement of water with ethanol in the presence of Zn (entry 6) resulted in a 84% yield increase compared to entry 1 (6.4C% to 11.8C%) caused almost entirely by the increase of **3** (5.4C% to 10.0C%). The replacement of water with methanol in the presence of Zn (entry 7) resulted in an almost identical yield and product distribution. When ethanol was used in conjunction with H₂, an extraordinarily high monomer yield of 34.8C% was obtained, a 81.3% increase from entry 2, and is consistent with a quantitative monomer yield for lignin substrate containing 59% cleavable ether bonds (see 4.2.2.3 ii).

All three reactions are selective in that only lignin was depolymerised while the cellulosic component remained intact. This is reflected by the retention of wood chip shape, lack of reduced alcohol sugars in the GC-MS, and the lower oil yields relative to the amount of monomer compared to the reactions run in water. The large difference in monomer yield between the reactions with Zn and the reaction with H₂ is explained by the fact that the reaction of Zn with alcohols to evolve hydrogen gas is much slower than that with water. When 2M HCl was added to the filtered solid of entries 6 and 7,

sustained effervescence was observed indicating that a significant portion of the metallic zinc survived, indicating that the hydrogen pressure within the reactor must have been very low at any given point. Comparing these entries (Table 11, entries 6-7) to entries 1-2 and 4-5 in Table 12, it is apparent that alcohol can serve as a reducing agent in the presence of Ni/C and likely participates in the reduction observed in these entries. Further discussion on the use of alcohol as a hydrogen source can be found in section 4.3.2.

Given its potential as a recyclable hydrogen source in the context of an industrial process, Zn was used as a reducing agent in alcohol-water solvent mixtures in an effort to improve monomer yields and reaction selective compared to entries 1 and 3. The addition of ethanol caused a substantial improvement of phenolic monomer yield to 23.0C% of which PG comprises 20.7C%. Methanol induced a similar, though lesser, result; increasing the phenolic monomer yield to 16.4C% of which **3** comprises 13.8C%. The yield enhancement can largely be attributed to improved solubility and dispersion of lignin in the solvent mixtures. The yields obtained are comparable to that of neutral water with a large hydrogen reservoir (entry 2) and significantly lower than that of H₂ in ethanol (entry 8), indicating that the rate of lignin degradation is still greater than the rate of hydrogen production, resulting in the condensation of some lignin product. The difference in yield between entries 1, 9 and 10 reflect the relative solubility of lignin in the given solvents as follows: H₂O < 1:1 MeOH/H₂O < 1:1 EtOH/H₂O.

The relative solubility of lignin affects the rate at which condensation occurs. Because lignin is degraded faster than it can be reduced, reactive intermediates accumulate in the reaction mixture. EtOH/H₂O can best solvate these reactive lignin fragments, keeping them more dispersed in solution and preventing aggregation on the

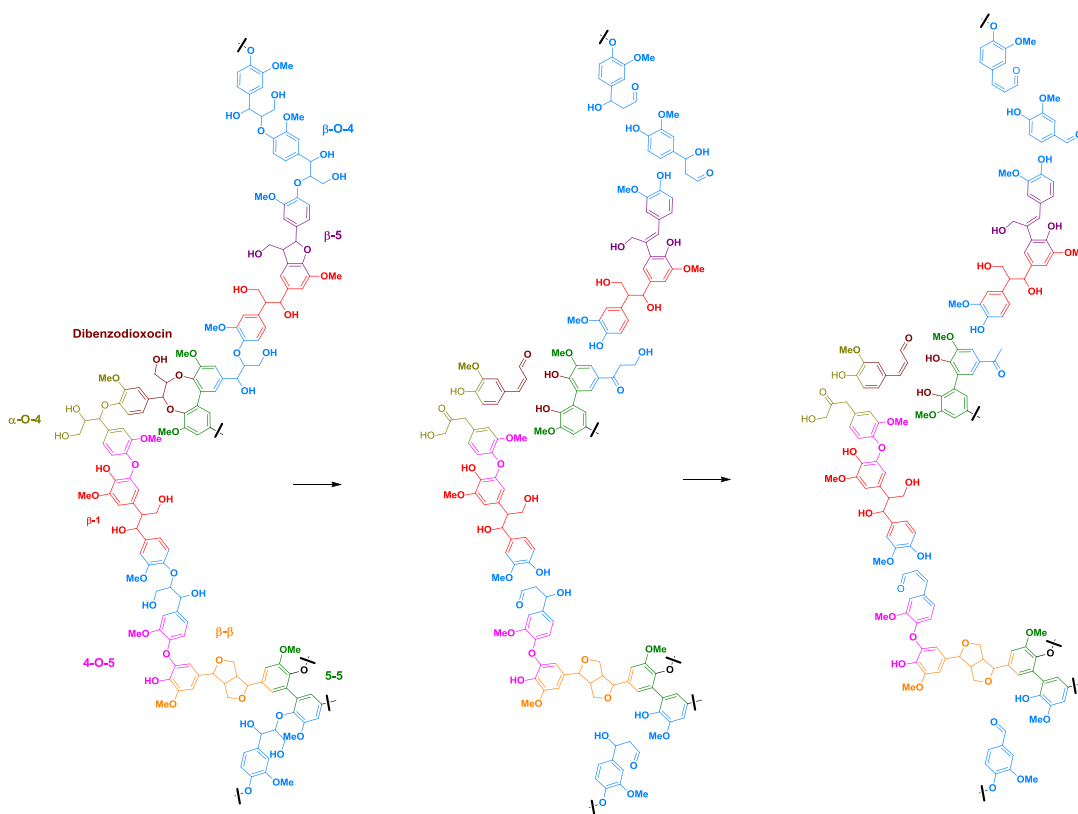
catalyst surface, and thus slowing condensation. A lower amount of reduced sugar alcohols relative to the monomer yield was noted for entry 9 when compared to entry 2 as seen in Figure 15, meaning cellulose hydrolysis was slowed with the addition of ethanol. This likely also improved the monomer yield due to fewer sugar alcohols competing for H₂. A final possibility is that some H₂ is produced from the oxidation of the alcohol solvent. However, given that methanol is shown to be a better hydrogen source at 200°C both in Table 12 and in literature^{146, 153} and that the yield of entry 10 is lower than that of entry 9, the hydrogen produced from alcohol is minimal.

When the reaction time was increased to 18 hours, only a marginal 1C% increase in monomer yield was observed in EtOH/H₂O (entry 11). A more substantial increase of 2.5C% was observed in MeOH/H₂O (entry 12). A possible explanation for this is that lignin is extracted and degraded slower in MeOH/H₂O than in EtOH/H₂O while cellulose is hydrolysed quicker, resulting in a lower monomer yield. This explanation is consistent with the expectant solubility of the cellulosic and lignin fractions in both solvent systems. It would make sense then that additionally monomer would be obtained with lengthened reaction time in the case of MeOH/H₂O. Nonetheless, both entries demonstrate the impressive stability of the reduced lignin product mixture at high temperatures for an extended time. An increase of reaction temperature resulted in a significant increase in monomer yield for both EtOH/H₂O (entry 13, 27.9C%) and MeOH/H₂O (entry 14, 25.8C%). This can be attributed almost entirely to the catalytic oxidation of alcohol over the nickel catalyst, providing another source of hydrogen within the reactor. Evidence of such can be seen in entries 8-11 in Table 12 which demonstrate reductive depolymerization in the absence of zinc metal and H₂ at the same reaction temperature.

The only difference between entry 14 in Table 11 and entry 11 in Table 12 is the substitution of ZnO for Zn, in which case a 14.5% monomer yield was obtained. The yield increase seen in MeOH/H₂O (entry 14) is more pronounced than that seen in EtOH/H₂O (entry 13) due to methanol being a superior source of hydrogen (see 4.3.2).

4.3.1.2 Mechanism

Lignin depolymerization under the tested conditions occurs primarily through the cleavage of ether linkages as evident by the preservation of the 3 carbon chain in the major products (basic conditions are an exception and are explained below). There are 4 possible paths, shown in Scheme 1, that result in the cleavage of alkyl aryl ether linkages in lignin: 1) elimination 2) retro-aldol followed by subsequent reduction and cleavage 3) homolysis and 4) Ni-catalysed bond cleavage. The 4-O-5 bond, an aryl ether, can only be broken by path 4. Path 4 is unique in that it requires contact with the catalyst surface whereas paths 1-3 can happen anywhere in the reaction mixture. Lignin in raw biomass is insoluble with softwood lignin being even less soluble compared to hardwood lignin due to crosslinking caused by 5-5' bonds. Due to the rigidity and low solubility, contact with the catalyst surface is minimal, making path 4 non-competitive with paths 1-3 until lignin can be better solubilized. Solubility is likely conferred upon fragmentation through paths 1-3, after which bond cleavage (path 4) and reduction on the catalyst surface can more readily occur.¹⁴⁶



Scheme 11. Depolymerization of a sample lignin fragment via the elimination pathway. Elimination results in the cleavage of α -O-4 and β -O-4 ether bonds and the formation of carbonyl species. Carbon linkages and the 4-O-5 linkages remain intact.

We previously demonstrated that alkyl aryl ether cleavage predominately occurs by elimination (path 1) in neutral aqueous and alcohol solutions in the absence of Ni. Scheme 2 illustrates the elimination pathway for a lignin fragment containing the most prominent linkages identified in softwood lignin.²⁸ Elimination results in chain cleavage at β -O-4 and α -O-4 bonds, producing a free phenol and hydroxy carbonyl species. In the case of the β -O-4 bond, elimination can occur at the α or γ carbon to give a β -hydroxy ketone or aldehyde, respectively, which were observed in the dimer study. Under reductive conditions, these products are converted to **3** and **5**. When reduction cannot occur, or is slow, the hydroxy ketone or aldehyde can be consumed in condensation reactions with phenols or undergo a retro-aldol reaction, forming vanillin and

acetovanillone in the case of monophenols. These latter products were shown to be able to be reduced to 4-methylguaiacol and 4-ethylguaiacol, both of which appear as ubiquitous trace products in this study. The presence of these products, particularly 4-methylguaiacol, indicates that depolymerization occurs by elimination to some extent. While alkyl aryl ether cleavage on Ni also lead to the formation of the β -hydroxy ketone or aldehyde, their subsequent transformation to vanillin and acetovanillone is less likely to occur before reduction, as they are already on the catalyst surface. With this in mind, the formation of these downstream products is an expected result brought about by limited contact with both the catalyst surface and other reactive species due to insolubility and rigidity during early chain fragmentation. No other linkages in lignin result in chain fragmentation upon elimination. Phenyl coumaran (β -5) is the only other linkage that shows any change and undergoes a ring opening reaction as evident by the lack of signal in the GC-MS despite being one of the more abundant linkages. Interestingly, 2 signals attributed to β -5 dimer structures **8** and **9** are observed as shown in the product spectrum of Entry 8 (Figure 16).¹⁵⁴⁻¹⁵⁵ Compound **9** could be formed through either elimination as shown in Scheme 11, or through C-O cleavage over Ni similar to path 4 in Scheme 10 followed by reduction of the double bond. A product containing the completely reduced terminal alcohol was expected but not observed, nor has it been observed in literature.^{143, 154-155} Compound **8** is almost certainly formed by a retro-aldol process (path 2) as evident by the loss of the γ -carbon as shown in Scheme 12.

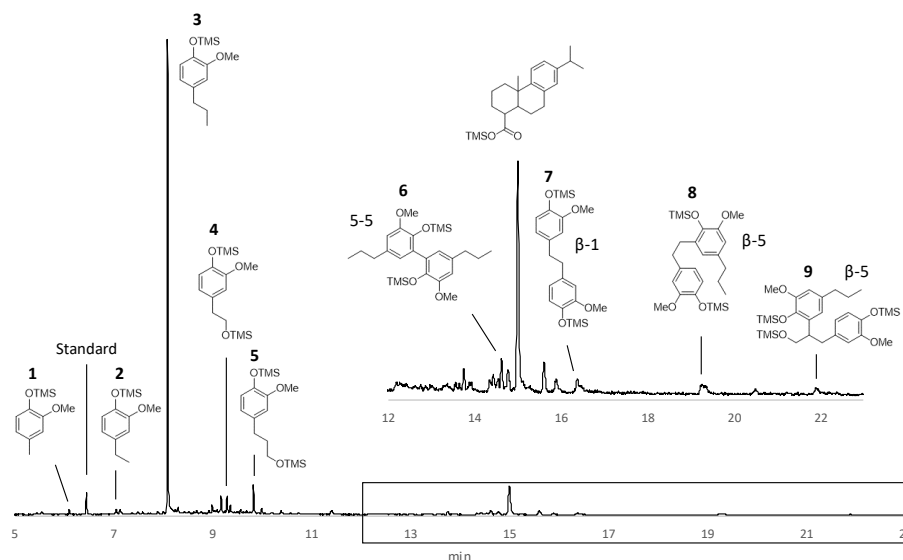
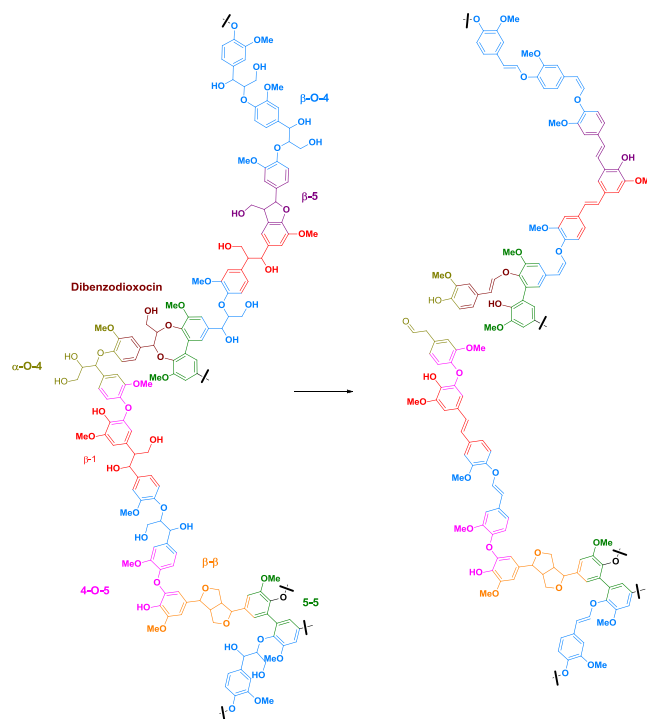


Figure 16. GC-MS chromatogram and peak identification of trimethylsilylated lignin monomers (1-5) and dimers (6-9) (reaction conditions: Entry 8 Table 11). The internal standard is 2-isopropylphenol. A relatively high abundance of dehydroabietic acid (15 min) is observed due to the reaction being conducted without extractive pre-treatment.

Pathway 2 is a retro-aldol reaction that results in the loss of the γ -carbon as shown in Scheme 1 and is activated in alkali conditions as evident by the change in product selectivity towards **2** seen in entries 3-5. Two possible mechanisms for the retro-aldol process were identified during the study of the β -O-4 dimer model and are shown in Scheme 5. The mechanism shown on the left side is a two-step reaction that requires a free phenol be dehydrated to quinone methide before proceeding whereas the mechanism on the right is a single concerted process. Within the lignin polymer, there are very few free phenols which would largely prevent the retro-aldol reaction if the nonconcerted mechanism was dominant. If that were the case, it would be expected that elimination would occur, resulting in the selective production of products **3** and **5**, which are obtained in a lower amount than **2** in entries 3-5. Therefore, it must be that the concerted mechanism is dominant and that retro-aldol reactions can occur virtually anywhere in the

polymer chain as shown in Scheme 12. The retro-aldol reaction does not result in chain fragmentation for any linkages except for α -O-4, and instead forms a more rigid and robust polymer bonded primarily through vinyl ethers. The formation of double bonds prevents ether cleavage through elimination, meaning that reduction is necessary for depolymerization to proceed any further. However, the double bonds along the polymer backbone severely restrict movement by preventing rotation and the loss of all hydroxy groups further limit solubility, preventing interaction with the catalyst surface and greatly slowing reduction. This results in low monomer yields for entries 3-5 for no reason than that the reaction is slow. GPC results, shown in Figure 17, confirm that there is a greater relative concentration of short oligomers to monomers for alkaline entries (3-4) than neutral entries (1-2).



Scheme 12. Depolymerization of a sample lignin fragment via the retro-aldol pathway. Only α -O-4 bonds are cleaved by the retro-aldol reaction that occurs in the presence of base. β -O-4 linkages are converted to vinyl ethers while β -1 linkages containing α and γ hydroxyl groups are converted to stilbene moieties.

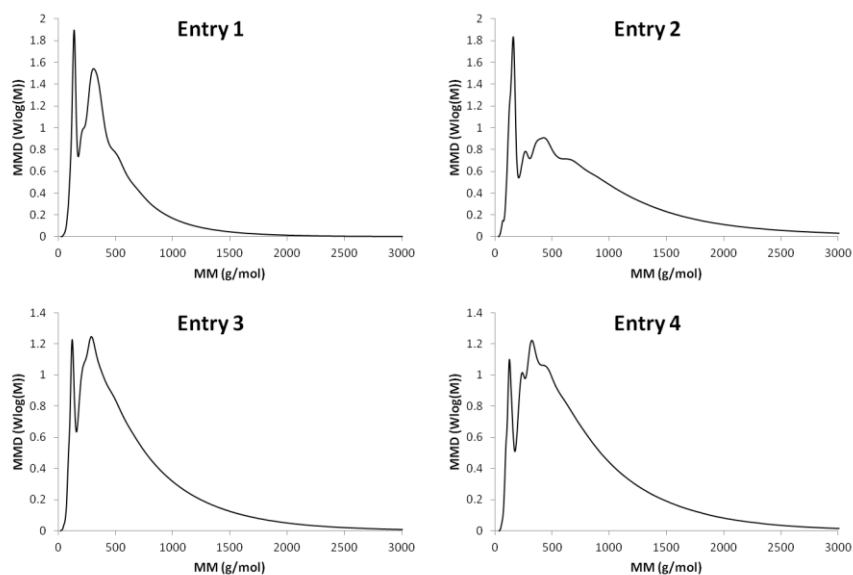
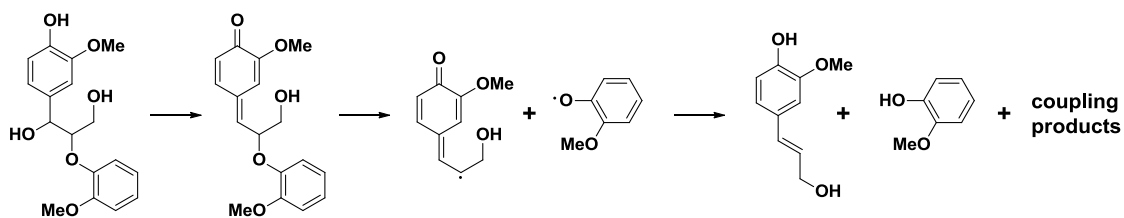


Figure 17. Mass distribution of products in DCM oil of entries 1-4. Entry 1: Ni/C, Zn, H₂O. Entry 2: Ni/C, 4 atm H₂, H₂O. Entry 3: Ni/C, Zn, 4% NaOH. Entry 4: Ni/C, 4 atm H₂, 4% NaOH.

A few studies have cited homolysis as a prominent ether cleavage mechanism and provide the mechanism shown in Scheme 13.¹⁵⁶⁻¹⁵⁷ Assuming this mechanism is correct, the homolytic cleavage of the β -O-4 bond is predicated on the conversion of the phenol moiety to quinone methide; a process that requires a free 4-hydroxyl group which sometimes occur at chain termini but is rare within the lignin polymer. Therefore, it is unlikely that homolysis could be a competitive process in the case of β -O-4 cleavage. Additionally, the rate of homolysis relative to elimination was previously investigated using the dimer shown in Scheme 13. It was found that even in pure ethanol, homolysis of the dimer is significantly slower than elimination. It is possible that α -O-4 homolytic cleavage could occur as the radical would be stabilized at the benzyl carbon. However, given that this would be a higher energy species (less stabilized) than the quinone methide stabilized radical, it is expected that such a process would be slower than the noncompetitive β -O-4 homolytic cleavage. Therefore, it is unlikely that homolysis is a significant pathway in aqueous and alcohol solvents.



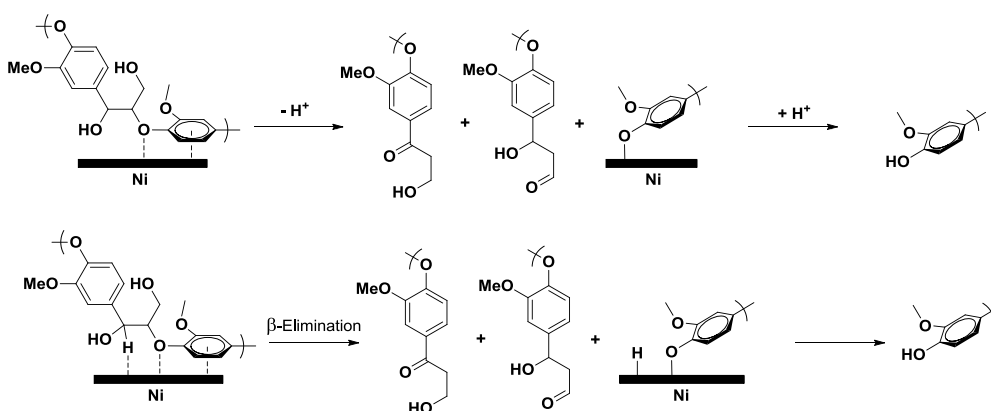
Scheme 13. Homolytic cleavage mechanism of guaiacylglycerol- β -guaiacyl ether.

Once soluble oligomers are made available in solution through fragmentation by paths 1 and 2, path 4 becomes active. We previously demonstrated that β -O-4 bond cleavage was catalysed in both the absence and presence of H_2 and was the dominant decomposition mechanism for guaiacylglycerol- β -guaiacyl ether under all neutral pH conditions. The catalytic activity of Ni/C in the absence of a hydrogen source has also

been noted in literature, however, the proposed mechanism involved metal insertion which is not possible for a heterogeneous catalyst and would result in C_{aryl}-O cleavage rather than C_{aliphatic}-O cleavage according to the literature cited.^{146, 158} Path 4 is therefore broken into two paths dependent on whether H₂ is available.

Ni-arene activated C-O cleavage, path 4a, occurs when H₂ is scarce and likely results in the same immediate products as elimination. Hydrogenolysis, path 4b, occurs when H₂ is readily available and results in simultaneous bond cleavage and reduction. In both cases it is likely that initial interaction occurs via adsorption of the aromatic ring via the overlap of π orbitals with the d-orbitals of the metal. This interaction with nickel has been shown to significantly weaken the C-O bond such that ring opening can occur in furan,¹⁵⁹ likely through π backbonding as evident by the increased sp³ character of the carbon bonds when chemisorped onto the metal.¹⁶⁰ However, in the case of α -O-4 and β -O-4 ethers, the C_{aliphatic}-O bond in which both atoms lay outside the π system is cleaved, meaning that π backbonding will have little effect on the bond strength. Although interaction with the aryl system does not directly impact the C_{aliphatic}-O bond, it does bring the oxygen into proximity with the nickel surface which has been shown to exhibit stronger binding to carbonyls than other metals such as Pd and Ru;^{159, 161-164} it is likely this interaction with the oxygen that activates the C_{aliphatic}-O bond. Further evidence of the O-Ni interaction can be seen by comparing the product selectivity of Pd/C and Ni/C in Table 11. Ni/C appears to be more effective at reducing the terminal alcohol, indicating greater binding of oxygen to Ni. Once activated and in the absence of hydrogen, the phenol moiety is quickly eliminated through either simple elimination via solvent or H elimination via the nickel surface (path 4a), as shown in scheme 6. When hydrogen is

present, hydrogenation (path4b) is the dominant pathway. Evidence of this was found in the previous dimer study by monitoring the decomposition of 2-methoxy-4-(2-(2-methoxyphenoxy)vinyl)phenol, the immediate product in basic conditions. It was found that hydrogenation of the double bond occurred first, followed very quickly by hydrogenolysis. 2-Methoxy-4-vinylphenol was only detected in trace amounts that had no correlation to the reaction progression.



Scheme 14. Proposed mechanisms for path 4a: Ni-arene activation of C-O bond. Top: Nickel promotes elimination by weakening the β -O-4 through surface interaction with oxygen. Bottom: Nickel removes the α -H to induce β -elimination.

Nickel can also cleave 4-O-5 bonds as evident by the total lack of aryl ether dimer in the chromatogram shown in Figure 16 despite occurring with the same frequency as β -1 and β -5 bonds which were observed. Diaryl ethers are activated in a manner similar to furan where the $C_{\text{aryl}}\text{-O}$ bond is sufficiently weakened by π backbonding so as to be able to undergo hydrolysis in the presence of water or hydrogenation in the presence of hydrogen on the nickel surface.¹⁶⁵ Despite the lack of water in entry 5 (Table 11), 4-O-5 hydrogenolysis products lacking a hydroxyl group, such as 1-methoxy-3-propylbenzene, were never observed. Given this result and the previously established affinity of oxygen for Ni, it is possible that the metal binding occurs selectively to the aryl moiety with more

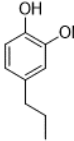
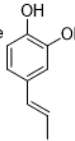
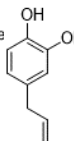
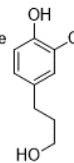
oxygen, resulting in cleavage solely on the 5 side of the 4-O-5 bond to yield two monophenols.

4.3.2 Lignin depolymerization in pine sawdust utilizing hydrogen transfer from alcohol

Several studies have reported alcohols as a convenient source of hydrogen in the presence of a metal catalyst. However, these processes typically require the use of noble metal catalysts and temperature exceeding 230°C.^{153, 166-167} A few studies have utilized this technology for lignin valorization processes and report yields up to 41% using hardwood substrate.^{143, 168-169} The work by Song *et al.* also employs this technology but is especially notable in that they were able to achieve a near quantitative yield at only 200°C using birch sawdust as a substrate. Interestingly, when similar conditions were employed using pine sawdust as substrate (entry 1, Table 12) a moderate yield of 13.6C% was obtained with the major products being eugenol and isoeugenol as opposed to the fully reduced compound **3**. The monomer yield is strongly tied to the biomass processed. It has been shown that biomass containing a large percentage of syringyl moieties, such as hardwood, is far more susceptible to depolymerization and far less susceptible to repolymerization due to the occupation of the 3 and 5 positions of the aromatic ring by methoxy groups, reducing crosslinking through largely uncleavable C-C bonds such as β -5, and 5-5 and preventing condensation at these sites.^{27-28, 170} This phenomena can be observed in the results of Van den Bosch *et al.* wherein they report a 50% yield using hardwood (birch), a 21% yield using softwood (pine-spruce), and a 27% yield using grass (miscanthus).¹⁴³ However, considering that a near quantitative yield was obtained when a large hydrogen reservoir was available (entry 8, Table 11), it is not merely the lignin

substrate that affects the reaction yield but rather the relative rates of hydrogen production and lignin condensation.

Table 12. Reductive delignification of pine sawdust utilizing hydrogen generation from an alcohol solvent

Entry	Conditions ^a	Temp(°C)	<i>t</i> (h)	Product Yields (C%)				Other	Total	Oil (%wt)
				3	11	10	5			
										
1	Ni/C, MeOH	200	6	1.8	0.9	10.6	0.3	-	13.6	25.0
2	Ni/C, EtOH	200	6	-	0.5	4.3	0.2	-	5.1	18.3
3	Ni/C, <i>t</i> -BuOH	200	6	-	0.2	1.3	-	-	1.5	nd
4	Ni/C, ZnO, MeOH	200	6	13.1	0.5	2.3	0.6	0.3	16.8	13.3
5	Ni/C, ZnO, EtOH	200	6	10.9	0.1	0.9	0.8	0.3	13.0	13.0
6	Ni/C, ZnO, MeOH	200	18	18.0	-	0.4	1.0	0.3	19.6	17.3
7	Ni/C, ZnO, EtOH	200	18	16.1	-	0.5	1.3	0.6	18.5	19.8
8	Ni/C, ZnO, MeOH	220	6	18.9	-	0.3	1.2	0.6	20.9	16.5
9	Ni/C, ZnO, EtOH	220	6	18.6	-	-	1.1	1.0	20.7	13.3
10	Ni/C, ZnO, 3:1 MeOH/H ₂ O	220	6	19.4	-	0.5	1.3	0.8	22.0	27.5
11	Ni/C, ZnO, 1:1 MeOH/H ₂ O	220	6	12.3	-	0.3	1.0	0.9	14.5	31.5
12	Ni/C, ZnO, MeOH	240	6	22.8	-	-	1.7	1.2	25.7	20.3
13	Ni/C, <i>t</i> -BuOH	240	6	0.4	-	-	-	0.4	0.7	nd
14	Ni/C, MeOH	240	6	24.0	-	-	1.9	1.5	27.4	22.6
15	Ni/C, BHT ^b , MeOH	240	6	5.5	0.5	15.9	0.3	-	22.3	nd
16	Ni/C, ZnO, MeOH	260	6	20.5	-	-	1.3	2.4	24.2	25.3
17	Ni/C, ZnO, MeOH	280	6	18.0	-	-	1.0	3.3	22.3	36.3

^a400 mg pine sawdust, 4 mL of solvent, 14mg of Ni (140mg 10% Ni/C), 200 mg (2.46 mmol) of ZnO made from 6-10 μm Zn metal when used. ^b47.5mg butylated hydroxytoluene used.

Entry 2 was performed under the same conditions as entry 8 from Table 11 barring the addition of hydrogen gas and resulted in 5.1C%, a significantly lower yield than entry 1. Song et al. also reported a decrease in yield when depolymerization was performed in ethanol though considerably less substantial (48% vs 54% in methanol) which they attributed to differences in lignin solubility. While solubility certainly plays a role in that it slows condensation by keeping the lignin fragments more dispersed,

consideration must also be given to the rate at which the alcohol solvent is oxidized to produce H₂. These results are consistent with Mostafa et al. who reported that ethanol decomposition over a Pt catalyst was both significantly slower and less efficient in terms of hydrogen production than methanol. In order to further illustrate this relation and potentially confirm that the alcohol solvent and not an endogenous chemical such as formic acid, cellulose, or hemicellulose is the hydrogen source, *tert*-butanol, which cannot be oxidized without significant structural rearrangement, was used as solvent at both 200°C and 240°C resulting in monomer yields of 1.5C% and 0.7C%, respectively. These results lead us to conclude that no endogenous hydrogen source exists using the reaction conditions shown in Table 12.

The addition of ZnO powder was made in entries 4 and 5 to introduce acidic sites which have been hypothesized to aid in alcohol decomposition.^{167, 171} Substantial increases in monomer yield were noted for both MeOH (entry 4, 16.8C%) and EtOH (entry 5, 13.0C%), and perhaps more importantly, the product selectively was strongly shifted to compound **3**. This is especially notable in EtOH which in the absence of ZnO was totally free of compound **3**, indicating that ZnO increases the rate of alcohol decomposition. Compounds **10** and **11** have been shown to be formed from the dehydration of compound **3**.¹⁴⁶ The fact that these products are seen predominantly in their reduced form means that either they were produced earlier in the reaction, that the alcohol solvent was decomposed quicker allowing for quicker reduction, or both. It was also noted that the addition of ZnO drastically lowered the oil yield in both cases but especially for methanol, despite increasing the monomer yield. This indicates that ZnO slows lignin depolymerization, prevents the decomposition of cellulose, or both. Figure

18 shows the chromatograms of all 6h reactions performed in methanol within the elution time of reduced sugar alcohols. It can be seen that there is little difference between entries 1 and 4 which indicates that ZnO has little effect on the cellulosic components. Thus the oil yield must be entirely attributed to the lignin component, meaning that ZnO stabilizes the lignin structure and slows depolymerization. In accordance with this conclusion, extended reaction times resulted in significant yield increases for both methanol (entry 6) and ethanol (entry 7) solvents in the presence of ZnO. Therefore, we can conclude that ZnO has 2 effects on the reaction kinetics that ultimately favour monomer production: 1) ZnO increases the rate of alcohol decomposition thereby increasing the rate at which H₂ is produced 2) ZnO slows lignin depolymerization preventing the accumulation of condensation susceptible immediate depolymerization products.

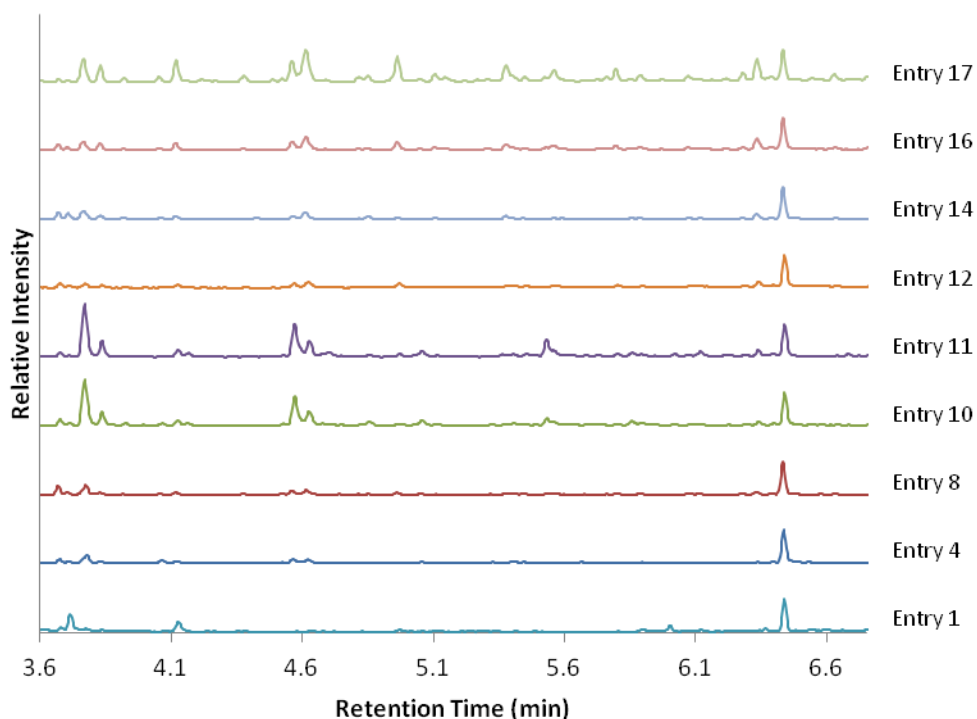


Figure 18. GC-MS chromatograms of 6h methanol entries from Table 12 depicting the amount of hemicelluloses/cellulose derived alcohols relative to the concentration of internal standard. Each chromatogram is normalized to the internal standard (peak at 6.42 minutes). Other peaks represent the abundance of 5 or 6 aliphatic carbon chains containing one or two hydroxyl groups. The lack of aromatic moieties indicates that these alcohols must be derived from polysaccharides.

Even with the addition of ZnO, the monomer yields of entries 4 and 5 are well below the maximum obtained with H₂ (entry 8 Table 11). In other words, the alcohol decomposition is too slow relative to the rate of lignin depolymerization. The temperature dependence of the alcohol decomposition over a Pt catalyst was thoroughly investigated by Mostafa et al. and methanol decomposition was shown to have an onset temperature of 175°C, less than 10% conversion at 200°C, and reached over 90% conversion at 300°C.¹⁵³ When the lignin depolymerization temperature was increased to 220°C, significant gains in monomer yield were observed for both methanol (entry 8) and

ethanol (entry 9) with little difference in the overall yield and product distribution between them. Reaction selectivity for lignin degradation remained excellent as shown by the minimal change in the amount of cellulose derived alcohols present in the chromatogram (Figure 18). Reaction efficiency was superior to reactions conducted at extended reaction time in both solvents as evident by the higher monomer yields and lower oil yields, although ethanol appears to be more selective than methanol at 220°C. Therefore, it is likely that the relative rate alcohol decomposition versus rate of depolymerization was increased for both solvents with a greater relative change occurring in ethanol. These results are consonant with the previously described lignin fragmentation/depolymerization mechanism in that elimination, which would be more favoured in more polar methanol, is the predominant lignin depolymerization pathway before chain solubility is achieved.



Methanol's decomposition pathways have been described by Equations 9-12.

Equation 9 was shown to be greatly favored when decomposition was performed on a Pt catalyst.¹⁵³ While H₂ is the salient reaction product, CO can still be utilized through the water-gas shift (Equation 11) through the addition of water. Water can also be reduced to produce carbon dioxide and hydrogen gas directly, bypassing the water-gas equilibrium (Equation 10). In this way, the addition of water can increase H₂ output by 50%.

Replacing 1 mL of methanol with 1 mL of H₂O (entry10) resulted in a small increase in

monomer yield and can be attributed to the activation of one or both decomposition processes. Selectivity was greatly affected by the addition of water. The oil yield increased disproportionately from the monomer yield and sugar derived alcohols were abundant in the product mixture as shown in Figure 18, indicating that cellulosic components are decomposed along with lignin. However, this is far from an optimized solvent ratio, as only 0.02 mL of methanol is needed for the complete reduction of the lignin fraction of the biomass (assuming 3 reductions per monomer unit), meaning that a much smaller volume of water is necessary. It is expected that the water concentration could be reduced to 2% of the added amount, which would restore selectivity while maintaining enhanced H₂ production resulting in a superior monomer yield. The addition of more water (entry 11) resulted in further loss of selectivity and a markedly decreased monomer yield.

A reaction temperature of 240°C resulted in the highest monomer yield obtained in the absence of H₂ and Zn metal, 27.4%. Interestingly, at this temperature ZnO no longer appears to be beneficial. A slightly higher monomer yield was obtained in the absence of ZnO while little difference can be seen in the product distribution and selectivity. In an effort to confirm whether radical processes were activated at this temperature, BHT was added to the reaction mixture in place of ZnO (entry 15). A marked change in product distribution was observed, with eugenol being the major product, with only a 5% drop in overall yield. The only plausible explanation is that BHT stabilizes eugenol which would normally be hydrogenated very quickly. This could only occur if BHT simultaneously slowed alcohol decomposition and lignin repolymerization. In any

case, this proves that it is possible to tune the reaction kinetics so as to select for either the saturated or unsaturated carbon chain.

Higher temperatures resulted in both decreased monomer yields and a loss of selectivity. This is likely the result of cellulosic sugars being decomposed over the catalyst surface, causing carbon build up and catalyst deactivation. This behaviour has been observed for even small alcohols such as isopropanol and 1-butanol.¹⁵³ The increasing extent of cellulose decomposition from 240-280°C is evident in the chromatograms shown in Figure 18.

4.3.3 Application to agricultural waste product substrates

One of the foremost problems in establishing a biorefinery is identifying a profitable substrate. The use of hardwood and softwood as a primary substrate has inherent disadvantages such as slower growth, a time lag of several years between planting and harvesting, and only being able to harvest the wood. Woody substrates can be obtained from mills as well but only 1606 tonnes of unutilized primary mill residues are produced annually in the US (data from 2002).¹⁷² Agricultural waste product or “bioenergy crops” are more practical substrates as they are fast growing and either utilize a product that already is mass produced and largely unutilized or can be specifically grown in the stead of other crops for energy and chemical applications. Corn stover represents one the most abundant sources of biomass residues and is already utilized for cellulosic ethanol production, making it a prime substrate for lignin valorization. Sugarcane bagasse is another excellent substrate, as it is cleaner than corn stover, does not have concerns about residue removal affecting soil conditions,¹⁷³ and is often used for cellulosic ethanol production as well. Switchgrass represents a class of potential crops known as “bioenergy

crops” that have been studied for their low cost and relatively high energy content. These perennial grasses would be cultivated solely for biomass valorization should such processes be industrially realized.

The conditions from entry 12 were applied to each substrate. All substrates resulted in a lignin oil containing a mixture of *p*-hydroxyphenyl-(H), guaiacyl-(G), and syringyl-(S) units. The relative amounts of each unit were determined by integrating the H_{2,6}, G₂ and S_{2,6} signals in the aromatic region of the HSQC spectra and are shown in Table 13 along with the lignin and extractive content.^{143, 149} All substrates also yielded various amounts of dihydro-*p*-coumaric methyl ester and dihydroferulic methyl ester which was not seen when using a pine substrate. These products are derivatives of *p*-coumaric acid and ferulic acid, which has been found to couple lignin to hemicellulose through an ester linkage with hemicellulose and an ether linkage with lignin in grasses and herbaceous crops.^{31, 174} These products then are the result of hydrogenolysis of the ether bond, hydrogenation of the alkene, and finally transesterification with methanol.

Table 13. Characterization of biomass substrates

Substrate	Lignin oil			Ratio H/G/S	Klason lignin (wt%)	Extractives (wt%)
	%H	%G	%S			
Pine	0	100	0	0.0/1.0/0.0	23.0	13.2
Corn stover	27.1	23.7	49.3	1.1/1.0/2.1	15.1	10.7
Sugarcane bagasse	35.0	28.5	36.5	1.2/1.0/1.3	18.0	2.2
Switchgrass	14.2	56.8	29.0	1.0/4.0/2.0	20.0	6.3

Corn stover resulted in an intermediate monomer yield (34.5C%) and the highest oil yield despite having the lowest lignin content due to the high amount of extractives. Sugarcane bagasse resulted in an excellent monomer yield of 46.4C% and the lowest oil

yield due to the exceptionally low amount of extractives remaining in bagasse. Switchgrass resulted in a significantly lower monomer yield compared to other substrates and had an intermediate oil yield. The lignin product oil from each substrate was examined by GPC to compare the ratio of monomeric product to oligomeric product (Figure 19). It can be seen that the product oil of sugarcane bagasse contains very few oligomers compared to both corn stover and switchgrass derived oils as evident by the much smaller peak centered around 400 g/mol, which corresponds to lignin dimer structures. It has previously been shown that delignification is correlated to the G/S ratio with a higher S content resulting in higher delignification¹⁷⁰ and higher monomer yields during reductive depolymerization.¹⁴³ This occurs due to increased frequency of β -5 and 5-5 bonds between G units due to the missing methoxy group. It is logical then to assume that H units would result in additional C-C bonding through the aromatic ring. The results of this reaction set make sense in this context, though species-specific properties appear to obfuscate the trend. An obvious example of this can be seen in the monomer distribution.

Sugarcane bagasse has an almost even distribution of H/G/S but the H units are predominantly from *p*-coumaric acid and so do not participate in C-C bond formation, resulting in a high monomer yield. Corn stover on the other hand has a similar proportion of H units but few can be attributed to *p*-coumaric acid, meaning that they must be incorporated within the lignin polymer chain and likely result in a greater frequency of C-C bonds. The high S content and low G content found in corn stover balances the H content and so results in an intermediate monomer yield. Switchgrass has a lower S and H content and higher G content than either of the other two substrates meaning that a

yield between that of pine and corn stover should be anticipated. However, a significantly lower yield than both pine and corn stover is obtained. Likely, this is the result of increased incidence of β -5 and 5-5 bonds compared to pine and corn stover. The GPC results support this conclusion, as an increased dimer peak is observed relative to the other substrates.

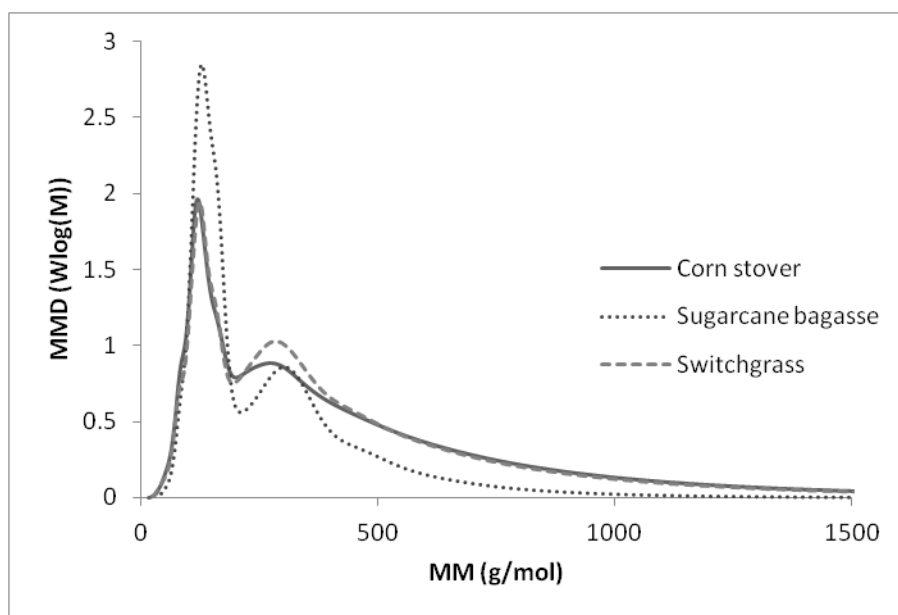
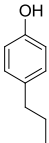
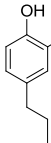


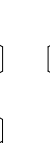


Figure 19. Mass distributions of lignin product oil from corn stover, sugarcane bagasse, and switchgrass feedstocks.

It can be concluded that the developed method is effective at depolymerising a multitude of substrates. However, given the differences in lignin structure and the importance of the relative rates of lignin decomposition and alcohol decomposition, the reaction parameters should be optimized for each individual substrate. Additionally, we have shown that selecting a substrate is not as simple as looking at the monophenolic unit ratios. It is important to know how the units are incorporated within the lignocellulosic structure. Of the substrates tested, sugarcane bagasse is the most promising. It is

depolymerised efficiently and by its nature has very little extractive and so requires no pre-treatment.

Table 14. Reductive delignification of agricultural waste products utilizing hydrogen generation from methanol

Entry	Substrate	Product Yields (C%)					Other	Total	Oil Yield (% wt)
									
1	Corn stover	7.6	6.0	10.8	3.8	2.3	4.0	34.5	23.8
2	Sugarcane bagasse	4.8	9.6	14.9	10.3	4.8	2.1	46.4	13.8
3	Switchgrass	1.0	5.7	3.5	1.6	3.0	1.4	16.2	17.0

4.4 Conclusions

The catalytic reductive depolymerization of lignin from a pine substrate was investigated. Preservation of the cellulose matrix, lignin extraction and solubilization, rate of hydrogen generation, and lignin decomposition mechanism were identified to be the most important factors governing monomer yields. These factors were shown to be affected by solvent choice, temperature, and pH. A quantitative monomer yield of 35 C% was realized using Ni/C and H₂ in ethanol with 4-propylguaiacol composing 32 C%. Ethanol and methanol solvents in the presence of Ni metal were identified as a hydrogen source for reductive depolymerization and the relevant reactions to maximize hydrogen production were examined. The presence of co-catalyst or catalyst support containing acidic sites was shown to increase hydrogen production at temperatures below 240°C. The omission of an external reducing agent resulted in a monomer yield of 26 C% using Ni/C and methanol. The lignin component of two agricultural waste crops, corn stover

and sugarcane bagasse, and an energy crop, switchgrass, were characterized by HSQC NMR and depolymerized under the same conditions. Differences in monophenol yields between substrates were attributed to differences in crosslinking which is related to the relative monomer ratios present in the native lignin of each substrate.

CHAPTER 5: CONCLUSIONS AND FUTURE WORK

5.1 Conclusions

5.1.1 Determination of the hydrothermal degradation mechanism of a lignin dimer under neutral and basic conditions

A lignin dimer model compound was used to assess the degradation mechanism of the β -O-4 bond in neutral and basic solution. The immediate degradation products were not able to be isolated due to their high reactivity and downstream product analysis could not differentiate between hydrolysis or elimination as the primary bond cleavage pathway. The hydrolysis cleavage product, 1-(4-hydroxy-3-methoxyphenyl)propane-1,2,3-triol, was synthesized and subjected to hydrothermal conditions. The products of the triol decomposition were markedly different than those of the dimer compound, suggesting that the triol is not formed in appreciable amounts. DFT transition state energy calculations were performed and agree that elimination is the dominant pathway under basic conditions. This study outlines the first complete β -O-4 decomposition pathway under neutral and basic conditions that accounts for commonly observed products such as vanillin and acetovanillone.

5.1.2 Lignin dimer decomposition under reductive conditions

Ni/C + H₂ and two Ni/Zn bimetallic systems (Ni/C + Zn and Ni/Zn) were used for β -O-4 bond cleavage and carbonyl reduction. Under neutral conditions, the β -O-4 cleavage is catalyzed by nickel metal and dominates the dimer decomposition. In neutral water, Ni/C with H₂ gave the highest yields. Switching the solvent from water to mixtures of water and ethanol brought significant increases in monomer yield with a maximum of

77.3 C% at a EtOH:H₂O ratio of 9:1. Under basic conditions, the vinyl ether was formed and converted to the final reduction product 4-ethylguaiacol in all three reduction systems. The best monomer yield (78.1 C%) among all conditions was obtained for Ni/Zn + H₂O + 8 equivalent NaOH. In this case, Ni/Zn greatly promoted the vinyl ether (**10**) formation and products from the β-O-4 bond cleavage reaction were detected only in trace quantities.

5.1.3 Selective depolymerization of lignin in a raw biomass substrate

Several catalyst systems for reductive lignin depolymerization from a pine substrate were investigated. A quantitative monomer yield of 35 C% was realized using Ni/C and H₂ in ethanol with 4-propylguaiacol composing 32 C%. Small alcohols in the presence of Ni metal were identified as a hydrogen source for reductive depolymerization and the relevant reactions to maximize hydrogen production were examined. The omission of an external reducing agent resulted in a monomer yield of 26 C% using Ni/C and methanol. The lignin component of two agricultural waste crops, corn stover and sugarcane bagasse, and an energy crop, switchgrass, were characterized by HSQC NMR and successfully depolymerized under the same conditions.

5.2 Continued and future work

5.2.1 Application of lignin derived monophenols

At the time of this writing, there is a considerable amount of research being devoted to the development of lignin depolymerization technologies. Currently, reductive depolymerization methods such as those outlined above can give nearly quantitative monophenol yields, producing 4-propylphenol, 4-propylguaiacol, and 4-propylsyringol as

the most common products. However, it is important not to lose sight of the primary goal, which is to produce renewable chemical building blocks to replace petroleum based chemicals. These products pose a problem towards meeting that goal, as they are difficult to incorporate into useful commercial polymers due to poor positioning of ring substituents and a lack of functional groups on the carbon chain. Without substantial modification, these products are fit only for phenol-formaldehyde resins which are often mechanically inferior compared to current commercial resins. Substituents at the para and ortho positions reduce crosslinking and the carbon chain reduces crystallinity resulting in lower T_g values and reduced mechanical strength. Therefore, chemical modification is necessary for these monophenolic chemicals to have commercial purpose. Such procedures are likely to be quite costly, making competition with readily available petroleum based feedstocks impractical.

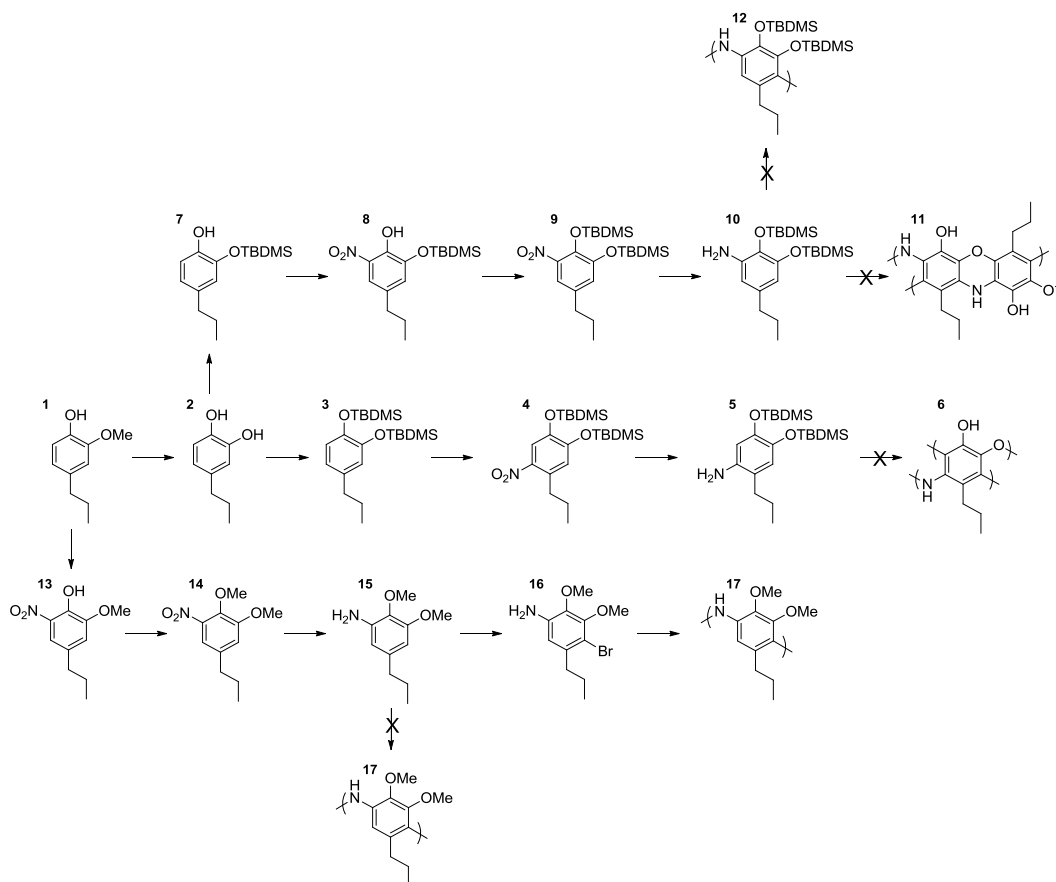
Although these chemicals are unsuitable as replacements for current commercial polymer products, high value polymers can be developed with the constraint of utilizing this new renewable feedstock. One potential application for these materials is use in charge storage devices. Hydroquinone type structures have been used as cathode materials and in supercapacitors.¹⁷⁵ Both 4-propylguaiacol and 4-propylsyringol are capable of similar oxidation-reduction reactions upon demethylation of a single methoxy group. Therefore, these chemicals have the potential to be used in high value applications, thereby mitigating the cost of chemical modification.

This section details the chemical routes attempted to make a polyconjugated material starting from 4-propylguaiacol. Although all attempts failed to make a polymer of acceptable molecular weight for use in charge storage devices, it is worthwhile to report

these reactions here so that the finding may be of use to another researcher as many of the attempted reactions resulted in significant deviations from predictions made according to related reactions found in literature. A revised reaction scheme towards a polyconjugated material based on these findings is proposed.

5.2.2 Reactions and Schemes

Scheme 15 outlines the paths taken from starting material, 4-propylguaiacol, to several potential polyconjugated materials that could be used for charge storage applications.



Scheme 15. Reaction intermediates leading from starting material, 4-propylguaiacol, to polyconjugated materials 6, 11, 12, and 17.

Synthesis of 4-propylcatechol (2): 4-propylguaiacol (5 g, 30 mmol) was dissolved in 50 mL dichloromethane. Boron tribromide (7.5 g, 30 mmol) was added dropwise by syringe at room temperature while stirring vigorously. The solution was stirred at room temperature for 4 hours then quenched with 300 mL of water. The mixture was extracted 3x with dichloromethane and dried with MgSO_4 . Clear liquid that solidifies to white solid at room temperature. 98% yield. ^1H NMR chemical shifts: 0.913 (t, $J = 7.4$ Hz, 3H), 1.580 (m, 2H), 2.465 (t, $J = 7.8$ Hz, 2H), 5.300 (s, 2H), 6.607 (dd, $J = 7.7, 1.7$ Hz, 1H), 6.699 (d, $J = 1.8$ Hz, 1H), 6.769 (d, $J = 7.8$ Hz, 1H).

Synthesis of ((4-propyl-1,2-phenylene)bis(oxy))bis(tert-butyldimethylsilane) (3):

Compound 2 (1.7 g, 11.3 mmol), TBDMSCl (3.7 g, 24.5 mmol), and imidazole (2.28 g, 33.5 mmol) were dissolved in dichloromethane and stirred while refluxing for 16 hours. The resultant mixture was filtered, washed 5x with HCl (pH 4), and dried with MgSO₄. Clear liquid. 89% yield. ¹H NMR chemical shifts: 0.181 (s, 6H), 0.188 (s, 6H), 0.900 (t, J = 7.4 Hz, 3H), 0.980 (s, 9H), 0.986 (s, 9H), 1.575 (m, 2H), 2.453 (t, J = 7.8 Hz, 2H), 6.596 (dd, J = 7.7, 1.7 Hz, 1H), 6.637 (d, J = 1.8 Hz, 1H), 6.717 (d, J = 7.8 Hz, 1H).

Synthesis of ((4-nitro-5-propyl-1,2-phenylene)bis(oxy))bis(tert-butyldimethylsilane)

(4): Compound 3 (3.823 g, 10 mmol) was dissolved in 25 mL DCM with 0.38 g Aliquat 336. The solution was cooled to 0°C. While stirring vigorously, 1.25 mL 70% HNO₃, and 5 drops H₂SO₄ were added. The solution was allowed to stir overnight and warm to room temperature. The solution was neutralized with NaHCO₃ and extracted 3x with DCM. The DCM was removed and the mixture separated on a column with hexane to yield a light yellow liquid. 61% yield. ¹H NMR chemical shifts: 0.230 (s, 6H), 0.241 (s, 6H), 0.975 (t, J = 7.8 Hz, 3H), 0.992 (s, 9H), 0.994 (s, 9H), 1.630 (m, 2H), 2.810 (t, J = 7.8 Hz, 2H), 6.691 (s, 1H), 7.541 (s, 1H).

Synthesis of 4,5-bis((tert-butyldimethylsilyl)oxy)-2-propylaniline (5): Compound 4 (2.6 g, 6.1 mmol) was dissolved in 30 mL ethanol. To this solution, 250 mg 5% Pt/C was added. The flask was vacuumed and refilled with 1 atm H₂ three times then connected to a hydrogen reserve that maintained 1 atm of H₂ throughout the reaction. The mixture was stirred for 48 hours at room temperature. The mixture was then filtered and the ethanol removed under reduced pressure. The mixture was separated on a column with hexane to yield a pale yellow oil. 91% yield. ¹H NMR chemical shifts: 0.160 (s, 6H), 0.185 (s, 6H),

0.973 (t, J = 7.8 Hz, 3H), 0.979 (s, 9H), 0.984 (s, 9H), 1.593 (m, 2H), 2.361 (t, J = 7.8 Hz, 2H), 3.291 (s, 2H), 6.213 (s, 1H), 6.527 (s, 1H).

Attempted synthesis of poly(4,5-diol-2-propylaniline) (6): Under an inert atmosphere, compound 5 (0.1 g, 0.25 mmol) was placed in a 10mL round bottom flask along with 1.35 mL of 1M tetrabutylammonium fluoride (1.35 mmol). An immediate color change was observed. The reaction was typically let stir uncapped for 16 hours. 3 mL of 1M HCl solution was then added and the mixture cooled to 0°C. 4.2 electron equivalents of oxidant dissolved in 2 mL DI water was added over 20 minutes. Oxidants tried: FeCl₃, K₂S₂O₈, and H₂O₂. GPC analysis of the products suggests that only dimeric-trimeric structures are produced.

Synthesis of 2-((tert-butyldimethylsilyl)oxy)-4-propylphenol (7): Compound 2 (1.7 g, 11.3 mmol), TBDMSCl (1.68 g, 11.3 mmol), and imidazole (1.14 g, 16.8 mmol) were dissolved in dichloromethane and stirred while refluxing for 16 hours. The resultant mixture was filtered, washed 5x with HCl (pH 4), and dried with MgSO₄ Clear liquid. Product was not separated from the double protected product (3) or constitutional isomer. 2.88g recovered.

Synthesis of 2-((tert-butyldimethylsilyl)oxy)-6-nitro-4-propylphenol (8): The mixture of products from the previous reaction (2.88 g, 10.8 mmol product 7) were dissolved in 30mL ACN and cooled to 0°C. Tert-butyl nitrite (1.17 g, 11.3 mmol) was added dropwise to the stirring solution. The solution was allowed to stir for 3h and warm to room temperature. Solvent was removed under reduced pressure and the resultant red-orange liquid separated on a column with 1:120 EtOAc:Hexane. 39% yield. ¹H NMR

chemical shifts: 0.217 (s, 6H), 0.932 (t, $J = 7.8$ Hz, 3H), 1.024 (s, 9H), 1.605 (m, 2H), 2.810 (t, $J = 7.8$ Hz, 2H), 6.968 (d, 2.3 Hz, 1H), 7.523 (d, 2.3Hz, 1H), 10.470 (s, 1H).

Synthesis of ((3-nitro-5-propyl-1,2-phenylene)bis(oxy))bis(tert-butyldimethylsilane)

(9): Compound 8 (1.31 g, 4.2 mmol), TBDMSCl (0.75 g, 5 mmol), and imidazole (0.51 g, 7.5 mmol) were dissolved in 20mL dichloromethane and stirred while refluxing for 16 hours. The resultant mixture was filtered, washed 5x with HCl (pH 4), and dried with $MgSO_4$. The product mixture was separated on a column with hexane. 97% yield. 1H NMR chemical shifts: 0.102 (s, 6H), 0.243 (s, 6H), 0.927 (t, $J = 7.4$ Hz, 3H), 0.986 (s, 9H), 0.991 (s, 9H), 1.606 (m, 2H), 2.499 (t, $J = 7.8$ Hz, 2H), 6.849 (d, 2.3 Hz, 1H), 7.173 (d, 2.3Hz, 1H).

Synthesis of 2,3-bis((tert-butyldimethylsilyl)oxy)-5-propylaniline (10): Compound 9

(1.73 g, 4.1 mmol) was dissolved in 30 mL ethanol. To this solution, 250 mg 5% Pt/C was added. The flask was vacuumed and refilled with 1atm H_2 three times then connected to a hydrogen reserve that maintained 1 atm of H_2 throughout the reaction. The mixture was stirred for 48 hours at room temperature. The mixture was then filtered and the ethanol removed under reduced pressure. The mixture was separated on a column with hexane to yield a pale green-yellow oil. 96% yield. 1H NMR chemical shifts: 0.177 (s, 6H), 0.199 (s, 6H), 0.894 (t, $J = 7.4$ Hz, 3H), 0.957 (s, 9H), 1.023 (s, 9H), 1.551 (m, 2H), 2.367 (t, $J = 7.8$ Hz, 2H), 3.575 (s, 2H), 6.100 (d, $J = 2.4$ Hz, 1H), 6.172 (d, $J = 2.4$ Hz, 1H).

Attempted synthesis of poly(2,3-diol-5-propylaniline) (11): Under an inert atmosphere, compound 10 (0.1 g, 0.25 mmol) was placed in a 10 mL round bottom flask along with 1.35 mL of 1M tetrabutylammonium fluoride (1.35 mmol). An immediate color change

was observed. The reaction was typically let stir uncapped for 16 hours. 3 mL of 1M HCl solution was then added and the mixture cooled to 0°C. 4.2 electron equivalents of oxidant dissolved in 2mL DI water was added over 20 minutes. Oxidants tried: FeCl₃, (NH₄)₂S₂O₈, and H₂O₂. GPC analysis of the products suggests that only dimeric-trimeric structures are produced (MW < 2000).

Attempted synthesis of poly(2,3-bis((tert-butyldimethylsilyl)oxy)-5-propylaniline)

(12): Biphasic method: Under an inert atmosphere, compound 10 (0.1 g, 0.25 mmol) was dissolved in hexane. 3 mL of 1M HCl solution was then added and the mixture cooled to 0°C. 4.2 electron equivalents of oxidant dissolved in 2mL DI water was added over 20 minutes. Oxidants tried: FeCl₃, (NH₄)₂S₂O₈, and H₂O₂. GPC analysis of the products suggests that only dimeric structures are produced (MW < 1000). **Monophasic method:** Under an inert atmosphere, compound 10 (0.1g, 0.25mmol) was dissolved in ACN. 0.2mL of concentrated H₂SO₄ was added and the solution cooled to 0°C. 10 drops of 50% H₂O₂ were added and the solution was allowed to stir for 48 hours while warming to room temperature. GPC and NMR suggest that no reaction occurred.

It is apparent that the TBDMS protecting group is too bulky for reactions to occur at the 4 position, thereby preventing polymerization. Removing the protecting group does not result in polymer formation either, however, likely due to unproductive oxidation of the diol moiety. Therefore, a smaller protecting group is necessary for successful polymerization.

Synthesis of 2-methoxy-6-nitro-4-propylphenol (13): Compound 1 (5 g, 30 mmol) was dissolved in 25 mL DCM with 0.13 g Aliquat 336. The solution was cooled to 0°C. While stirring vigorously, 2.5 mL 50% HNO₃, and 1 mL 0.3M KNO₂ solution were

added. The solution was allowed to stir for 4 hours and warm to room temperature. The solution was extracted 3x with DCM. The DCM was removed and the mixture separated on a column with 1:30 EtOAc:Hexane to yield an orange liquid. 55% yield. ^1H NMR chemical shifts: 0.954 (t, $J = 7.2$ Hz, 3H), 1.646 (m, 2H), 2.568 (t, $J = 7.8$ Hz, 2H), 3.943 (s, 3H), 6.965 (d, 1.9 Hz, 1H), 7.502 (d, 1.9Hz, 1H), 10.649 (s, 1H).

Synthesis of 1,2-dimethoxy-3-nitro-5-propylbenzene (14): Compound 13 (3.45 g 16 mmol) was dissolved in 40mL acetone. Anhydrous potassium carbonate (7 g, 51 mmol) and methyl iodide (4.83 g, 0.34 mmol) were added to the solution and stirred briefly. The solution was brought to reflux and and stirred for 16 hours. The solution changed from an orange-red to pale orange-yellow. The solvent was removed under reduced pressure, the excess potassium carbonate neutralized with 2M HCl and the mixture extracted 3x with DCM and dried over MgSO_4 . Yellow liquid. 98% yield. ^1H NMR chemical shifts: 0.959 (t, $J = 7.4$ Hz, 3H), 1.653 (m, 2H), 2.583 (t, $J = 7.2$ Hz, 2H), 3.909 (s, 3H), 3.959 (s, 3H), 6.912 (d, 1.9 Hz, 1H), 7.142 (d, 1.9Hz, 1H).

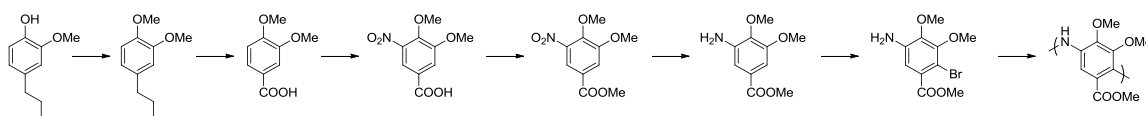
Synthesis of 2,3-dimethoxy-5-propylaniline (15): Compound 14 (3.6 g, 16 mmol) was dissolved in 30 mL ethanol. To this solution, 250 mg 5% Pt/C was added. The flask was vacuumed and refilled with 1 atm H_2 three times then connected to a hydrogen reserve that maintained 1 atm of H_2 throughout the reaction. The mixture was stirred for 48 hours at room temperature. The mixture was then filtered and the ethanol removed under reduced pressure to yield a pale yellow oil that reddened on exposure to air. 96% yield. ^1H NMR chemical shifts: 0.937 (t, $J = 7.4$ Hz, 3H), 1.602 (m, 2H), 2.443 (t, $J = 7.4$ Hz, 2H), 3.797 (s, 3H), 3.815 (s, overlapped with methoxy peaks, 2H) 3.839 (s, 3H), 6.164 (d, 1.9 Hz, 1H), 6.223 (d, 1.9Hz, 1H).

Synthesis of 4-bromo-2,3-dimethoxy-5-propylaniline (16): Compound 15 (2.65 g, 14 mmol) was dissolved in 10mL DMF and cooled to -70°C using dry ice. NBS(2.54 g, 14 mmol) was dissolved in 40mL DMF and added to the cooled solution of compound 15 over 20 minutes. The reaction was let stir for 16 hours and allowed to slowly warm to room temperature. The isomer distribution of 4-bromo:6-bromo was found to be 9:1 in the crude product. The mixture was poured into 300 mL of DI water along with 15 mL of 1M NaOH. The mixture was extracted 5x with DCM and dried over MgSO_4 . The product mixture was separated on a column using 1:30 EtOAc:Hexane containing a trace amount of Et_3N . Although the NMR yield was roughly 75%, only 54% isomerically pure product could be recovered. Yellow-brown oil. ^1H NMR chemical shifts: 0.967 (t, $J = 7.4$ Hz, 3H), 1.593 (m, 2H), 2.583 (t, $J = 7.4$ Hz, 2H), 3.793 (s, 2H), 3.851 (s, 3H) 3.864 (s, 3H), 6.424 (s, 1H).

Synthesis of poly(2,3-dimethoxy-5-propylaniline) (17): Oxidative method: Under an inert atmosphere, compound 15 (0.1 g, 0.5 mmol) was placed in a 10mL round bottom flask along 3 mL of 1M HCl or 0.5M H_2SO_4 . The solution was cooled to 0°C . 4.2 electron equivalents of oxidant dissolved in 2mL DI water was added over 20 minutes. Oxidants tried: FeCl_3 , $(\text{NH}_4)_2\text{S}_2\text{O}_8$, and H_2O_2 . GPC analysis of the products suggests that only oligomeric structures are produced ($\text{MW} < 2000\text{-}4000$). It is hypothesized that polymerization is hindered by activation of the 6-position (ortho), contrary to literature substituted polyaniline synthesis studies, resulting in phenazine formation and chain termination. Therefore, any oxidative polymerization method is unsuitable for the synthesis of the desired polymer. **Buchwald–Hartwig coupling method:** Compound 16 (2 g, 7.3 mmol), potassium tert-butoxide (1.26 g, 11 mmol), $\text{Pd}_2(\text{dba})_3$ (0.07 g, 0.07

mmol), and $P(t-Bu)_3$ (0.03 g, 0.14 mmol) were dissolved in 20mL dioxane and sealed in a pressure tube under an inert atmosphere. The resulting solution was stirred at 110°C for 48 hours. The solution was poured into 300mL of water, extracted 3x with DCM, dried over $MgSO_4$, and the solvent removed under reduced pressure. A red-brown solid was obtained. GPC analysis indicated that the product was a low molecular weight polymer (~2000-4000 g/mol). Changing the phosphine ligands did not result in improvement to molecular weight. A large amount of what appeared to be dehalogenated starting material could be seen in the product NMR, indicating that β -elimination is a prominent reaction pathway. Therefore, hydrogen abstraction from the carbon chain (β -elimination) results in chain termination and prevents the formation of a higher molecular weight polymer.

It can be concluded then, that synthesis of the desired polymer structure with appreciable MW (>10000) is likely impossible. Oxidative methods lack the selectivity to yield a high MW polymer while any metal-mediated polymerization technique will result in β -elimination due to the carbon chain. Therefore, it is advisable to remove the carbon chain and attempt to polymerize the resultant product according to Scheme 16. The final polymer could be completely demethylated by BBr_3 , to yield the redox active polymer.



Scheme 16. Proposed synthesis scheme for a potential charge storage material

REFERENCES

1. Nashawi, I. S.; Malallah, A.; Al-Bisharah, M., Forecasting World Crude Oil Production Using Multicyclic Hubbert Model. *Energy & Fuels* **2010**, *24* (3), 1788-1800.
2. Andrews, T., Using an AGCM to Diagnose Historical Effective Radiative Forcing and Mechanisms of Recent Decadal Climate Change. *Journal of Climate* **2014**, *27* (3), 1193-1209.
3. Li, C.; Zhao, T.; Ying, K., Quantifying the contributions of anthropogenic and natural forcings to climate changes over arid-semiarid areas during 1946–2005. *Climatic Change* **2017**, *144* (3), 505-517.
4. Solomon, S. C.; Liu, H.-L.; Marsh, D. R.; McInerney, J. M.; Qian, L.; Vitt, F. M., Whole Atmosphere Simulation of Anthropogenic Climate Change. *Geophys. Res. Lett.* **2018**, *45*, 1567-1576.
5. Kraaijenbrink, P. D. A.; Bierkens, M. F. P.; Lutz, A. F.; Immerzeel, W. W., Impact of a global temperature rise of 1.5 degrees Celsius on Asia's glaciers. *Nature* **2017**, *549* (7671), 257-260.
6. Mahmoud, S. H.; Gan, T. Y., Impact of anthropogenic climate change and human activities on environment and ecosystem services in arid regions. *Sci Total Environ* **2018**, *633*, 1329-1344.
7. Douville, H.; Plazzotta, M., Midlatitude Summer Drying: An Underestimated Threat in CMIP5 Models? *Geophysical Research Letters* **2017**, *44* (19), 9967-9975.
8. Yan, X.; Cai, Y. L., Multi-Scale Anthropogenic Driving Forces of Karst Rocky Desertification in Southwest China. *Land Degradation & Development* **2015**, *26* (2), 193-200.
9. Feng, L.; Jia, Z.; Li, Q., The dynamic monitoring of aeolian desertification land distribution and its response to climate change in northern China. *Sci Rep* **2016**, *6*, 39563.
10. Faleiro, F.; Baptista, M.; Santos, C.; Aurelio, M. L.; Pimentel, M.; Pegado, M. R.; Paula, J. R.; Calado, R.; Repolho, T.; Rosa, R., Seahorses under a changing ocean: the impact of warming and acidification on the behaviour and physiology of a poor-swimming bony-armoured fish. *Conserv Physiol* **2015**, *3* (1), cov009.
11. Rosa, R.; Rummer, J. L.; Munday, P. L., Biological responses of sharks to ocean acidification. *Biol Lett* **2017**, *13* (3).

12. Wulff, A.; Karlberg, M.; Olofsson, M.; Torstensson, A.; Riemann, L.; Steinhoff, F. S.; Mohlin, M.; Ekstrand, N.; Chierici, M., Ocean acidification and desalination: climate-driven change in a Baltic Sea summer microplanktonic community. *Mar Biol* **2018**, *165* (4), 63.
13. Garcia, E.; Clemente, S.; Hernandez, J. C., Effects of natural current pH variability on the sea urchin *Paracentrotus lividus* larvae development and settlement. *Mar Environ Res* **2018**, *139*, 11-18.
14. Soares, M. O., Climate change and regional human pressures as challenges for management in oceanic islands, South Atlantic. *Mar Pollut Bull* **2018**, *131* (Pt A), 347-355.
15. Leung, J. Y. S.; Nagelkerken, I.; Russell, B. D.; Ferreira, C. M.; Connell, S. D., Boosted nutritional quality of food by CO₂ enrichment fails to offset energy demand of herbivores under ocean warming, causing energy depletion and mortality. *Sci Total Environ* **2018**, *639*, 360-366.
16. *Wood Production, Wood Technology, and Biotechnological Impacts*. Aplicada International: Germany, 2007.
17. Brunow, G., Lignin line and lignin-based product family trees. In *Biorefineries – industrial processes and products*, Kamm, B.; Gruber, P. R.; Kamm, M., Eds. WILEY-VCH Verlag GmbH & Co.: 2006; pp 151–63.
18. Saake, B.; Lehnen, R., Lignin. In *Encyclopedia of Industrial Chemistry*, Ullmann, Ed. Wiley-VCH Verlag GmbH & Co. KGaA: Weinheim, 2012; pp 21–36.
19. Buchanan; Gruissem; Jones, *Biochemistry & molecular biology of plants*. 1st edition ed.; 2000.
20. Taiz, L.; Zeiger, E., *Plant physiology*. 3rd ed.; Sinauer Associates: Sunderland, 2003; Vol. 91.
21. Ji, Z.; Ma, J.-F.; Zhang, Z.-H.; Xu, F.; Sun, R.-C., Distribution of lignin and cellulose in compression wood tracheids of *Pinus yunnanensis* determined by fluorescence microscopy and confocal Raman microscopy. *Industrial Crops and Products* **2013**, *47*, 212-217.
22. Sticklen, M. B., Plant genetic engineering for biofuel production: towards affordable cellulosic ethanol. *Nat Rev Genet* **2008**, *9*, 433–443.
23. Sixta, H., *Handbook of Pulp*. 2008.

24. Luo, H.; Abu-Omar, M. M., Chemicals From Lignin. In *Encyclopedia of Sustainable Technologies*, 2017; Vol. 3, pp 573-585.
25. A., E.; Z., H.; T., H., Hemicellulose. In *Polysaccharides I. Advances in Polymer Science*, Springer, Berlin, Heidelberg: 2005; Vol. 186.
26. Lam, T. B. T.; Kadoya, K.; Iiyama, K., Bonding of hydroxycinnamic acids to lignin: ferulic and *p*-coumaric acids are predominantly linked at the benzyl position of lignin, not the β -position, in grass cell walls. *Phytochemistry* **2001**, *57*, 987–992.
27. Santos, R. B.; Capanema, E. A.; Balakshin, M. Y.; Chang, H.-M.; Jameel, H., Effect of Hardwoods Characteristics on Kraft Pulping Process: Emphasis on Lignin Structure. *BioResources* **2011**, *6* (4), 3623-3637.
28. Santos, R. B.; Hart, P. W.; Jameel, H.; Chang, H.-m., Wood based lignin reactions important to the biorefinery and pulp and paper industries. *BioResources* **2013**, *8* (1), 1456-1477.
29. Holladay, J. E.; Bozell, J. J.; White, J. F.; Johnson, D., Top Value-Added Chemicals from Biomass. Energy, U. S. D. o., Ed. 2007; Vol. 2.
30. Hua, X.; Capretti, G.; Focher, B.; Marzetti, A.; Kokta, B. V.; Kaliaguine, S., Characterization of Aspen Explosion Pulp by CP/MAS ^{13}C NMR. *Appl. Spectrosc.* **1993**, *47*, 1693-1695.
31. Bauer, S.; Sorek, H.; Mitchell, V. D.; Ibanez, A. B.; Wemmer, D. E., Characterization of *Miscanthus giganteus* lignin isolated by ethanol organosolv process under reflux condition. *J Agric Food Chem* **2012**, *60* (33), 8203-12.
32. Nguyen, J. D.; Matsuura, B. S.; Stephenson, C. R. J., A Photochemical Strategy for Lignin Degradation at Room Temperature. *JACS* **2014**, *136*, 1218–1221.
33. Harms, R. G.; Markovits, I. I. E.; Drees, M.; Herrmann, W. A.; Cokoja, M.; Kühn, F. E., Cleavage of CO Bonds in Lignin Model Compounds Catalyzed by Methyldioxorhenium in Homogeneous Phase. *ChemSusChem* **2014**, *7*, 429 – 434.
34. Huo, W.; Li, W.; Zhang, M.; Fan, W.; Chang, H.-m.; Jameel, H., Effective C–O Bond Cleavage of Lignin β -O-4 Model Compounds: A New $\text{RuHCl}(\text{CO})(\text{PPh}_3)_3/\text{KOH}$. *Catal. Lett.* **2014**, *144*, 1159–1163.
35. Sedai, B.; Diaz-Urrutia, C.; Baker, R. T.; Wu, R.; Silks, L. A.; Hanson, S. K., Comparison of Copper and Vanadium Homogeneous Catalysts for Aerobic Oxidation of Lignin Models. *ACS Catal.* **2011**, *1*, 794-804.

36. Son, S.; Toste, F. D., Non-Oxidative Vanadium-Catalyzed C O Bond Cleavage: Application to Degradation of Lignin Model Compounds. *Angew. Chem., Int. Ed.* **2010**, *49*, 3791-3794.
37. Galkin, M. V.; Sawadjoon, S.; Rohde, V.; Dawange, M.; Samec, J. S. M., Mild Heterogeneous Palladium-Catalyzed Cleavage of β -O-4'-Ether Linkages of Lignin Model Compounds and Native Lignin in Air. *ChemCatChem* **2014**, *6*, 179-184.
38. Zhang, J.; Chen, Y.; Brook, M. A., Reductive Degradation of Lignin and Model Compounds by Hydrosilanes. *ACS Sustainable Chem. Eng.* **2014**, *2*, 1983-1991.
39. Parsell, T. H.; Owen, B. C.; Klein, I.; Jarrell, T. M.; Marcum, C. L.; Hauptert, L. J.; Amundson, L. M.; Kenltämaa, H. I.; Ribeiro, F.; Miller, J. T.; Abu-Omar, M. M., Cleavage and hydrodeoxygenation (HDO) of C-O bonds relevant to lignin conversion using Pd/Zn synergistic catalysis. *Chem. Sci.* **2013**, *4*, 806-813.
40. Crestini, C.; Pastorini, A.; Tagliatesta, P., Metalloporphyrins immobilized on montmorillonite as biomimetic catalysts in the oxidation of lignin model compounds. *J. Mol. Catal. A Chem.* **2004**, *208*, 195-202.
41. Hanson, S. K.; Wu, R.; Silks, L. A., C-C or C-O Bond Cleavage in a Phenolic Lignin Model Compound: Selectivity Depends on Vanadium Catalyst. *Angew. Chem., Int. Ed.* **2012**, *51*, 3410-3413.
42. Chan, J. M. W.; Bauer, S.; Sorek, H.; Sreekumar, S.; Wang, K.; Toste, F. D., Studies on the vanadium-catalyzed nonoxidative depolymerization of miscanthus giganteus-derived lignin. *ACS Catal.* **2013**, *3*, 1369-1377.
43. Zeng, H.; Cao, D.; Qiu, Z.; Li, C. J., Palladium-Catalyzed Formal Cross-Coupling of Diaryl Ethers with Amines: Slicing the 4-O-5 Linkage in Lignin Models. *Angewandte Chemie* **2018**, *57* (14), 3752-3757.
44. Jiang, W.; Wu, S., Mechanism Study on Depolymerization of the α -O-4 Linkage Lignin Model Compound in Supercritical Ethanol System. *Waste and Biomass Valorization* **2017**.
45. Demirbas, A., Mechanisms of liquefaction and pyrolysis reactions of biomass. *Energy Convers Manage* **2000**, *41*, 633-646.
46. De Wild, P. J.; Huijgen, W. J. J.; Gosselink, R. J. A., Lignin pyrolysis for profitable lignocellulosic biorefineries. *Biofuels, Bioproducts and Biorefining* **2014**, *8* (5), 645-657.

47. Jackson, M. A.; Compton, D. L.; Boateng, A. A., Screening heterogeneous catalysts for the pyrolysis of lignin. *Journal of Analytical and Applied Pyrolysis* **2009**, *85* (1-2), 226-230.
48. Zhao, Y.; Deng, L.; Liao, B.; Fu, Y.; Guo, Q.-X., Aromatics Production via Catalytic Pyrolysis of Pyrolytic Lignins from Bio-Oil. *Energy & Fuels* **2010**, *24* (10), 5735-5740.
49. Wahyudiono; Sasaki, M.; Goto, M., Recovery of phenolic compounds through the decomposition of lignin in near and supercritical water. *Chemical Engineering and Processing: Process Intensification* **2008**, *47* (9-10), 1609-1619.
50. Fang, Z.; Sato, T.; Smith, R. L., Jr.; Inomata, H.; Arai, K.; Kozinski, J. A., Reaction chemistry and phase behavior of lignin in high-temperature and supercritical water. *Bioresour Technol* **2008**, *99* (9), 3424-30.
51. Sturgeon, M. R.; Kim, S.; Lawrence, K.; Paton, R. S.; Chmely, S. C.; Nimlos, M.; Foust, T. D.; Beckham, G. T., A Mechanistic Investigation of Acid-Catalyzed Cleavage of Aryl-Ether Linkages: Implications for Lignin Depolymerization in Acidic Environments. *ACS Sustainable Chem. Eng.* **2014**, *2*, 472-485.
52. Gao, Y.; Zhang, J.; Chen, X.; Ma, D.; Yan, N., A Metal-Free, Carbon-Based Catalytic System for the Oxidation of Lignin Model Compounds and Lignin. *ChemPlusChem* **2014**, *79* (6), 825-834.
53. Hanson, S. K.; Wu, R.; Silks, L. A. P., C-C or C-O bond cleavage in a phenolic lignin model compound: selectivity depends on vanadium catalyst. *Angew Chem Int Ed* **2012**, *51*.
54. Li, Y.; Chang, J.; Ouyang, Y., Selective Production of Aromatic Aldehydes from Lignin by Metalloporphyrins/H₂O₂ System. *Advanced Materials Research* **2013**, *805-806*, 273-276.
55. Kües, U., *Wood Production, Wood Technology and Biotechnological Impacts*. Micología Aplicada International, Germany 2007.
56. Boerjan, W.; Ralph, J.; Baucher, M., Lignin biosynthesis. *Annu. Rev. Plant Biol.* **2003**, *54*, 519-546.
57. Fengel, D.; Wegener, G., *Wood. Chemistry, Ultrastructure, Reactions*. Berlin, 1984.
58. Zakzeski, J.; Bruijninx, P. C. A.; Jongerijs, A. L.; Weckhuysen, B. M., The Catalytic Valorization of Lignin for the Production of Renewable Chemicals. *Chem. Rev.* **2010**, *110*, 3552-3599.

59. Beste, A.; Buchanan, A. C., Computational study of bond dissociation enthalpies for lignin model compounds. Substituent effects in phenethyl phenyl ethers. *J. Org. Chem.* **2009**, *74*, 2837-2841.
60. Beste, A.; Buchanan, A. C.; Harrison, R. J., Computational prediction of α/β selectivities in the pyrolysis of oxygen-substituted phenethyl phenyl ethers. *J. Phys. Chem. A* **2008**, *112*, 4982-4988.
61. Faravelli, T.; Frassoldati, A.; Migliavacca, G.; Ranzi, E., Detailed kinetic modeling of the thermal degradation of lignins. *Biomass Bioenergy* **2010**, *34*, 290-301.
62. Azadi, P.; Inderwildi, O. R.; Farnood, R.; King, D. A., Liquid fuels, hydrogen and chemicals from lignin: A critical review. *Renewable Sustainable Energy Rev.* **2013**, *21*, 506-523.
63. Hage, R. E.; Brosse, N.; Chrusciel, L.; Sanchez, C.; Sannigrahi, P.; Ragauskas, A., Characterization of milled wood lignin and ethanol organosolv lignin from miscanthus. *Polym. Degrad. Stab.* **2009**, *94*, 1632-1638.
64. X., E.; R., P.; A., C. M.; J., L., Effect of different organosolv treatments on the structure and properties of olive tree pruning lignin. *J. Ind. Eng. Chem.* **2013**, *20*, 1103-1108.
65. Bauer, S.; Sorek, H.; Mitchell, V. D.; Ibáñez, A. B.; Wemmer, D. E., Characterization of *Miscanthus giganteus* lignin isolated by ethanol organosolv process under reflux condition. *J. Agric. Food Chem.* **2012**, *60*, 8203-8212.
66. Bozell, J. J.; O'Lenick, C. J.; Warwick, S., Biomass fractionation for the biorefinery: Heteronuclear multiple quantum coherencenuclear magnetic resonance investigation of lignin isolated from solvent fractionation of switchgrass. *J. Agric. Food Chem.* **2011**, *59*, 9232-9242.
67. Zhang, Y. H. P.; Ding, S. Y.; Mielenz, J. R.; Cui, J. B.; Elander, R. T.; Laser, M.; Himmel, M. E.; McMillan, J. R.; Lynd, L. R., Fractionating recalcitrant lignocellulose at modest reaction conditions. *Biotechnol. Bioeng.* **2007**, *97*, 214-223.
68. Pu, Y.; Hu, F.; Huang, F.; Davison, B.; Ragauskas, A., Assessing the molecular structure basis for biomass recalcitrance during dilute acid and hydrothermal pretreatments. *Biotechnol. Biofuels* **2013**, *6*.
69. Hu, G.; Cateto, C.; Pu, Y. Q.; Samuel, R.; Ragauskas, A. J., Structural characterization of switchgrass lignin after ethanol organosolv pretreatment. *Energy Fuels* **2012**, 740-745.

70. Samuel, R.; Foston, M.; Jiang, N.; Allison, L.; Ragauskas, A. J., Structural changes in switchgrass lignin and hemicelluloses during pretreatments by NMR analysis. *Polym. Degrad. Stab.* **2011**, *96*, 2002–2009.
71. Westermark, U.; Samuelsson, B.; Lundquist, K., Homolytic cleavage of the β -ether bond in phenolic β -O-4 structures in wood lignin and in guaiacylglycerol- β -guaiacyl ether. *Res. Chem. Intermed.* **1995**, *21*, 343-352.
72. Lundquist, K.; Ericsson, L., Acid degradation of lignin. 3. Formation of formaldehyde. *Acta Chem. Scand.* **1970**, *24*, 3681-3686.
73. Lundquist, K.; Ericsson, L., Acid degradation of lignin. 6. Formation of methanol. . *Acta Chem. Scand.* **1971**, 756-758.
74. Lundquist, K.; Lundgren, R., Acid degradation of lignin. 7. Cleavage of ether bonds. *Acta Chem. Scand.* **1972**, *26*, 2005-2023.
75. Li, S. M.; Lundquist, K.; Westermark, U., Cleavage of arylglycerol beta-aryl ethers under neutral and acid conditions. *Nord. Pulp Pap. Res. J.* **2000**, *15*, 292-299.
76. Yasuda, S.; Terashima, N.; Ito, T., Chemical structures of sulfuric acid lignin. II. Chemical structures of condensation products from arylglycerol- β -aryl ether type structures. *Mokuzai Gakkaishi* **1981**, *27*, 216-222.
77. Ito, T.; Terashima, N.; Yasuda, S., Chemical structures of sulfuric acid lignin. III. Reaction of arylglycerol- β -aryl ether with 5% sulfuric acid. *Mokuzai Gakkaishi* **1981**, *27*, 484-490.
78. Yasuda, S.; Terashima, N., Chemical structures of sulfuric acid lignin. V. Reaction of three arylglycerol- β -aryl ethers [α -, β -, and γ -13C] with 72% sulfuric acid. *Mokuzai Gakkaishi* **1982**, *28*, 383–387.
79. Yasuda, S.; Terashima, N.; Hamanaka, A., Chemical structures of sulfuric acid lignin. VI. Physical and chemical properties of sulfuric acid lignin. *Mokuzai Gakkaishi* **1983**, *29*, 795–800.
80. Yasuda, S., Chemical structures of sulfuric acid lignin. VII. Reaction of phenylcoumaran with sulfuric acid. *Mokuzai Gakkaishi* **1984**, *30*, 166–172.
81. Yasuda, S.; Adachi, K.; Terashima, N.; Ota, K., Chemical structures of sulfuric acid lignin. VIII. Reactions of 1,2-diaryl-1,3-propanediol and pinoresinol with sulfuric acid. *Mokuzai Gakkaishi* **1985**, *31*, 125–131.

82. Yasuda, S.; Ota, K., Chemical structures of sulfuric-acid lignin. 10. Reaction of syringylglycerol- β -syringyl ether and condensation of syringyl nucleus with guaiacyl lignin model compounds in sulfuric acid. *Holzforschung* **1987**, *41*, 59-65.
83. Yokoyama, T.; Matsumoto, Y., Revisiting the mechanism of β -O4 bond cleavage during acidolysis of lignin. Part 1: Kinetics of the formation of enol ether from non-phenolic C-6-C-2 type model compounds. *Holzforschung* **2008**, *62*, 164-168.
84. Yokoyama, T.; Matsumoto, Y., Revisiting the mechanism of β -O4 bond cleavage during acidolysis of lignin. Part 2: Detailed reaction mechanism of a non-phenolic C-6-C-2 type model compound. *J. Wood Chem. Technol.* **2010**, *30*, 269-282.
85. Ito, H.; Imai, T.; Lundquist, K.; Yokoyama, T.; Matsumoto, Y., Revisiting the mechanism of β -O-4 bond cleavage during acidolysis of lignin. Part 3: Search for the rate-determining step of a non-phenolic C-6-C-3 type model compound. *J. Wood Chem. Technol.* **2011**, *31*, 172-182.
86. Imai, T.; Yokoyama, T.; Matsumoto, Y., Revisiting the mechanism of β -O-4 bond cleavage during acidolysis of lignin IV: Dependence of acidolysis reaction on the type of acid. *J. Wood Sci.* **2011**, *57*, 219-225.
87. Imai, T.; Yokoyama, T.; Matsumoto, Y., Revisiting the mechanism of β -O-4 bond cleavage during acidolysis of lignin: Part 5: On the characteristics of acidolysis using hydrobromic acid. *J. Wood Chem. Technol.* **2012**, *32*, 165-174.
88. Yokoyama, T., Revisiting the mechanism of β -o-4 bond cleavage during acidolysis of lignin. Part 6: A review. *J. Wood Chem. Technol.* **2015**, *35*, 27-42.
89. Hauteville, M.; Lundquist, K.; Vonunge, S., NMR-studies of lignins. 7. H-1-NMR spectroscopic investigation of the distribution of erythro and threo forms of β -O-4 structures in lignins. *Acta Chem. Scand. Ser. B* **1986**, *40*, 31-35.
90. Miksche, G. E., Zum alkalischen abbau von Arylclycerin- β -(2,6-dimethoxy-4-alkylaryl)-atherstrukturen. *Acta Chem. Scand.* **1973**, *27*, 1355-1368.
91. Bardet, M.; Robert, D. R.; Lundquist, K., On the reactions and degradation of the lignin during steam hydrolysis of aspen wood. *Svensk Papperstidn.* **1985**, *88*, 61-67.
92. Minami, E.; Kawamoto, H.; Saka, S., Reaction behavior of lignin in supercritical methanol as studied with lignin. *J. Wood Sci.* **2003**, *49*, 158-165.

93. Tsujino, J.; Kawamoto, H.; Saka, S., Reactivity of lignin in supercritical methanol studied with various lignin model compounds. *Wood Sci. Technol.* **2003**, *37*, 299–307.
94. Ibbett, R.; Gaddipati, S.; Davies, S.; Hill, S.; Tucker, G., The mechanisms of hydrothermal deconstruction of lignocellulose: new insights from thermal–analytical and complementary studies. *Bioresour. Technol.* **2011**, *102*, 9272–9278.
95. Zakzeski, J.; Weckhuysen, B. M., Lignin solubilization and aqueous phase reforming for the production of aromatics chemicals and hydrogen. *ChemSusChem* **2011**, *4*, 369–378.
96. Kobayashi, T.; Kohn, B.; Holmes, L.; Faulkner, R.; Davis, M.; Maciel, G. E., Molecular-level consequences of biomass pretreatment by dilute sulfuric acid at various temperatures. *Energy Fuels* **2011**, *25*, 1790–1797.
97. Thring, R. W., Alkaline degradation of ALCELL lignin. *Biomass Bioenergy* **1994**, *7*, 125–130.
98. Karagöz, S.; Bhaskar, T.; Muto, A.; Sakata, Y., Effect of Rb and Cs carbonates for production of phenols from liquefaction of wood biomass. *Fuel* **2004**, *83*, 2293–2299.
99. Karagoz, S.; Bhaskar, T.; Muto, A.; Sakata, Y.; Uddin, M. A., Low-Temperature Hydrothermal Treatment of Biomass: Effect of Reaction Parameters on Products and Boiling Point Distributions. *Energy Fuels* **2004**, *18*, 234–241.
100. Xu, C.; Lancaster, J., Conversion of secondary pulp/paper sludge to bio-oils by direct liquefaction in hot compressed or sub- and near-critical water. *Water Res.* **2008**, *42*, 1571–1582.
101. Xu, C.; Lad, N., Production of heavy oils with high caloric values by direct liquefaction of woody biomass in sub-/near-critical water. *Energy Fuels* **2008**, *22*, 635–642.
102. Tymchyshyn, M.; Xu, C., Liquefaction of bio-mass in hot-compressed water for the production of phenolic Compounds. *Bioresour. Technol.* **2010**, *101*, 2483–2490.
103. Akhtar, J.; Kuang, S. K.; Amin, N. S., Liquefaction of empty palm fruit bunch (EPFB) in alkaline hot compressed water. *Renewable Energy* **2010**, *35*, 1220–1227.
104. Radoykova, T.; Nenkova, S.; Stanulov, K., Production of phenol compounds by alkaline treatment of poplar wood bark. *Chem. Nat. Compd.* **2010**, *46*, 807–808.
105. Roberts, V. M.; Stein, V.; Reiner, T.; Lemonidou, A.; Li, X.; Lercher, J. A., Towards Quantitative Catalytic Lignin Depolymerization. *Chem. Eur. J.* **2011**, *17*, 5939–5948.

106. Lavoie, J. M.; Baré, W.; Bilodeau, M., Depolymerization of steam-treated lignin for the production of green chemicals. *Bioresour. Technol.* **2011**, *102*, 4917–4920.
107. Beauchet, R.; Monteil-Rivera, F.; Lavoie, J. M., Conversion of lignin to aromatic-based chemicals (L-chems) and biofuels (L-fuels). *Bioresour. Technol.* **2012**, *121*, 328–334.
108. Mahmood, N.; Yuan, Z.; Schmidt, J.; Xu, C. C., Production of polyols via direct hydrolysis of kraft lignin: Effect of process parameters. *Bioresour. Technol.* **2013**, *139*, 13–20.
109. Kim, H. G.; Park, Y., Manageable Conversion of Lignin to Phenolic Chemicals Using a Microwave Reactor in the Presence of Potassium Hydroxide. *Ind. Eng. Chem. Res.* **2013**, *52*, 10059–10062.
110. Erdocia, X.; Prado, R.; Corcuera, M. Á.; Labidi, J., Base catalyzed depolymerization of lignin: Influence of organosolv lignin nature. *Biomass Bioenergy* **2014**, *66*, 379–386.
111. Toledano, A.; Serrano, L.; Labidi, J., Improving base catalyzed lignin depolymerization by avoiding lignin repolymerization. *Fuel* **2014**, *116*, 617–624.
112. Xia, G.-G.; Chen, B.; Zhang, R.; Zhang, Z. C., Catalytic hydrolytic cleavage and oxy-cleavage of lignin linkages. *J. Mol. Catal. A Chem.* **2014**, *388–389*, 35–40.
113. Krutov, S. M.; Evtuguin, D. V.; Ipatova, E. V.; Santos, S. A. O.; Sazanov, Y. N., Modification of acid hydrolysis lignin for value-added applications by micronization followed by hydrothermal alkaline treatment. *Holzforschung* **2015**, *69*, 761–768.
114. Miller, J. E.; Evans, L.; Littlewolf, A.; Trudell, D. E., Batch microreactor studies of lignin and lignin model compound depolymerization by bases in alcohol solvents. *Fuel* **1999**, *78*, 1363–1366.
115. Yuan, Z.; Cheng, S.; Leitch, M.; Xu, C., Hydrolytic degradation of alkaline lignin in hot-compressed water and ethanol. *Bioresour. Technol.* **2010**, *101*, 9308–9313.
116. Toledano, A.; Serrano, L.; Labidi, J., Improving base catalyzed lignin depolymerization by avoiding lignin repolymerization. *Fuel* **2014**, *116*, 617–624.
117. Gierer, J.; Lenz, B.; Noren, I.; Soederberg, S., Reactions of lignin during sulfate cooking. III. The split ring of aryl-alkyl ether bonds in milled wood lignin by alkali. *Tappi J.* **1964**, *47*, 233–239.

118. Dong, C.; Feng, C.; Liu, Q.; Shen, D.; Xiao, R., Mechanism on microwave-assisted acidic solvolysis of black-liquor lignin. *Bioresour. Technol.* **2014**, *162*, 136–141.
119. Shen, D.; Liu, N.; Dong, C.; Xiao, R.; Gu, S., Catalytic solvolysis of lignin with the modified HUSYs in formic acid assisted by microwave heating. *Chem. Eng. J.* **2015**, *270*.
120. Nakatsubo, F.; Higuchi, T., Synthesis of Guaiacylglycerol-beta-Coniferyl and beta-Coniferyl Aldehyde Ethers. *Holzforschung* **1975**, *29*, 165-168.
121. Kim, Y. H.; Kim, K. H.; Szulejko, J. E.; Bae, M. S.; Brown, R. J., Experimental validation of an effective carbon number-based approach for the gas chromatography-mass spectrometry quantification of 'compounds lacking authentic standards or surrogates'. *Anal. Chim. Acta* **2014**, *830*, 32-41.
122. Dabral, S.; Mottweiler, J.; Rinesch, T.; Bolm, C., Base-catalysed cleavage of lignin β -O-4 model compounds in dimethyl carbonate. *Green Chem.* **2015**, *17*, 4908-4912.
123. Tachon, N.; Benjelloun-Mlayah, B.; Delmas, M., Organosolv Wheat Straw Lignin as a Phenol Substitute for Green Phenolic Resins. *BioResources* **2016**, *11* (3), 5797-5815.
124. Sarkar, S.; Adhikari, B., Lignin-modified phenolic resin: synthesis optimization, adhesive strength, and thermal stability. *J. Adhes. Sci. Technol.* **2000**, *14* (9), 1179-1193.
125. Barkhau, R. A.; Malcolm, E. W.; Dimmel, D. R., Insoluble Lignin Models (4): Condensation Reactions of a Polymer-Bound Guaiacylpropanol Model. *J. Wood Chem. Technol.* **1990**, *10* (2), 269-291.
126. Crestini, C.; Pastorini, A.; Tagliatesta, P., Metalloporphyrins immobilized on montmorillonite as biomimetic catalysts in the oxidation of lignin model compounds. *Journal of Molecular Catalysis A: Chemical* **2004**, *208* (1-2), 195-202.
127. Roberts, V. M.; Stein, V.; Reiner, T.; Lemonidou, A.; Li, X.; Lercher, J. A., Towards quantitative catalytic lignin depolymerization. *Chemistry* **2011**, *17* (21), 5939-48.
128. Kozliak, E. I.; Kubátová, A.; Artemyeva, A. A.; Nagel, E.; Zhang, C.; Rajappagowda, R. B.; Smirnova, A. L., Thermal Liquefaction of Lignin to Aromatics: Efficiency, Selectivity, and Product Analysis. *ACS Sustainable Chem. Eng.* **2016**, *4* (10), 5106-5122.
129. Molinari, V.; Giordano, C.; Antonietti, M.; Esposito, D., Titanium nitride-nickel nanocomposite as heterogeneous catalyst for the hydrogenolysis of aryl ethers. *JACS* **2014**, *136* (5), 1758-61.

130. Zhang, J.; Teo, J.; Chen, X.; Asakura, H.; Tanaka, T.; Teramura, K.; Yan, N., A Series of NiM (M = Ru, Rh, and Pd) Bimetallic Catalysts for Effective Lignin Hydrogenolysis in Water. *ACS Catal.* **2014**, *4* (5), 1574-1583.
131. Galkin, M. V.; Sawadjoon, S.; Rohde, V.; Dawange, M.; Samec, J. S. M., Mild Heterogeneous Palladium-Catalyzed Cleavage of β -O-4'-Ether Linkages of Lignin Model Compounds and Native Lignin in Air. *ChemCatChem* **2014**, *6*, 179-184.
132. Yao, K. X.; Liu, X.; Li, Z.; Li, C. C.; Zeng, H. C.; Han, Y., Preparation of a Ru-Nanoparticles/Defective-Graphene Composite as a Highly Efficient Arene-Hydrogenation Catalyst. *ChemCatChem* **2012**, *4* (12), 1938-1942.
133. Zhang, W.-x.; Wang, C.-B.; Lien, H.-L., Treatment of chlorinated organic contaminants with nanoscale bimetallic particles. *Catal. Today* **1998**, *40*, 387-395.
134. Yin, J.; Maguire, C. K.; Yasuda, N.; Brunskill, A. P. J.; Klapars, A., Impact of Lead Impurities in Zinc Dust on the Selective Reduction of a Dibromoimidazole Derivative. *Org. Process Res. Dev.* **2017**, *21* (1), 94-97.
135. Zielinski, M.; Wojcieszak, R.; Monteverdi, S.; Mercy, M.; Bettahar, M., Hydrogen storage in nickel catalysts supported on activated carbon. *Int. J. Hydrogen Energy* **2007**, *32* (8), 1024-1032.
136. Beauchet, R.; Monteil-Rivera, F.; Lavoie, J. M., Conversion of lignin to aromatic-based chemicals (L-chems) and biofuels (L-fuels). *Bioresour Technol* **2012**, *121*, 328-34.
137. Toledano, A.; Serrano, L.; Labidi, J., Organosolv lignin depolymerization with different base catalysts. *Journal of Chemical Technology & Biotechnology* **2012**, *87* (11), 1593-1599.
138. Erdocia, X.; Prado, R.; Corcuera, M. Á.; Labidi, J., Base catalyzed depolymerization of lignin: Influence of organosolv lignin nature. *Biomass and Bioenergy* **2014**, *66*, 379-386.
139. Mu, W.; Ben, H.; Ragauskas, A.; Deng, Y., Lignin Pyrolysis Components and Upgrading—Technology Review. *BioEnergy Research* **2013**, *6* (4), 1183-1204.
140. Constant, S.; Robitzer, M.; Quignard, F.; Di Renzo, F., Vanillin oligomerization as a model of side reactions in lignin fragmentation. *Catalysis Today* **2012**, *189* (1), 123-128.

141. Nguyen, T. D. H.; Maschietti, M.; Belkheiri, T.; Åmand, L.-E.; Theliander, H.; Vamling, L.; Olausson, L.; Andersson, S.-I., Catalytic depolymerisation and conversion of Kraft lignin into liquid products using near-critical water. *The Journal of Supercritical Fluids* **2014**, *86*, 67-75.
142. Yan, N.; Zhao, C.; Dyson, P. J.; Wang, C.; Liu, L. T.; Kou, Y., Selective degradation of wood lignin over noble-metal catalysts in a two-step process. *ChemSusChem* **2008**, *1* (7), 626-9.
143. Van den Bosch, S.; Schutyser, W.; Vanholme, R.; Driessen, T.; Koelewijn, S. F.; Renders, T.; De Meester, B.; Huijgen, W. J. J.; Dehaen, W.; Courtin, C. M.; Lagrain, B.; Boerjan, W.; Sels, B. F., Reductive lignocellulose fractionation into soluble lignin-derived phenolic monomers and dimers and processable carbohydrate pulps. *Energy & Environmental Science* **2015**, *8* (6), 1748-1763.
144. Parsell, T.; Yohe, S.; Degenstein, J.; Jarrell, T.; Klein, I.; Gencer, E.; Hewetson, B.; Hurt, M.; Kim, J. I.; Choudhari, H.; Saha, B.; Meilan, R.; Mosier, N.; Ribeiro, F.; Delgass, W. N.; Chapple, C.; Kenttämaa, H. I.; Agrawal, R.; Abu-Omar, M. M., A synergistic biorefinery based on catalytic conversion of lignin prior to cellulose starting from lignocellulosic biomass. *Green Chem.* **2015**, *17* (3), 1492-1499.
145. Galkin, M. V.; Samec, J. S., Selective route to 2-propenyl aryls directly from wood by a tandem organosolv and palladium-catalysed transfer hydrogenolysis. *ChemSusChem* **2014**, *7* (8), 2154-8.
146. Song, Q.; Wang, F.; Cai, J.; Wang, Y.; Zhang, J.; Yu, W.; Xu, J., Lignin depolymerization (LDP) in alcohol over nickel-based catalysts via a fragmentation–hydrogenolysis process. *Energy & Environmental Science* **2013**, *6* (3), 994.
147. Van den Bosch, S.; Schutyser, W.; Koelewijn, S. F.; Renders, T.; Courtin, C. M.; Sels, B. F., Tuning the lignin oil OH-content with Ru and Pd catalysts during lignin hydrogenolysis on birch wood. *Chemical communications* **2015**, *51* (67), 13158-61.
148. Dence, C. W., In *Methods in Lignin Chemistry*, Springer-Verlag Berlin Heidelberg, 1992; pp 33-61.
149. Kim, H.; Ralph, J., Solution-state 2D NMR of ball-milled plant cell wall gels in DMSO-d(6)/pyridine-d(5). *Org Biomol Chem* **2010**, *8* (3), 576-91.
150. Chang, V. S.; Nagwani, M.; Holtzapple, M. T., Lime Pretreatment of Crop Residues Bagasse and Wheat Straw. *Applied Biochemistry and Biotechnology* **1998**, *74*, 135-159.
151. Chang, V. S.; Holtzapple, M. T., Fundamental factors affecting biomass enzymatic reactivity. *Applied Biochemistry and Biotechnology* **2000**, *84-86*, 5-37.

152. Karagöz, S.; Bhaskar, T.; Muto, A.; Sakata, Y., Effect of Rb and Cs carbonates for production of phenols from liquefaction of wood biomass. *Fuel* **2004**, *83* (17-18), 2293-2299.
153. Mostafa, S.; Croy, J. R.; Heinrich, H.; Cuenya, B. R., Catalytic decomposition of alcohols over size-selected Pt nanoparticles supported on ZrO₂: A study of activity, selectivity, and stability. *Applied Catalysis A: General* **2009**, *366* (2), 353-362.
154. Lapierre, C.; Pollet, B.; Monties, B., Thioacidolysis of Spruce Lignin: GC-MS Analysis of the Main Dimers Recovered After Raney Nickel Desulphuration. *Holzforschung* **1991**, *45*, 61-68.
155. Yue, F.; Lu, F.; Sun, R. C.; Ralph, J., Syntheses of lignin-derived thioacidolysis monomers and their uses as quantitation standards. *J Agric Food Chem* **2012**, *60* (4), 922-8.
156. Westermark, U.; Samuelsson, B.; Lundquist, K., Homolytic cleavage β -O-4 in wood lignin & in guaiacylglycerol- β -guaiacyl ether. *Res. Chem. Intermed.* **1995**, *21*, 343-352.
157. Li, S.; Lundquist, K., Cleavage of arylglycerol β -aryl ethers under neutral and acid conditions. *Nordic Pulp and Paper Research Journal* **2000**, *15*, 292-299.
158. Kelley, P.; Lin, S.; Edouard, G.; Day, M. W.; Agapie, T., Nickel-mediated hydrogenolysis of C-O bonds of aryl ethers: what is the source of the hydrogen? *Journal of the American Chemical Society* **2012**, *134* (12), 5480-3.
159. Sitthisa, S.; Resasco, D. E., Hydrodeoxygenation of Furfural Over Supported Metal Catalysts: A Comparative Study of Cu, Pd and Ni. *Catalysis Letters* **2011**, *141* (6), 784-791.
160. Bradley, M. K.; Robinson, J.; Woodruff, D. P., The structure and bonding of furan on Pd(111). *Surface Science* **2010**, *604*, 920-925.
161. Derrouiche, S.; Bianchi, D., Heats of adsorption of the linear and bridged CO species on a Ni/Al₂O₃ catalyst by using the AEIR method. *Applied Catalysis A: General* **2006**, *313* (2), 208-217.
162. Dulaurent, O.; Nawdali, M.; Bourane, A.; Bianchi, D., Heat of adsorption of carbon monoxide on a Ru/Al₂O₃ catalyst using adsorption equilibrium conditions at high temperatures. *Applied Catalysis A: General* **2000**, *201*, 271-279.
163. Zeinalipour-Yazdi, C. D.; Cooksy, A. L.; Efstathiou, A. M., CO adsorption on transition metal clusters: Trends from density functional theory. *Surface Science* **2008**, *602* (10), 1858-1862.

164. Gómez-Monedero, B.; Ruiz, M. P.; Bimbela, F.; Faria, J., Selective hydrogenolysis of α -O-4, β -O-4, 4-O-5 C-O bonds of lignin-model compounds and lignin-containing stillage derived from cellulosic bioethanol processing. *Applied Catalysis A, General* **2017**, *541*, 60-76.
165. He, J.; Zhao, C.; Lercher, J. A., Ni-catalyzed cleavage of aryl ethers in the aqueous phase. *Journal of the American Chemical Society* **2012**, *134* (51), 20768-75.
166. Toubiana, J.; Sasson, Y., The true catalyst in hydrogen transfer reactions with alcohol donors in the presence of RuCl₂(PPh₃)₃ is ruthenium(0) nanoparticles. *Catalysis Science & Technology* **2012**, *2* (8), 1644.
167. D'Hondt, E.; Van de Vyver, S.; Sels, B. F.; Jacobs, P. A., Catalytic glycerol conversion into 1,2-propanediol in absence of added hydrogen. *Chemical communications* **2008**, (45), 6011-2.
168. Hu, J.; Shen, D.; Wu, S.; Zhang, H.; Xiao, R., Composition Analysis of Organosolv Lignin and Its Catalytic Solvolysis in Supercritical Alcohol. *Energy & Fuels* **2014**, *28* (7), 4260-4266.
169. Barta, K.; Matson, T. D.; Fettig, M. L.; Scott, S. L.; Iretskii, A. V.; Ford, P. C., Catalytic disassembly of an organosolv lignin via hydrogen transfer from supercritical methanol. *Green Chemistry* **2010**, *12* (9), 1640.
170. Santos, R. B.; Jameel, H.; Chang, H.-m.; Hart, P. W., Impact of Lignin and Carbohydrate Chemical Structures on Degradation Reactions During Hardwood Kraft Pulping Processes. *BioResources* **2013**, *8* (1), 158-171.
171. Croy, J. R.; Mostafa, S.; Liu, J.; Sohn, Y.; Heinrich, H.; Cuenya, B. R., Support Dependence of MeOH Decomposition Over Size-Selected Pt Nanoparticles. *Catalysis Letters* **2007**, *119* (3-4), 209-216.
172. Milbrandt, A., A Geographic Perspective on the Current Biomass Resource Availability in the United States. Energy, U. S. D. o., Ed. National Renewable Energy Laboratory: 2005.
173. Wilhelm, W. W.; Johnson, J. M. F.; Karlen, D. L.; Lightle, D. T., Corn Stover to Sustain Soil Organic Carbon Further Constrains Biomass Supply. *Agronomy Journal* **2007**, *99* (6), 1665.
174. Buranov, A. U.; Mazza, G., Lignin in straw of herbaceous crops. *Industrial Crops and Products* **2008**, *28* (3), 237-259.
175. Vlad, A.; Arnould, K.; Ernould, B.; Sieuw, L.; Rolland, J.; Gohy, J.-F., Exploring the potential of polymer battery cathodes with electrically conductive molecular backbone. *Journal of Materials Chemistry A* **2015**, *3* (21), 11189-11193.